hep-ph/0008183

Yukawa Unification as a Window into the Soft Supersymmetry Breaking Lagrangian

S. F. King and M.Oliveira

Department of Physics and Astronomy, University of Southampton

Southampton, SO17 1BJ, U.K

Abstract

We study Yukawa unification, including the effects of a physical neutrino mass consistent with the Superkamiokande observations, in a string/D-brane inspired $SU(4) \otimes SU(2)_L \otimes SU(2)_R$ model which allows the most general non-universal scalar and gaugino masses, including the usual D-term contributions which arise in $SO(10)$. We investigate how the tight constraints from rare decays such as $b \to s\gamma$ and $\tau \to \mu\gamma$ can provide information about the family dependent supersymmetry breaking soft Lagrangian, for example the trilinears associated with the second and third family. Many of our results also apply to $SO(10)$ to which the model approximately reduces in a limiting case. In both models we find that Yukawa unification is perfectly viable providing the non-universal soft masses have particular patterns. In this sense Yukawa unification acts as a window into the soft supersymmetry breaking Lagrangian.

February 1, 2008

I. INTRODUCTION

One of the earliest successes of the Minimal Supersymmetric Standard Model (MSSM) [1] was that it could allow for the unification of the gauge couplings at high energy ($Q = M_X$) [2], thereby opening the door for Supersymmetric Grand Unified Theories (SUSY GUTs) [3, 4, 5, 6]. SUSY GUTs typically involve some third family Yukawa unification [6, 7, 8, 9, 10]. For example minimal $SU(5)$ [11] predicts bottom-tau Yukawa unification at M_X ($\lambda_b = \lambda_\tau$) and allows for the prediction of the top quark mass (m_t) in terms of the ratio m_b/m_τ. In models like $SO(10)$, and in the $SU(4)\otimes SU(2)_L\otimes SU(2)_R$ (422) Pati-Salam model [12], complete third family Yukawa unification holds ($\lambda_t = \lambda_b = \lambda_\tau$). Thus the ratio of the vacuum expectation values (VEVs) of the up/down Higgs bosons doublets – $\tan\beta = v_2/v_1$ – can be predicted. Since the top and bottom Yukawa couplings start out equal at the GUT scale, and their renormalization group (RG) evolution is very similar (they differ only by the $U(1)$ couplings at one loop) their low energy values are approximately equal so we expect $\tan\beta \sim m_t/m_b \sim 40$.

In this paper we shall include the neutrino Yukawa coupling in the analysis giving quadruple Yukawa unification ($\lambda_t = \lambda_b = \lambda_\tau = \lambda_\nu$) as was first done in Ref. [10]. In the light of the Superkamiokande results [13] (assuming hierarchical neutrino masses and the see-saw mechanism) we regard the third family neutrino mass (m_ν) as an input which allows for an additional prediction – the mass scale at which the heavy right-handed neutrinos decouple – M_ν. However such predictions depend sensitively on the parameters of the soft SUSY breaking Lagrangian, as we now discuss.

Yukawa unification (assuming the MSSM and SUSY GUTs) at first was thought to lead to an acceptable top mass prediction, given the experimentally permitted range of top and bottom quark masses and α_s, with a unified Yukawa coupling at M_X of order one ($\lambda_X \sim 1$) [8, 10, 14, 15, 16, 17]. However, when low energy SUSY

corrections to the running bottom quark mass due to the decoupling of SUSY particles were included [18, 19], the initial good agreement was spoiled. The SUSY corrections to the bottom quark mass are :

$$\Delta m_b = \frac{\delta m_b}{m_b} = \frac{\mu \tan\beta}{4\pi}\left[\frac{8}{3}\alpha_s m_{\tilde{g}} I(m^2_{\tilde{g}}, m^2_{\tilde{b}_1}, m^2_{\tilde{b}_2}) + \frac{\lambda_t^2}{4\pi} A_t I(\mu^2, m^2_{\tilde{t}_1}, m^2_{\tilde{t}_2},)\right] \qquad (1)$$

where the function $I(x, y, z)$ is given in [18]. The corrections can be positive or negative depending on the sign of μ, and being proportional to $\tan\beta$, are rather large.

With universal soft masses and *negative* μ, the SUSY corrections to the bottom mass lead to large negative $\Delta m_b = \delta m_b/m_b \sim -20\%$ corrections which implies a larger b quark mass before the SUSY corrections, which effectively lowers the previously successful top mass prediction to $m_t \sim 150$ GeV which is too small [18]. With universal soft masses and *positive* μ the top mass is predicted to be too large, outside its perturbative upper limit. It has already been pointed out in the literature that δm_b can be made small by either assuming explicit non-universal scalar soft masses [20, 21, 22] or by introducing approximate Peccei-Quinn and R symmetries [19, 23]. However in the framework of $SO(10)$ the degree of non-universality one could assume until recently appeared rather limited. For example, if both Higgs doublets arise from a single $\underline{10}$ dimensional representation then they will necessarily have a common soft scalar mass at the GUT scale, and the same applies for the light Higgs bidoublet of the Pati-Salam model. Such universality is also a problem for electroweak symmetry breaking where one requires a large hierarchy of vacuum expectation values (VEVs) starting from very symmetrical initial conditions where the two Higgs doublet soft masses are equal, and where the approximately equal top and bottom Yukawa couplings tend to drive both Higgs masses negative equally, making large $\tan\beta$ rather difficult to achieve.

A large step forward for both these problems has been to realise the importance

of D-term contributions to scalar masses [24], which naturally split the two Higgs doublet masses. If the up-type Higgs doublet mass at the GUT scale is smaller than the down-type Higgs doublet mass, then this makes electroweak symmetry breaking with large $\tan\beta$ much more natural. Assuming negative μ, the D-terms also allow a choice of non-universal scalar masses which reduces the correction to the b-quark mass and hence allow a larger top quark mass. Although these problems appear to be resolved with D-terms, one still faces difficulties with rare decays such as $b \to s\gamma$, which is also enhanced for large $\tan\beta$, and negative μ [25]. This problem can be avoided either by increasing the masses of all the superpartners, or by considering positive μ which will tend to cancel the SUSY contributions, however both these procedures lead to fine-tuning. Another possibility which we pursue in this paper is to consider the effect of non-universality in the family space, which may lead to additional contributions to $b \to s\gamma$ which can cancel those coming from the family universal sources. We explicitly check that the contributions that we introduce do not introduce problems elsewhere such as with $\tau \to \mu\gamma$.

The main purpose of this paper is to provide a detailed analysis of Yukawa unification, post-Superkamiokande, allowing the most general non-universal soft SUSY breaking masses possible. Apart from non-universality in the soft scalar masses arising from D-terms, we shall also consider more general types of non-universality which may arise in models such as the string/D-brane inspired $SU(4) \otimes SU(2)_L \otimes SU(2)_R$ model [26],[27], which reduces to the $SO(10)$ model in a limiting case. This allows more general soft scalar mass non-universality including similar D-term contributions as in $SO(10)$ (since the relevant broken $U(1)$ factors all arise from the breaking of the $SU(4) \otimes SU(2)_L \otimes SU(2)_R$ subgroup), and also permits violations of gaugino mass universality which have not so far been studied. The underlying theme of our approach is that the sensitivity of Yukawa unification to soft SUSY breaking parameters is to be welcomed, since it provides a window into the soft SUSY breaking Lagrangian,

both from the point of view of family universal and family non-universal soft SUSY breaking parameters.

The layout of the remainder of the paper is as follows. In the section II we present our calculational approach, and in section III we review the SUSY corrections to the bottom and tau masses. Section IV deals with the effect of neutrino Yukawa couplings on Yukawa unification and in section V we present results for gauge and Yukawa unification, assuming minimal supergravity (mSUGRA) with universal soft SUSY breaking parameters and including the neutrino threshold in addition to the usual low energy thresholds. In section VI we turn to Yukawa unification in the $SU(4) \otimes SU(2)_L \otimes SU(2)_R$ model, including the effect of physics above the GUT scale, and non-universal soft scalar and gaugino masses permitted in this model. We also consider the effect of D-terms in the $SO(10)$ limit of the model, and then study $b \to s\gamma$ and $\tau \to \mu\gamma$ including non-universality in the family-dependent trilinear parameters. Section VII concludes the paper.

II. FRAMEWORK

In this section we will summarize how we implemented the RGEs and matching boundary conditions of the model. In the region $Q < M_Z$ the effective theory is $SU(3)_c \otimes U(1)_{em}$, thus 3-loop QCD [28] plus 2-loop QED RGEs [29] apply. Between $Q = M_Z$ and $Q = M_S$, where M_S is the scale that parameterises the energy at which the theory effectively becomes supersymmetric (see Appendix B for details), we considered 2-loop Standard Model (SM) RGEs in the gauge and Yukawa couplings [15, 29, 30]. In the region $M_S < Q < M_X$ we evolved 2-loop (1-loop) gauge/Yukawa (all other parameters) MSSM RGEs [15, 31], properly adapted and extended to take into account the presence (and decoupling) of right handed neutrinos ν^c.

A. Input

The low energy input was : the running electromagnetic coupling $\alpha_e^{-1}(M_Z) = 127.8$, the pole tau lepton mass $M_\tau = 1.784$ GeV and several values for the pole bottom quark mass $M_b = 4.7, 4.8, .., 5.1$ GeV. We have converted the pole bottom mass into "running" bottom mass in the $\overline{\rm MS}$ scheme using two loop QCD perturbation theory [29] :

$$m_b(Q = M_b) = \frac{M_b}{1 + \frac{4}{3}\frac{\alpha_s(M_b)}{\pi} + K_b\left(\frac{\alpha_s(M_b)}{\pi}\right)^2} \tag{2}$$

where $K_b = 12.4$. The corresponding running masses, for $\alpha_s = 0.120$, are $m_b(M_b) =$ 4.06, 4.15, 4.24, 4.33, 4.42 GeV. The experimental range for m_b estimated from bottomonium and B masses is 4.0–4.4 GeV [32]. The strong coupling $\alpha_s(M_Z)$ was taken to be in the range 0.110–0.130.

The low energy input was complemented by the Super-Kamiokande atmospheric neutrino data that suggests $m^2_{\nu_3} - m^2_{\nu_2} = 10^{-2}$ to 10^{-3} eV^2 [13]. Assuming that the neutrino masses are hierarchical we required that $m_{\nu_3} \sim 0.05$ eV.

The universal high energy inputs assumed initially are motivated by mSUGRA: spontaneously broken supergravity in which the local N=1 supersymmetry breaking occurs in a "hidden" sector and is only transmitted to the "visible" sector through weak gravitational – flavour blind – interactions. Thus we assume to begin with universal soft SUSY breaking masses (USBM) given by a common gaugino mass $M_{1/2}$ and soft scalar masses m_0 at $Q = M_X$. The trilinear A-terms were set to zero. In section VI we relax the universality assumption.

In the Yukawa sector we assumed that the third family Yukawa couplings have their origin in a unified renormalizable interaction which fixes their values to be λ_X.

B. Running and matching boundary conditions

The process by which the output was generated relied in the initial estimation and successive iterative refinement of *a priori* unknown parameters such as M_t and $\tan\beta$. The procedure is described in detail in section VII of Ref. [16].

Starting at $Q = M_Z$, $\alpha_s(M_Z)$ and $\alpha_e(M_Z)$ were firstly run down to $Q = 1$ GeV (where the up, down and strange quark running masses were fixed [29]) and secondly up to $Q = M_Z$ using $SU(3)_c \otimes U(1)_{em}$ RGEs. In the "running up" process the heavy (charm, tau and bottom) fermion pole masses were converted to running ones using the expressions in Ref. [29]. At $Q = M_Z$, α_e was corrected for the decoupling of heavy gauge bosons, Higgs and Nambu-Goldstone bosons, and ghosts [33]. Afterwards the value of s^2_θ [5] was used to obtain g' and g. The bottom and tau Yukawa couplings, in the Standard Model, were evaluated using $\lambda^{SM}_{b,\tau}(M_Z) = m_{b,\tau}(M_Z)/v$, where the VEV is $v = 174$ GeV. Next, the gauge and the Yukawa couplings were run from $Q = M_Z$ to the estimated pole top mass $Q = M_t$ using 2-loop SM RGEs, at which point M_t was converted to $\overline{\rm MS}$ running mass $m_t(M_t)$, joining the list of parameters to be integrated to $Q = M_S$. All along, threshold corrections in the gauge couplings were included by changing the 1-loop β-functions (using the "step" approximation.) At $Q = M_S$ the

$\overline{\rm MS}$ gauge couplings α_i were converted to the DR ones [5, 8, 34] and corrected for the cumulative effect of decoupling of all the SUSY particles [34]. The top, bottom and tau Yukawa couplings were then converted from the SM to the MSSM normalization and corrected for the SUSY corrections [34] :

$$\lambda_t^{MSSM} = \lambda_t^{SM}/\sin\beta \tag{3}$$

$$\lambda_b^{MSSM} = \lambda_b^{SM}/\cos\beta - \delta m_b/v_1 \tag{4}$$

$$\lambda_\tau^{MSSM} = \lambda_\tau^{SM}/\cos\beta - \delta m_\tau/v_1 \tag{5}$$

Afterwards we run up all the above couplings, together with an estimate for $\lambda_\nu^{MSSM}(M_S)$, in two stages, firstly from $Q = M_S$ to $Q = M_\nu$ and afterwards from $Q = M_\nu$ to $Q = M_X$, properly excluding (including) ν_τ^c in the former (latter) stage. In our model M_X was fixed to be the scale at which only the $U(1)$ and $SU(2)$ gauge couplings unify : $\alpha_1(M_X) = \alpha_2(M_X) \neq \alpha_3(M_X)$.

At M_X gauge and Yukawa unification were tested leading to eventual wiser choices to the next estimates for M_t, $\tan\beta$, M_X and M_ν.

The iteration cycle was completed by setting the USBM to their unification values after which all the couplings and masses of the model were run down from $Q = M_X$ to $Q = M_S$ using the inverse "running up" procedure described above. Finally at $Q = M_S$ the 1-loop effective Higgs potential was minimized [35, 36] and the SUSY Higgs mixing parameter μ^2 and the corresponding soft term m_3^2 were determined using [16, 37, 38] :

$$\mu^2 = \frac{m_1^2 - m_2^2\,\tan^2\beta}{\tan^2\beta - 1} - \frac{1}{2}\,M_Z^2 \tag{6}$$

$$m_3^2 = (\mu_2^2 + \mu_1^2)\,\frac{\tan\beta}{\tan^2\beta + 1} \tag{7}$$

where $\mu_{2,1}^2 = m_{2,1}^2 + \mu^2$ and the up/down soft Higgs boson masses are $m_{2,1}^2 = m_{2,1}^{2tree} + \Sigma_{2,1}$. [1]

[1] The $\Sigma_{2,1}$ parameterise the 1-loop corrections to the tree level Higgs potential [39].

We note that the number of independent parameters the model can predict is four – as many as the constraints imposed (one gauge and three Yukawa unification conditions.) We took them to be M_X, M_t, $\tan\beta$ and M_ν. The latter was fixed by requiring that $m_{\nu_3} = 0.05$ eV.

III. SUPERSYMMETRIC BOTTOM AND TAU MASS CORRECTIONS

In the Standard Model it is frequent to work in off-shell mass schemes in which the running masses $m_f(Q)$ differ from their physical masses M_f (defined as the real part of the complex pole position of its propagator) by some finite correction [40]. For the quarks the most important corrections (arising from gluon loops) are well known and particularly affect bottom quark mass (see Eq. (2).) In supersymmetric models additional corrections are also present. For large values of $\tan\beta$ some of these SUSY corrections can indeed affect the running bottom mass m_b by 20 % [18, 19], thus their consideration is crucial for the prediction of M_t. In this section we review the origin of the SUSY corrections to the bottom quark (δm_b) and tau lepton mass (δm_τ.)

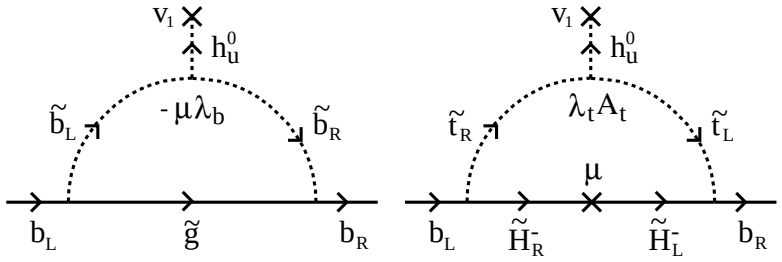

FIG. 1 Gluino and higgsino loop diagrams corresponding to the bottom mass corrections $\delta^{\tilde{g}} m_b$ and $\delta^{\tilde{H}} m_b$ of Eq. (8) and Eq. (9).

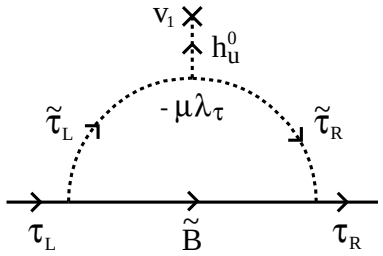

FIG. 2 Bino diagram corresponding to the tau mass correction $\delta^{\tilde{B}} m_\tau$ of Eq. (10).

In the MSSM, at tree level, the bottom quark acquires a mass exclusively through the non-vanishing VEV of $\langle h_d^0 \rangle = v_1$. However, at 1-loop level, the bottom quark also receives a "small" mass from $\langle h_u^0 \rangle = v_2$. The dominant processes responsible for the additional corrections to the bottom (tau) mass are characterized by gluino/sbottom and higgsino/stop (bino/stau) diagrams which we illustrate in Fig. 1 (and Fig. 2.) The corresponding expressions for $\delta^{\tilde{g}} m_b$, $\delta^{\tilde{H}} m_b$ and $\delta^{\tilde{B}} m_\tau$ are given by [18, 19, 41] :

$$\Delta^{\tilde{g}} m_b = \frac{\delta^{\tilde{g}} m_b}{m_b} = \frac{2\alpha_3}{3\pi}\, m_{\tilde{g}}\, \mu\, \tan\beta\, I(m^2_{\tilde{g}}, m^2_{\tilde{b}_1}, m^2_{\tilde{b}_2}) \tag{8}$$

$$\Delta^{\tilde{H}} m_b = \frac{\delta^{\tilde{H}} m_b}{m_b} = \frac{\alpha_t}{4\pi}\, A_t\, \mu\, \tan\beta\, I(\mu^2, m^2_{\tilde{t}_1}, m^2_{\tilde{t}_2}) \tag{9}$$

$$\Delta^{\tilde{B}} m_\tau = \frac{\delta^{\tilde{B}} m_\tau}{m_\tau} = \frac{\alpha'}{4\pi}\, m_{\tilde{B}}\, \mu\, \tan\beta\, I(m^2_{\tilde{B}}, m^2_{\tilde{\tau}_1}, m^2_{\tilde{\tau}_2}) \tag{10}$$

where $m_{\tilde{g}}$ ($m_{\tilde{B}}$) is the gluino (bino) mass, $\alpha_t = \lambda_t^2/4\pi$, $\alpha' = g'^2/4\pi$, A_t the top soft trilinear term and $m_{\tilde{b},\tilde{t},\tilde{\tau}}$ the sbottom, stop and stau masses. The function I is positive, symmetric, smallest for degenerate masses and approximately scales with the inverse of its biggest argument. [2] We also find convenient to define the total absolute and

[2] See footnote in appendix C.

relative bottom corrections :

$$\delta m_b = \delta^{\tilde{g}} m_b + \delta^{\tilde{H}} m_b \qquad \Delta m_b = \Delta^{\tilde{g}} m_b + \Delta^{\tilde{H}} m_b. \tag{11}$$

The bottom mass before the SUSY corrections are included – $m_b = \lambda_b v_1$ – is related to the bottom mass after the SUSY corrections are included – m_b^{SUSY} – through :

$$m_b^{SUSY} = m_b + \delta m_b = m_b(1 + \Delta m_b) \tag{12}$$

The pole mass after the SUSY corrections are included is given by Eq. (2) using m_b^{SUSY} in Eq. (12).

IV. DECOUPLING OF THE HEAVY RIGHT HANDED NEUTRINO

In this section we briefly discuss the decoupling of the heavy SM singlet right-handed neutrino with mass M_ν. We assume that the neutrino Yukawa matrix is dominated by a single entry in the 33 position, although in realistic models of neutrino mixing one would expect that there are at two entries which may have similar magnitude. We have checked that our results are insensitive to the presence of a large off-diagonal entry in the neutrino Yukawa matrix, assuming that the charged lepton Yukawa matrix does not have any large off-diagonal entries. [3] The decoupling is achieved via see-saw mechanism [42] which generates a small mass for the left-handed neutrino through the presence of a right-left Dirac Yukawa coupling. The part of the superpotential of interest is :

$$\mathcal{W} = \nu^c \, \lambda_\nu \, \nu \, h_u^0 + \tfrac{1}{2} \, M_\nu \, \nu^c \, \nu^c. \tag{13}$$

Thus the light neutrino tau acquires a mass $m_\nu = \lambda_\nu^2 v_2^2/(4M_\nu)$. In our model we used $m_\nu = 0.05$ eV suggested by Ref. [13] to fix $M_\nu \sim 10^{13}$ GeV (see results in Table IV in section V.C.)

V. mSUGRA RESULTS

We now proceed to discuss the results generated by the model described in the previous sections. Although many of the results presented here appear elsewhere, we find it useful to compile and review them here for the purposes of comparison to the new situations we discuss later such as the effect of neutrinos and non-universal soft masses. These have been organized in three categories which are suitable to expose their variation with $\alpha_s(M_Z)$ in the range 0.110–0.130, selected pole bottom masses

[3] We focus on the third family only, thus we simplify our notation by replacing $\nu_\tau \to \nu$ and $\nu_\tau^c \to \nu^c$.

$M_b = 4.7, 4.8, .., 5.1$ GeV and universal gaugino/soft scalar masses $M_{1/2}$, $m_0 < 1$ TeV. We plotted graphs showing the dependence of the results with α_s for various M_b and fixed $M_{1/2} = 400$, $m_0 = 200$ GeV; graphs scanning the $M_{1/2}$–m_0 parameter space for illustrative fixed α_s and M_b; and a set of numerical tables corresponding to the results obtained from nine models for which the input is listed in Table I.

TABLE I.

Case	$\alpha_s(M_Z)$	M_b	$m_b(M_b)$	$M_{1/2}$	m_0
A	0.1150	4.70	4.12	400	200
B	0.1150	4.70	4.12	800	400
C	0.1150	5.10	4.49	400	200
D	0.1150	5.10	4.49	800	400
E	0.1250	4.70	3.99	400	200
F	0.1250	4.70	3.99	800	400
G	0.1250	5.10	4.36	400	200
H	0.1250	5.10	4.36	800	400
I	0.1250	4.80	4.08	600	400

TABLE I. Input values of $\alpha_s(M_Z)$, the pole bottom mass M_b, the running bottom mass $m_b(M_b)$ obtained from M_b using two loop QCD corrections only (see Eq. (2)), and the universal gaugino and soft scalar masses $M_{1/2}$, m_0 (given in GeV units) at the unification scale $Q = M_X$ for a list of models we will refer in the main text as Case A,B,..,I.

A. Gauge unification

In Fig. 3 we plot the unified $U(1)$ and $SU(2)$ gauge couplings $\alpha_1^{-1}(M_X)$=$\alpha_2^{-1}(M_X)$= α_X^{-1} together with $\alpha_3^{-1}(M_X)$ against $\alpha_s(M_Z)$ for $M_{1/2} = 400$, $m_0 = 200$ GeV and several values of M_b. The mismatch $\Delta\alpha_X^{-1} = \alpha_3^{-1}(M_X) - \alpha_X^{-1}$ in gauge unification is small and decreasing for increasing α_s. In fact, for large values of $\alpha_s \sim 0.128$ complete gauge unification occurs. The sensitiveness of $\Delta\alpha_X^{-1}$ to M_b is quite small. Complete gauge unification can also be present for lower values of $\alpha_s \sim 0.125$ as is shown by case H in Table II where we find $\alpha_X^{-1} \sim \alpha_3 \sim 25.18$ ($M_{1/2} = 800$, $m_0 = 400$ GeV.)

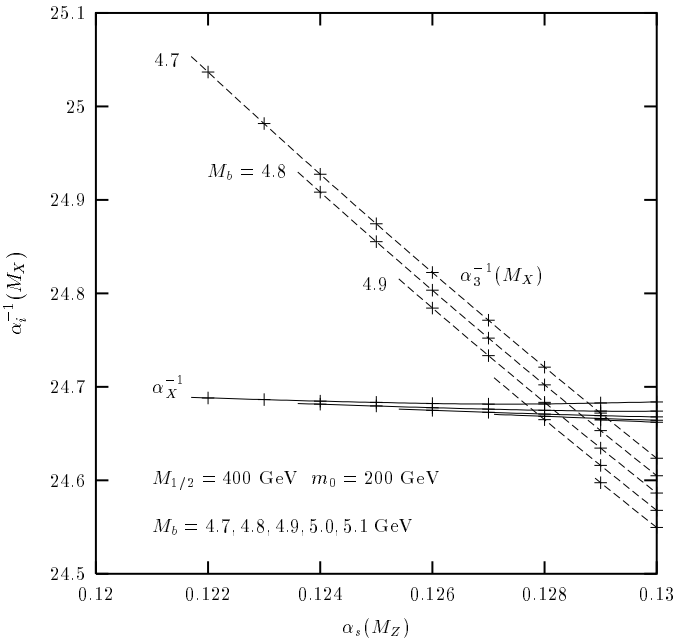

FIG. 3. Dependence of unified gauge couplings $\alpha_1^{-1}(M_X) = \alpha_2^{-1}(M_X) = \alpha_X^{-1}$ and $\alpha_3^{-1}(M_X)$ on $\alpha_s(M_Z)$ for several bottom masses M_b and fixed gaugino and soft scalar masses $M_{1/2}(M_X)$, $m_0(M_X)$.

TABLE II.

Case	α_X^{-1}	$\alpha_3^{-1}(M_X)$	$M_X/10^{16}$
A	24.70	25.46	1.64
B	25.21	25.83	1.37
C	24.70	25.38	1.52
D	25.18	25.75	1.26
E	24.68	24.87	1.83
F	25.20	25.25	1.54
G	24.68	24.80	1.70
H	25.18	25.17	1.42
I	24.98	25.09	1.66

TABLE II. Predicted values for the unified gauge coupling $\alpha_X^{-1} = \alpha_1^{-1}(M_X) = \alpha_2^{-1}(M_X)$, for the strong coupling $\alpha_3^{-1}(M_X)$ and for the unification scale M_X (given in GeV.)

Analysing Table II we find that $\delta\alpha_X^{-1} = \Delta\alpha_X^{-1}/\alpha_X^{-1} < 3\%$. Gauge unification also

depends on the SUSY spectrum. Generally, increasing $M_{1/2}$ and/or m_0 decreases M_X and $\delta\alpha_X^{-1}$. In short partial gauge unification is achieved for $M_X/10^{16} \sim 1-2$ GeV with $\alpha_X^{-1} \sim 25.0 \pm 0.5$ while complete unification $\alpha_X^{-1} = \alpha_3^{-1}(M_X)$ is favoured by large $\alpha_s(M_Z)$, $M_{1/2}$ and M_b.

B. Top mass prediction with SUSY bottom and tau mass corrections

We now turn to the predictions for the top mass. Experimentally the top mass has been measured to be [43] :

$$M_t \sim 174.3 \pm 3.2(\text{stat.}) \pm 4.0(\text{syst.}) \text{ GeV} \tag{14}$$

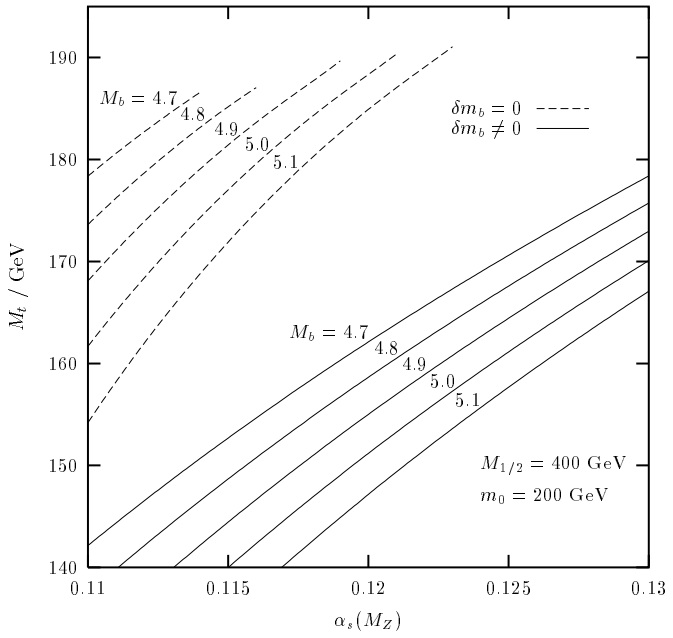

FIG. 4. Predicted values for the pole top mass M_t against $\alpha_s(M_Z)$ for several values of the pole bottom mass in the range $M_b = 4.7 - 5.1$ GeV. The dashed line refers to the top mass prediction when no SUSY correction to the bottom mass is considered ($\delta m_b = 0$). The prediction for the top mass when negative corrections to the bottom mass are included ($\mu < 0$) is indicated by the solid line ($\delta m_b \neq 0$.)

In Fig. 4 we compare the values for the pole top mass M_t prediction obtained when no SUSY correction to the bottom mass is considered ($\delta m_b = 0$), indicated

with a dashed line, and when they are included ($\delta m_b \neq 0$ and negative) plotted with a solid line. We see that the SUSY bottom corrections (for our choice of negative μ) decrease the top mass considerably.

In fact, the magnitude of the SUSY correction is so large that it excludes the possibility of an eventual positive sign for μ. The reason is because if we have a positive μ the SUSY bottom corrections are positive. Thus, in order to keep the bottom mass, after the SUSY corrections are included m_b^{SUSY}, in the allowed experimental range, the bottom mass before the SUSY corrections are included must decrease. In this case, third family unification leads to an increase in the top Yukawa coupling. However, it turns out that the required increase in the top Yukawa coupling is so large that it drives it, at high energy, well beyond perturbation theory. Numerically, we find that the RGEs fail to converge. [4]

At this point it is also interesting to comment on the effect the bino correction to the tau mass has on the prediction for the top mass. Again, a negative μ means that $\delta^{\tilde{B}} m_\tau$ is negative (see Eq. (10)). Thus, in order to keep the tau mass after the SUSY correction is included unchanged, the tau mass before the SUSY correction is included must increase, implying that, third family unification predicts a larger top mass. Numerically we find that the top mass increases by 3–4 GeV.

Returning to Fig. 4 we observe that when the bottom corrections are included the top mass prediction is only acceptable for large values of $\alpha_s(M_Z)$. For this reason, in the analysis that will follow, we will study the implications of including the SUSY bottom corrections in our model by taking $\alpha_s(M_Z)$ to be in the range 0.120–0.130.

[4] One can turn the argument around by saying that, if the top quark mass is fixed to be around 175 GeV then third family Yukawa unification at M_X requires, for positive μ, a very large bottom mass prediction after the SUSY corrections are included.

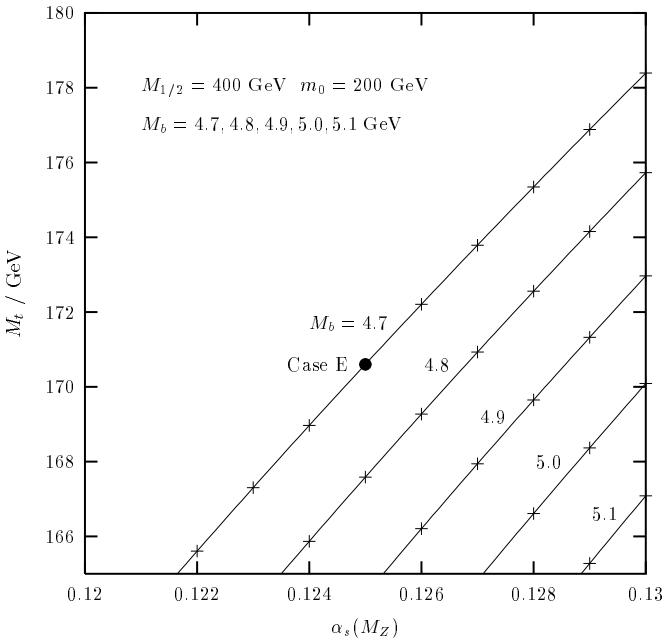

FIG. 5. Pole top mass prediction M_t against $\alpha_s(M_Z)$ for several values of the pole bottom mass M_b and fixed $M_{1/2}$, m_0.

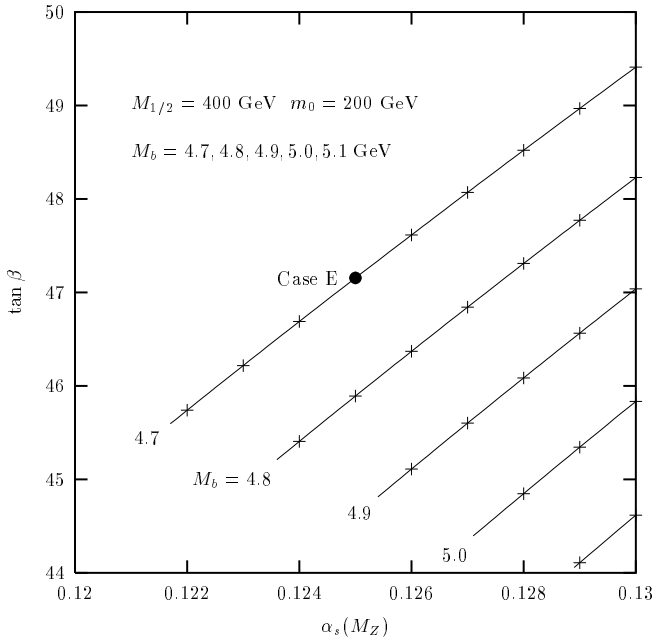

FIG. 6. Prediction for $\tan\beta$ against $\alpha_s(M_Z)$ for several values of the pole bottom mass M_b and fixed $M_{1/2}$, m_0.

In Fig. 5 and 6 the pole top mass M_t and $\tan\beta$ are plotted against α_s for several values of the bottom mass M_b. We can see that both are significantly sensitive to α_s and to M_b. For $M_b = 4.7$ (the first upper line) the top mass takes values within $165.6 < M_t < 178.4$ GeV and $45.73 < \tan\beta < 49.41$ for $0.122 < \alpha_s < 0.130$. Additionally for a fixed value of $\alpha_s = 0.125$ the top mass increases from 157.7 to 170.6 GeV and $\tan\beta$ from 41.99 to 47.15 when M_b decreases from 5.1 to 4.7 GeV. In Table III we list the numerical predictions for the top mass, $\tan\beta$ and the value of the unified Yukawa coupling λ_X.

TABLE III.

Case	M_t	$\tan\beta$	λ_X
A	152.7	42.16	0.426
B	158.1	44.16	0.469
C	135.3	35.94	0.317
D	139.7	37.51	0.340
E	170.6	47.15	0.569
F	176.2	49.40	0.643
G	157.7	41.99	0.428
H	163.3	44.06	0.473
I	170.7	47.34	0.561

TABLE III. Predicted values for the top mass (in GeV), $\tan\beta$ and for the value of the third family unified Yukawa coupling λ_X.

In Fig. 7 the strong correlation between M_t and λ_X is exposed. It is clear that since λ_X is not large the top quark mass prediction is far from its infrared (IR) fixed point ~ 200 GeV [44, 45].

In Fig. 8 we show that M_t increases with increasing SUSY particle masses. The reason for such dependence can be traced to the $SU(3)$ gauge group factors in the SM and MSSM RGEs : $\mathrm{d}\lambda_t^{SM,MSSM}/\mathrm{dt} \sim -b_t^{SM,MSSM} g_3^2$. Numerically we have $b_t^{SM} = 8 > b_t^{MSSM} = 16/3$ thus increasing M_S allows for a wider $M_Z < Q < M_S$ range of integration for the SM which favours an enhancement for the top mass.

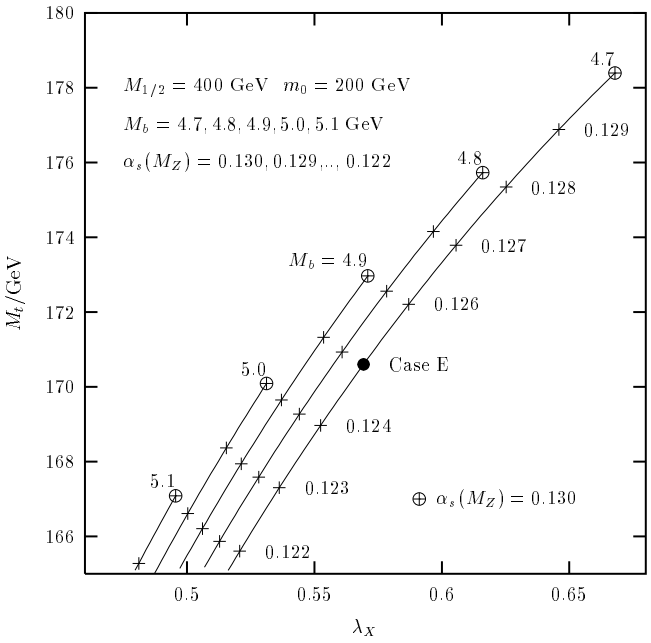

FIG. 7. Correlation between the top pole mass prediction M_t and the value of the unified gauge coupling at M_X, λ_X. Each line corresponds to a fixed choice of M_b and along it $\alpha_s(M_Z)$ decreases from a maximum value of 0.130 (indicated with a crossed circle) to lower values at 0.001 intervals marked with crosses.

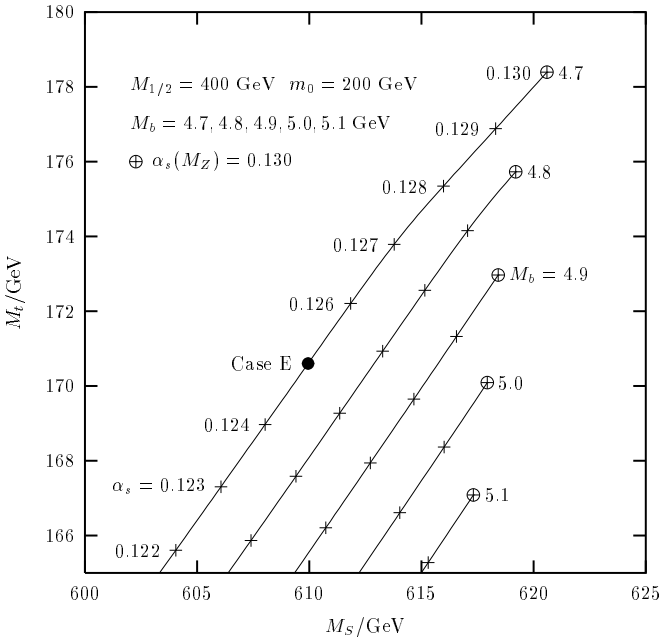

FIG. 8. Dependence of the top mass prediction M_t on the effective supersymmetry scale M_S. Each line corresponds to a fixed choice of M_b and along it $\alpha_s(M_Z)$ decreases from a maximum value of 0.130 (indicated with a crossed circle) to lower values at 0.001 intervals marked with crosses.

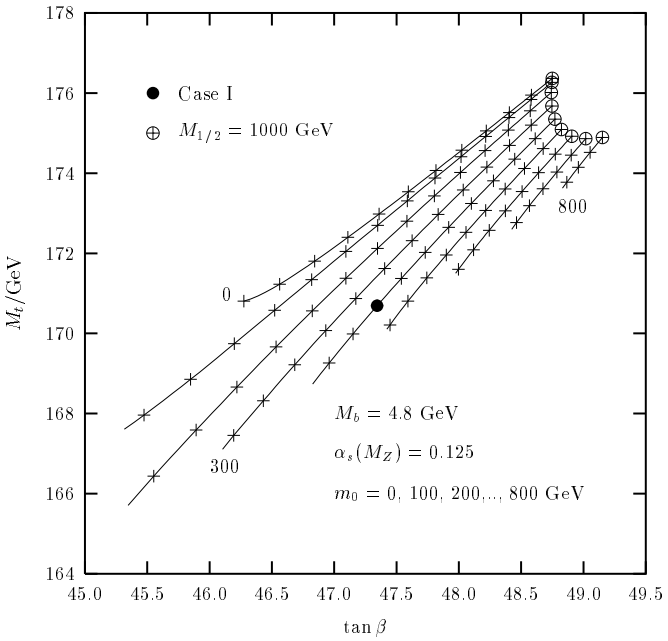

FIG. 9. Correlation between the top mass prediction M_t and the prediction for $\tan\beta$. Each line corresponds to a fixed choice of m_0 and along it $M_{1/2}$ decreases from a maximum value of 1 TeV (indicated with a crossed circle) to lower values at 50 GeV intervals marked with crosses.

Perhaps more interesting than Fig. 8 where variations in M_S are indirectly induced by α_s is Fig. 9 where $\alpha_s = 0.125$ is keep fixed but $M_{1/2}$ and m_0 are allowed to vary. The results are displayed in the M_t–$\tan\beta$ plane.

A quick estimate of the effect of including a consistent supersymmetric scale M_S on the top mass prediction can easily be computed. Taking, for example, $m_0 = 400$ GeV, varying $M_{1/2}$ from 600 to 700 GeV will increase M_t from 170.7 to 172.0 GeV (see Fig. 9) and M_S increases from 915 to 1047 GeV. Thus if we had considered a "rigid" $M_S \sim M_Z \sim 100$ GeV we would find a value for M_t decreased by $\Delta M_t \sim -8$ GeV.

C. Decoupling of the heavy tau neutrino

In Fig. 10 we show an example of third family Yukawa unification generated for case I. We note that the inclusion of the SUSY correction δm_b leads to low values for the unified Yukawa coupling $\lambda_X \sim 0.55$. Consulting Table III we find $0.32 < \lambda_X < 0.64$ in contrast with typical $\lambda_X \sim 1$ predictions when no SUSY corrections are considered. A low λ_X implies that the RGEs which govern the Yukawa evolution are dominated by the gauge terms, thus the effect of decoupling the right-handed tau neutrino is small.

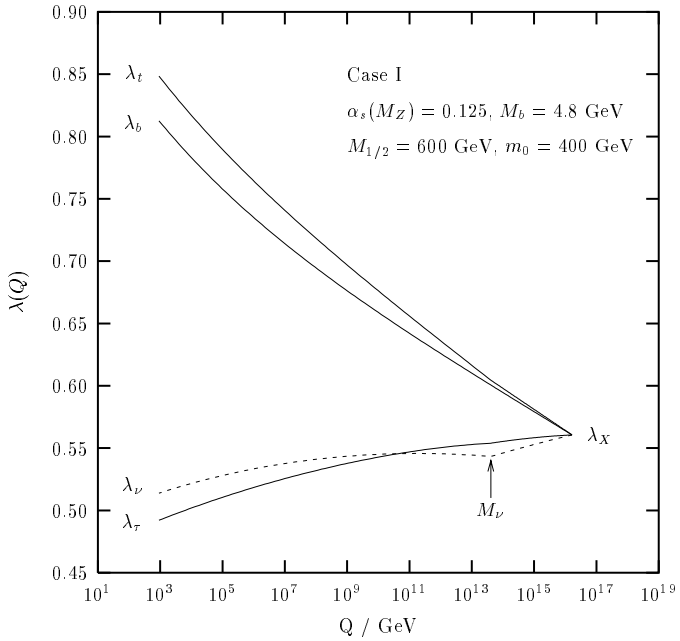

FIG. 10. Running of the third family $t - b - \tau - \nu_\tau$ Yukawa couplings between the unification scale $Q = M_X$ and the effective supersymmetry breaking scale $Q = M_S$. The decoupling of the tau right-handed neutrino at $Q = M_\nu$ mainly affects the running of λ_ν (dashed line.)

In Table IV we list the predicted values for the heavy right-handed neutrino mass scale M_ν which in our model is fixed by the requirement that the light left-handed neutrino tau has a mass of $m_\nu = 0.05$ eV. We see that M_ν is in the range $2 - 5 \times 10^{13}$ GeV.

TABLE IV.

Case	A	B	C	D	E	F	G	H	I
$M_\nu/10^{13}$	2.97	3.35	1.98	2.18	4.16	4.77	2.96	3.35	4.09

TABLE IV. Predicted values for the mass of the heavy right-handed neutrino M_ν (given in GeV) required to generate a light left-handed neutrino mass $m_{\nu_3} = 0.05$ eV.

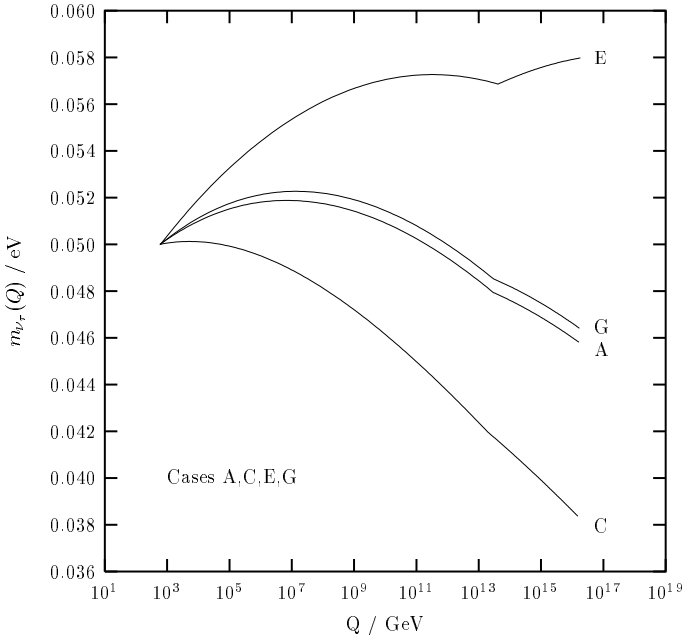

FIG. 11. Running of the tau neutrino mass from the unification scale to low energy for Cases A,C,E,G in Table I.

In Fig. 11 the evolution of m_{ν_3} from M_X to M_S is shown for cases A,C,E,G. For each line a different $M_\nu(Q = M_X)$ was chosen in order to assure the same $m_\nu = 0.05$ eV at low energy. For the purpose of illustration we have in Fig. 12 (and *only* in this plot) relaxed the constraint upon M_ν and set it to vary at ten log intervals from M_X to $10^{-5}M_X$. The effect of changing M_ν is shown in the M_t–λ_X plane. Comparing this plot with the tables throughout this article we can conclude that the uncertainties attached to α_s, M_b and M_S are far more important than the ones which might affect

the determination of M_ν. The predictions for M_t and λ_X increase for decreasing M_ν. The variation in M_t is quite small (typically less than 1 %). On the other hand variations in λ_X are larger and of about 3–4 %.

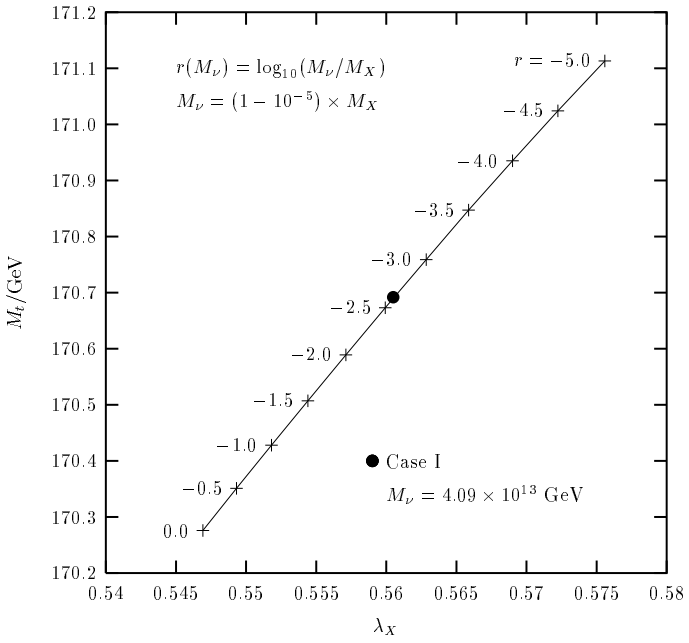

FIG. 12. Variations in the predictions for the top mass M_t and in the unified Yukawa coupling λ_X induced by changing M_ν in the range $(1-10^{-5}) \times M_X$. The dark circle refers to the choice of M_ν which for Case I gives $m_{\nu_3} = 0.05$ eV.

VI. YUKAWA UNIFICATION IN THE $SU(4) \otimes SU(2)_L \otimes SU(2)_R$ MODEL

In this section we will extend the analysis of the top quark mass, so far considered in the context of the MSSM with a right-handed tau neutrino, by assuming that above the unification scale, at which the gauge couplings meet, the gauge group is $SU(4) \otimes SU(2)_L \otimes SU(2)_R$ [12]. We will proceed in three steps. Firstly we review the model constrained by universal soft SUSY breaking masses (USBM). Secondly, the model is considered under non-USBM conditions and thirdly we will allow for the presence of D-terms which generally arise from the reduction of the gauge group rank [24]. Finally, we conclude by showing that the 422 model with non-universal

family dependent A-terms, is compatible with third family Yukawa unification (which requires a negative sign for μ) and with the experimental branch ratio for the $b \to s\gamma$ and $\tau \to \mu\gamma$ decays.

A. The model

Here we briefly summarize the parts of the model that are relevant for our analysis. For a more complete discussion see Ref. [26]. The SM fermions, together with the right-handed tau neutrino, are conveniently accommodated in the following $F^c = (\bar{4}, 1, \bar{2})$ and $F = (4, 2, 1)$ representations :

$$F^c_A = \begin{pmatrix} d^c & d^c & d^c & e^c \\ u^c & u^c & u^c & \nu^c \end{pmatrix}_A \qquad F_B = \begin{pmatrix} u & u & u & \nu \\ d & d & d & e \end{pmatrix}_B \tag{15}$$

The MSSM Higgs bosons fields are contained in $h = (1, \bar{2}, 2)$:

$$h = \begin{pmatrix} h_d^- & h_u^0 \\ h_d^0 & h_u^+ \end{pmatrix} \tag{16}$$

whereas the heavy Higgs bosons $\bar{H} = (\bar{4}, 1, \bar{2})$ and $H = (4, 1, 2)$ are denoted by :

$$\bar{H} = \begin{pmatrix} \bar{H}_d & \bar{H}_d & \bar{H}_d & \bar{H}_e \\ \bar{H}_u & \bar{H}_u & \bar{H}_u & \bar{H}_\nu \end{pmatrix} \qquad H = \begin{pmatrix} H_d & H_d & H_d & H_e \\ H_u & H_u & H_u & H_\nu \end{pmatrix}. \tag{17}$$

In addition to the Higgs fields in Eqs. (16) and (17) the model also involves an $SU(4)$ sextet field $D = (6, 1, 1) = (D_3, D_3^c)$. [5]

The superpotential of the minimal 422 model is : [6]

$$\begin{aligned} \mathcal{W} \;=\; & F^c_A \lambda_{AB} F_B h + \lambda_h S h h + \\ & \lambda_S S(\bar{H}H - M_H^2) + \lambda_H H H D + \lambda_{\bar{H}} \bar{H}\bar{H} D + F^c_A \lambda'_{AB} F^c_B \frac{HH}{M_P} \end{aligned} \tag{18}$$

[5] In fact, since we wish to keep the gauge couplings unified above M_X we also trivially include another pair of heavy Higgs boson fields in the $(4, 2, 1)$ and $(\bar{4}, \bar{2}, 1)$ representations and six more replicas of D's. This is sufficient to assure that, above the unification scale, the one loop RGEs beta functions of the gauge couplings are equal. [46]

[6] Note that FFD and F^cF^cD terms, associated with baryon number violating processes, can be forbidden by imposing a global R-symmetry. [47]

where S denotes a gauge singlet superfield, the λ's are real dimensionless parameters and $M_H \sim M_X$. Additionally, the Planck mass is denoted by $M_P \sim 2.4\times10^{18}$ GeV. As a result of the superpotential terms involving the singlet S, the Higgs fields develop VEVs $\langle H \rangle = \langle H_\nu \rangle \sim M_X$ and $\langle \bar{H} \rangle = \langle \bar{H}_\nu \rangle \sim M_X$ which lead to the symmetry breaking :

$$SU(4) \otimes SU(2)_L \otimes SU(2)_R \rightarrow SU(3)_c \otimes SU(2)_L \otimes U(1)_Y. \tag{19}$$

The singlet S itself also naturally develops a small VEV of the order of the SUSY breaking scale [47] so that the $\lambda_h S$ term in Eq. (18) gives an effective μ parameter of the correct order of magnitude. Under Eq. (19) the Higgs field h in Eq. (16) splits into the familiar MSSM doublets h_u and h_d whose neutral components subsequently develop weak scale VEVs $\langle h_u^0 \rangle = v_2$ and $\langle h_d^0 \rangle = v_1$ with $\tan\beta = v_2/v_1$. The neutrino field ν^c acquires a large mass $M_\nu \sim \lambda' \langle HH \rangle / M_P$ through the non-renormalizable term in $\mathcal{W}$ which, together with the Dirac ν^c – ν interaction (proportional to $\lambda \langle h_u^0 \rangle$), gives rise to a 2 × 2 matrix that generates, via see-saw mechanism, a suppressed mass for the left-handed neutrino state [26]. The D field does not develop a VEV but the terms HHD and $\bar{H}\bar{H}D$ combine the colour triplet parts of H, $\bar{H}$ and D into acceptable GUT scale mass terms [26].

In addition to the terms generated by the superpotential of Eq. (18) the lagrangian of the 422 model also includes the corresponding trilinear soft terms $\tilde{F}^c \tilde{A} \tilde{F} h + \tilde{\lambda}_h S h h$, [7] masses for the $SU(4)$, $SU(2)_L$, $SU(2)_R$ gauginos M_4, M_{2L}, M_{2R} and explicit soft masses for the scalar fields $\tilde{m}_F^2 |\tilde{F}|^2 + \tilde{m}_{F^c}^2 |\tilde{F}^c|^2 + \tilde{m}_h^2 |h|^2$.

Finally we remind that the symmetry breaking in Eq (19) leads to specific relations between the $SU(4)$, $SU(2)_{2R}$ and $U(1)_Y$ gauge couplings and gaugino masses at M_X

[7] Often re-parametrised by $\tilde{A} = A\lambda$ and $m_3^2 = \tilde{\lambda}_h \langle S \rangle$.

given by [48] : [8]

$$\frac{5}{\alpha_1} = \frac{2}{\alpha_4} + \frac{3}{\alpha_{2R}} \qquad\qquad \frac{5M_1}{\alpha_1} = \frac{2M_4}{\alpha_4} + \frac{3M_{2R}}{\alpha_{2R}} \tag{20}$$

B. The universal model

In this section we briefly review the 422 model with USBM. The main motivation for USBM is the smallness of flavour changing neutral currents (FCNC) and it's simplicity — few input parameters are needed to specify a otherwise complex and largely unconstrained parameter space.

The model is very similar to the one presented in the previous section except that we have imposed the high energy boundary conditions at the Planck scale instead of at M_X, thus we allowed for the running of the parameters between these two scales. The relevant input parameters were sign $\mu < 0$, $A_0 = 0$ and :

$$0 < M_{1/2} < 2 \text{ TeV} \qquad\qquad 0 < m_0 < M_{1/2} \tag{21}$$

where $M_{1/2} = M_4 = M_{2L} = M_{2R}$ is the common gaugino mass and $m_0^2 = \tilde{m}_F^2 = \tilde{m}_{F^c}^2 = \tilde{m}_h^2$ is the universal scalar mass ($\alpha_s = 0.120$, $M_b = 4.8$ GeV). The results are presented in scattered plots in Fig. 13 and Fig. 14.

In Fig. 13 we plot m_0 against $M_{1/2}$. The black (white) circles indicate points that do (not) satisfy EWSB, *i.e.* $m_1^2 - m_2^2 \gtrless M_Z^2$. [9] We observe that increasing m_0 is disfavoured by EWSB whereas increasing $M_{1/2}$ makes EWSB easier to occur. The interplay between these two dependencies dictates that only the region with $M_{1/2} \gtrsim m_0$, with a threshold for $M_{1/2} \sim 500 - 600$ GeV, is allowed. [10] The large gaugino mass (required in models with USBM and large $\tan\beta$) has important implications, it leads to a large negative m_2 parameter at low energy. Thus the EWSB condition in Eq. (6)

[8] See appendix D for a comprehensive derivation of these relations.

[9] This condition can be obtained from Eqs. (6) and (7) in the limit of large $\tan\beta$.

[10] Note that this value corresponds to the gaugino mass at the Planck scale which in our model decreases between M_P and M_X. At the GUT scale we obtained $M_{1/2} > 400$ GeV.

can only be satisfied if $|m_2^2| - \mu^2 \sim M_Z^2/2$ with $|m_2^2| \sim \mu^2 \gg M_Z^2/2$ — fine tuning $\mathcal{O}(500)$ is inevitable [20, 49]. Furthermore large values for μ, which is correlated with $M_{1/2}$, increase the SUSY correction to the bottom mass in Eq. (8) and Eq. (9) pushing the prediction for the top mass below the experimental lower bound.

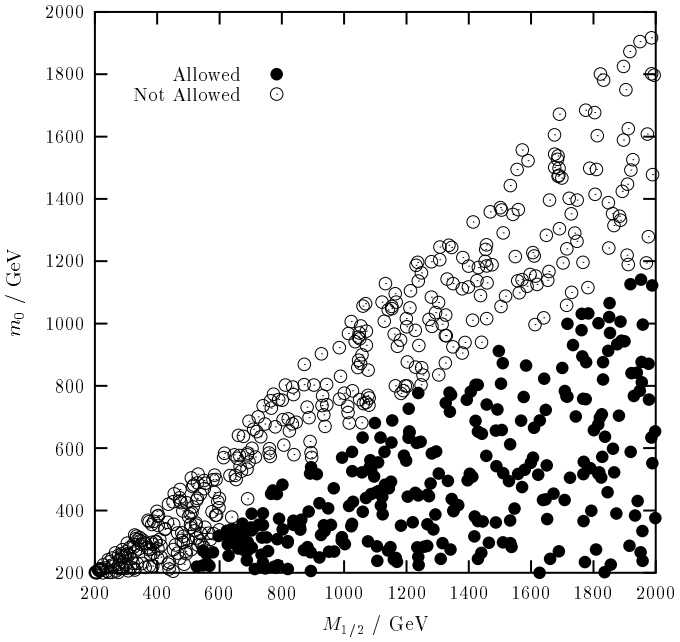

FIG. 13. Common scalar mass m_0 against unified gaugino mass $M_{1/2}$ fixed at the Planck scale. The white circles denote points that fail to satisfy the electro-weak symmetry breaking conditions.

In Fig. 14 we show the top mass prediction M_t against $M_{1/2}$. We can see that not only is M_t smaller than 170 GeV (even for $M_{1/2}$ as large as 2 TeV) but also that for fixed $M_{1/2}$ its dependence with m_0 is small. It is relevant to note that, in the attractive scenario of lowest $M_{1/2}$, corresponding to lighter sparticles and smallest fine tuning, the largest top mass prediction is unacceptable. Indeed, we found, by pushing the stability of the Higgs potential to the extreme, that for a low gaugino mass $M_{1/2} \sim 600$ GeV [11] we obtain $M_t \sim 157$ GeV ($\tan\beta = 43$). Nevertheless, the fact that in Fig. 14 the white circles are above of the blacks suggests that, if the scalar masses $\tilde{m}_F$, $\tilde{m}_{F^c}$, $\tilde{m}_h$ are allowed to increase (and/or split) and be bigger than

[11] Corresponding to $M_{1/2}(M_X) = 485$ GeV and gluino masses $m_{\tilde{g}}(M_Z) = 1145$ GeV.

$M_{1/2}$, then M_t may increase. Thus, the main problem is how to conciliate EWSB with scalar masses bigger than gaugino masses.

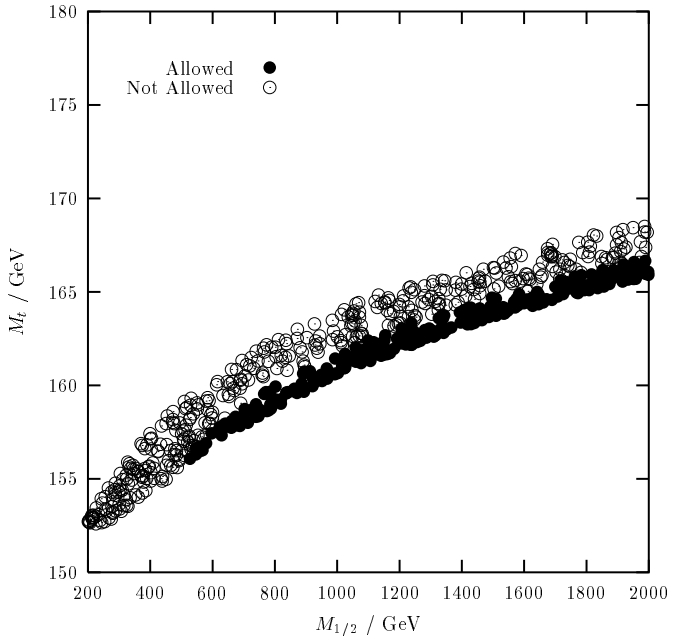

FIG. 14. Top mass prediction M_t against the common gaugino mass $M_{1/2}$ fixed at the Planck scale ($\alpha_s = 0.120$.)

C. The non-universal model

Over the past decade the numerous studies of models with USBM [14, 17, 18, 50, 51, 52, 53] at the GUT scale showed that they often face recurrent difficulties with low energy phenomenology. The unsatisfactory results have stimulated the interest in non-universal models [19, 20, 21, 48, 54, 55, 56, 57] which are well motivated from a theoretical point of view. As was emphasized in [55, 56], even when universality is imposed at the Planck scale, radiative corrections between M_P and M_X and heavy threshold effects lead to non-universal parameters at the GUT scale. Moreover, the most general SUGRA models (with non-canonical kinetic terms) in which supersymmetry is broken in a hidden sector, and/or superstring theories in which supersymmetry is broken by the F component of the moduli fields with different weights, show that non-universality can be generated at the Planck or string scale.

In this section we consider the 422 model with non-universal boundary conditions at M_P. The independent input parameters were $\tilde{m}_F^2$, $\tilde{m}_{F^c}^2$ (proportional to the unit matrix), $\tilde{m}_h^2$ and $M_4 = M_{2R} \neq M_{2L}$. [12] These parameters were made to vary at random in the ranges :

$$200 \text{ GeV} < M_4 = M_{2R} < 2 \text{ TeV} \tag{22}$$

$$\tfrac{1}{2} M_4 < M_{2L} < 2M_4 \tag{23}$$

$$200 \text{ GeV} < \tilde{m}_F \neq \tilde{m}_{F^c} \neq \tilde{m}_h < M_4. \tag{24}$$

The results are presented in Figs. 15–21 which main purpose was not to exhaustively scan all the parameter space but to be a guide of the configuration of the parameter space which most effectively increased M_t

In Fig. 15 we plot the top mass against M_4. Comparing with Fig. 14 we observe that while the average increase of M_t with M_4 is similar, the strict correlation present in the universal case is replaced, in the non-universal model, by a dispersed region of enhanced/suppressed M_t predictions. This plot also illustrates that one can expect $M_t \sim 170$ GeV (for $M_4 > 1000$ GeV) and shows that EWSB can occur under more relaxed conditions, which is obvious from the way the white and black circles distribute evenly. [13]

In Fig. 16 M_{2L} is plotted against M_4. We see that $M_{2L} > M_4$ is disfavoured by the condition on the Higgs potential to be bounded. The majority of black circles is concentrated in the $M_4 > M_{2L}$ region with $M_4 > 600$ GeV. This preference is illustrated by the left-right asymmetry around the x-axis of Fig. 17 which displays M_t against $M_4 - M_{2L}$.

[12] Note that, for the sake of simplicity, we have taken the $SU(4)$ and $SU(2)_R$ gaugino masses equal at M_P. Since their one-loop beta functions are identical, and the gauge couplings are roughly unified above M_X we also have $M_4(M_X) = M_{2R}(M_X)$.

[13] A similar graph is obtained when M_t is plotted against M_{2L} thus we spared from including it here.

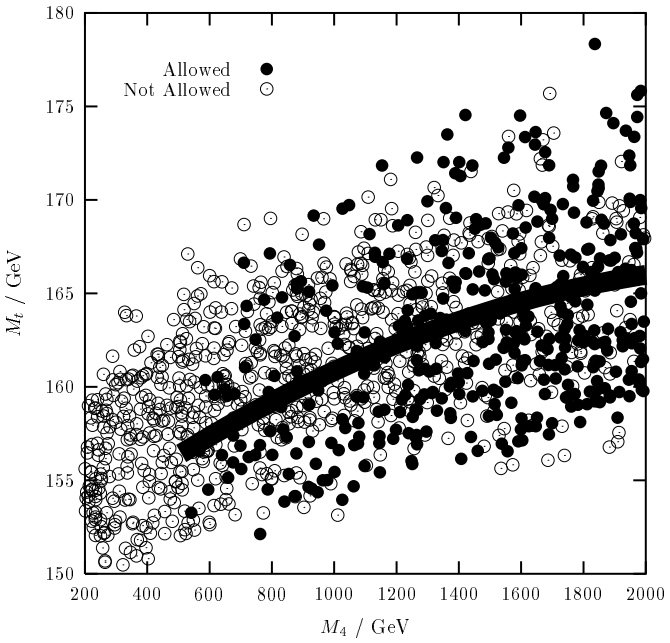

FIG. 15. Top mass prediction M_t against the $SU(4)$ gaugino mass M_4 fixed at the Planck scale in the non-universal model. The thick central line indicates the prediction for M_t in the universal model of Fig. 14 ($\alpha_s = 0.120$.)

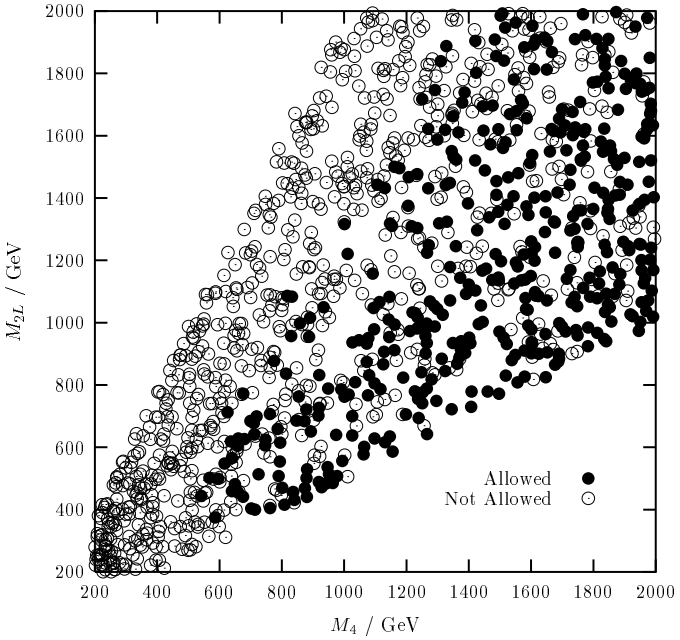

FIG. 16. The $SU(2)_L$ gaugino mass M_{2L} against the $SU(4)$ gaugino mass M_4.

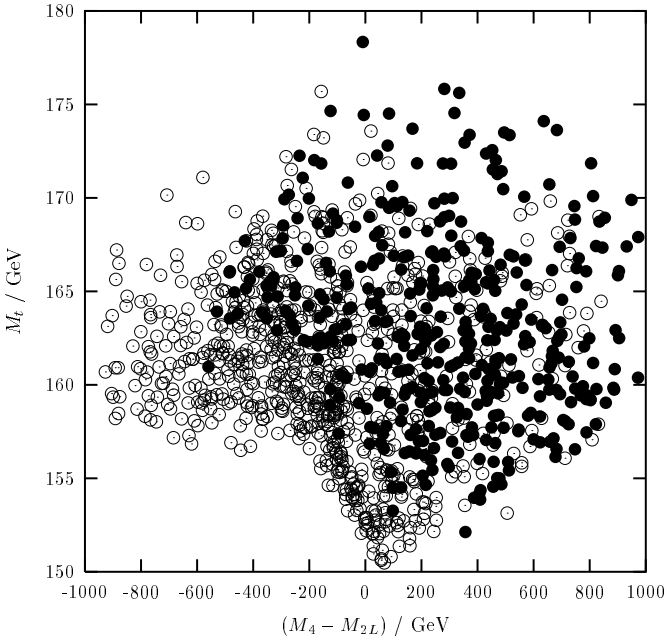

FIG. 17. Top mass prediction M_t against the difference between the $SU(4)$ and $SU(2)_L$ gaugino masses $M_4 - M_{2L}$. The stronger concentration of black circles on the right-half part of this figure indicates that EWSB favours M_4 to be bigger than M_{2L}.

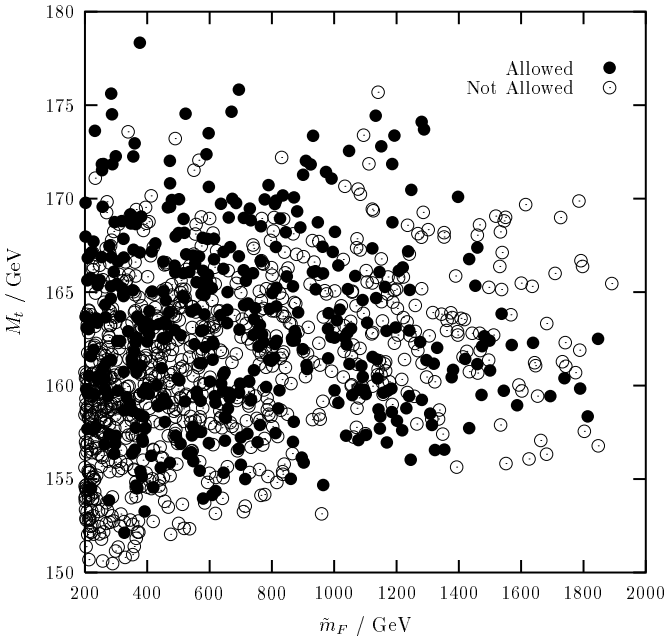

FIG. 18. The top mass prediction M_t against the left-handed SUSY scalar mass $\tilde{m}_F$. The lower $\tilde{m}_F$ the bigger the spread in M_t ($\alpha_s = 0.120$.)

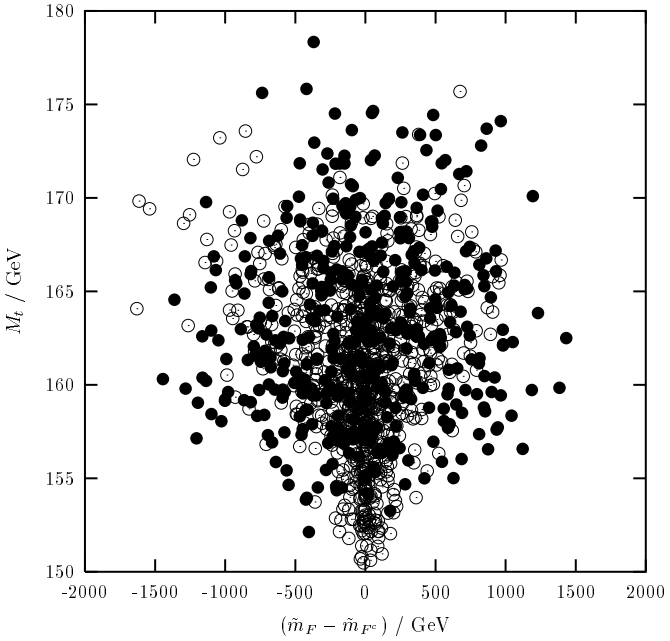

FIG. 19. Top mass prediction M_t against the difference between the left/right SUSY scalar masses $\tilde{m}_F - \tilde{m}_{F^c}$. This symmetric plot shows that the top mass does not favour an hierarchy between $\tilde{m}_F$ and $\tilde{m}_{F^c}$ ($\alpha_s = 0.120$.)

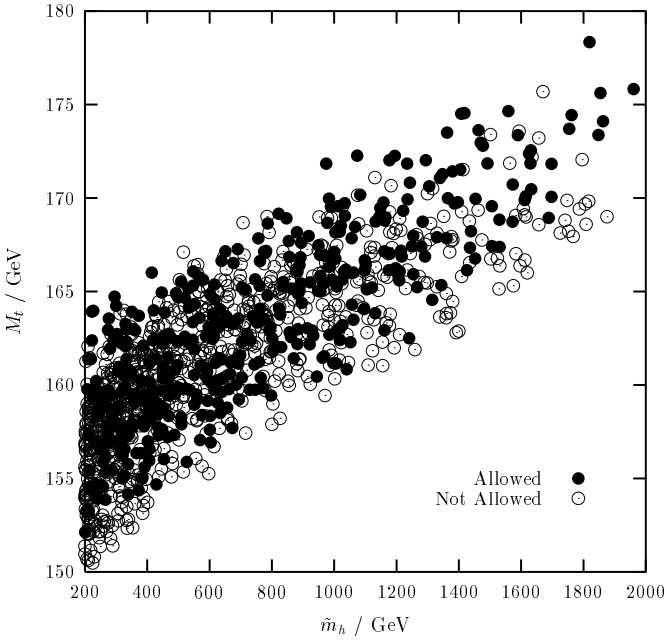

FIG. 20. Top mass prediction M_t against the soft Higgs mass $\tilde{m}_h$. We can see that a large top mass is favoured by a large Higgs parameter $\tilde{m}_h$ ($\alpha_s = 0.120$.)

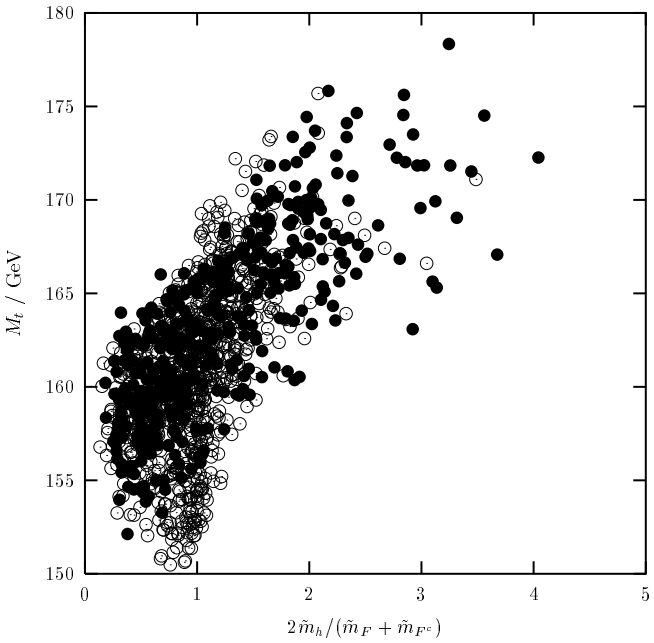

FIG. 21. Top mass prediction M_t against the ratio between the soft Higgs mass $\tilde{m}_h$ and the average of the SUSY scalar masses $\frac{1}{2}(\tilde{m}_F + \tilde{m}_{F^c})$. The bigger this ratio the bigger M_t is likely to be.

The Fig. 18 shows that, generally, as $\tilde{m}_F$ decreases M_t predictions are allowed to increase. A similar dependence of M_t on $\tilde{m}_{F^c}$ was found. Indeed, when M_t is plotted against the difference $\Delta\tilde{m}_F = \tilde{m}_F - \tilde{m}_{F^c}$ such as in Fig. 19 a symmetric left-right graph emerges around the x-axis. On the other hand, from Fig. 20 we can conclude that M_t increases with increasing soft Higgs mass $\tilde{m}_h$. These figures suggest that the top mass may be increased by increasing the splitting between the sfermions and Higgs soft mass. We therefore find interesting to plot in Fig. 21 M_t against the ratio $\tilde{m}_h/\langle\tilde{m}_F\rangle$ where $\langle\tilde{m}_F\rangle = (\tilde{m}_F + \tilde{m}_{F^c})/2$ is the average sfermion mass. Our suspictions are confirmed.

After combining the top mass dependencies on the input parameters suggested by the previous figures with numerous case-by-case analyses of "outputs" from our numerical model we arrived at the following conclusions. The top mass prediction is

strongly dependent on M_4. [14] Once M_4 is fixed, decreasing $\tilde{m}_F$ and $\tilde{m}_{F^c}$ increases both M_t and the Higgs potential stability parameter (that is positive for a "bounded-from-below" Higgs potential) : [15]

$$S^2 = \mu_2^2 + \mu_1^2 - 2|m_3^2| > 0 \tag{25}$$

However $\tilde{m}_{F,F^c}$ cannot be arbitrarily small since if $\tilde{m}_{F,F^c}$ are very small the sleptons became too light. Increasing M_{2L} and $\tilde{m}_h$ increases the top mass, however they also affect S. We found that the most efficient mechanism to increase M_t relied on decreasing M_{2L} (which decreased M_t moderately but increased S substantially) and increasing $\tilde{m}_h$ (which increased M_t significantly and decreased S moderately). For the sake of illustration, we found that, by pushing the EWSB conditions to the extreme ($S \sim 0$, *i.e.* tuning m_3), it was possible to get $M_t \sim 175$ GeV only if $M_4(M_P) \gtrsim 800$ GeV. In this case we got $M_{2L} = 500$ GeV, $\tilde{m}_F = 350$ GeV, $\tilde{m}_{F^c} = 450$ GeV and $\tilde{m}_h = 1000$ GeV. [16] Naturally, for a larger M_4 mass, S increases and an acceptable top mass is easier to obtain with less tuning in m_3.

The main conclusion is that in the 422 model with non-universal soft masses a top mass of around $M_t \sim 175$ GeV is only possible to obtain in the context of a large gluino mass $m_{\tilde{g}}(M_Z) \sim 1520$ GeV and large $\tan\beta \sim 50$, by implicitly tuning the EWSB conditions, and by choosing squark/slepton masses considerably smaller than the soft Higgs mass $\tilde{m}_F, \tilde{m}_{F^c} < \tilde{m}_h$.

[14] The reason is because, at the unification scale, the gluino masses are set to be $M_3(M_X) = M_4(M_X)$. Thus the sensitiviness of the results with M_4 is in fact a sensitiviness to the masses of the coloured sparticles.

[15] In the large $\tan\beta$ limit S^2 is given by $S^2 \sim m_1^2 - m_2^2 - M_Z^2 \sim m_3^2/\tan\beta$.

[16] The corresponding values at M_X are $M_4 = 653$ GeV, $M_{2L} = 408$ GeV, $\tilde{m}_F = 456$ GeV, $\tilde{m}_{F^c} = 567$ GeV, and $\tilde{m}_h = 972$ GeV.

D. D-term contributions

The symmetry breaking of the Pati-Salam to the SM gauge group given in Eq. (19) reduces the group rank from five to four. Although the GUT symmetry is broken at a very high energy it nevertheless has important consequences to low energy TeV phenomenology via D-term contributions to the scalar masses [21, 48, 58]. In the 422 model the GUT boundary conditions for the scalar masses are [48] : [17]

$$\tilde{m}_q^2 = \tilde{m}_F^2 + g_4^2 D^2 \tag{26}$$

$$\tilde{m}_{u^c}^2 = \tilde{m}_{F^c}^2 - (g_4^2 - 2g_{2R}^2) D^2 \tag{27}$$

$$\tilde{m}_{d^c}^2 = \tilde{m}_{F^c}^2 - (g_4^2 + 2g_{2R}^2) D^2 \tag{28}$$

$$\tilde{m}_l^2 = \tilde{m}_F^2 - 3g_4^2 D^2 \tag{29}$$

$$\tilde{m}_{e^c}^2 = \tilde{m}_{F^c}^2 + (3g_4^2 - 2g_{2R}^2) D^2 \tag{30}$$

$$\tilde{m}_\nu^2 = \tilde{m}_{F^c}^2 + (3g_4^2 + 2g_{2R}^2) D^2 \tag{31}$$

$$\tilde{m}_2^2 = \tilde{m}_h^2 - 2g_{2R}^2 D^2 \tag{32}$$

$$\tilde{m}_1^2 = \tilde{m}_h^2 + 2g_{2R}^2 D^2 \tag{33}$$

The D-term corrections, If D is sufficiently large, are important to consider because, firstly they leave an imprint in the scalar masses of the charges carried by the broken GUT generator (these charges determine the coefficients of the g^2 terms above), therefore the analysis of the sparticle spectra [58] might reveal the nature of the GUT symmetry breaking pattern; Secondly, they split the soft Higgs masses by $m_2^2 - m_1^2 \sim -4g_X^2 D^2$, which for positive D^2, makes radiative EWSB much easier to occur. Indeed, we found that once $D \gtrsim 150 - 200$ GeV then EWSB no longer requires the large gluino/squark masses characteristic of models with USBM.

[17] See appendix E for a detailed derivation of the D-terms in the 422 model. Note that in the limit of unified gauge couplings the D-terms give identical corrections to the fields in the $\underline{16}$ dimensional representation of $SO(10)$.

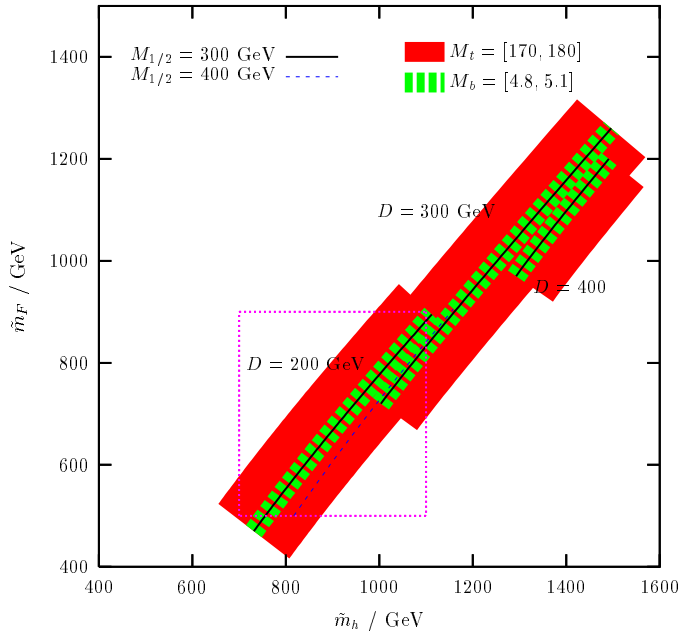

FIG. 22. Correlation between the sfermion masses $\tilde{m}_F = \tilde{m}_{F^c}$ and the Higgs soft mass $\tilde{m}_h$ required to obtain a top mass around 175 GeV ($\alpha_s = 0.120$.) Three illustrative choices for the value of the D-term are taken. The effect of experimental uncertainties in the top and bottom quark masses is indicated by the toned areas. The box around the $D = 200$ GeV label indicates the scanned region used to generate Figs. 23–31 (see main text for details.)

In Fig. 22 we summarize how an acceptable top mass prediction can be achieved in the 422 model in the $SO(10)$ limit of universal gaugino masses $M_{1/2}$ and universal squark and slepton mass parameters $\tilde{m}_F = \tilde{m}_{F^c}$ defined at the Planck scale, but with D-term corrections arising at the symmetry breaking scale. [18] The three solid lines establish the correlation between the sfermion masses $\tilde{m}_F = \tilde{m}_{F^c}$ (plotted in the y-axis) and the Higgs soft mass $\tilde{m}_h$ (plotted in the x-axis) required to obtain a top mass $M_t = 175$ GeV, for $D = 200, 300, 400$ GeV and $M_4 = M_{2R} = M_{2L} = 300$ GeV. For the $D = 200$ GeV line, EWSB failed to occur beyond the point where the line is discontinued in her way upward. [19] In all cases the lines were cut at the bottom edge at points where the left-handed stau mass became smaller than 100 GeV.

[18] Although we refer to this as the $SO(10)$ limit, in fact the two theories differ in the region between the GUT scale and the Planck scale.

[19] The $D = 300, 400$ GeV lines continue beyond the border of the figure.

The general behaviour in Fig. 22 with increasing D-term values — lines shifting to the top-right corner — results from the decrease of $\tilde{m}_L^2 \sim \tilde{m}_F^2 - 3g_X^2 D^2$ in Eq. (29) which demands an increasing $\tilde{m}_F^2$ parameter. The broader darker areas around the solid lines correspond to the uncertainty in the top mass 175 ± 5 GeV, while the thinner patches result from varying the pole bottom mass M_b in the range 4.8–5.1 GeV. We also analysed how the gaugino masses affect the solid lines. For example, for $D = 200$ GeV, taking $M_{1/2} = 400$ GeV generates the dashed line. If M_{2R} or M_{2L} are taken different from M_4 the prediction for the top mass is very similar to the one with universal gaugino masses with $M_{1/2} = M_4$.

In summary, Fig. 22 shows that if $D \gtrsim 200$ GeV then a successful prediction for M_t can be achieved, even for small gluino/squark masses — no fine tuning in EWSB conditions — as long as the soft Higgs mass $\tilde{m}_h$ is bigger than the sfermion masses $\tilde{m}_F$, $\tilde{m}_{F^c}$. As an example, setting $D = 200$ GeV and $M_{1/2} = 300$ GeV we found that $M_t \sim 175$ GeV could be obtained by fixing $\tilde{m}_F = \tilde{m}_{F^c} = 500$ GeV and $\tilde{m}_h = 750$ GeV. [20] This input lead to the following low energy predictions : $\tan\beta$=52, $\lambda_X = 0.70$ a gluino mass $m_{\tilde{g}} = 618$ GeV, a lightest neutralino mass $m_{\chi_1^0} = 88$ GeV (bino like, but with substantial higgsino component), a lightest chargino mass $m_{\chi_1^-} = 125$ GeV (higgsino like) and masses for the lightest sfermions $m_{\tilde{\nu}_\tau} = 179$ GeV, $m_{\tilde{\tau}_1} = 189$ GeV and $m_{\tilde{b}_2} = 377$ GeV. The lightest CP-even Higgs mass, computed using the one-loop expressions of Ref. [59] (that include the stop/sbottom corrections only) was found to be $m_h = 114$ GeV (note that this value should be read with some caution, we estimate an error of about 10 GeV in m_h.)

[20] The corresponding values at M_X are $M_{1/2} = 247$ GeV, $\tilde{m}_{F,F^c} = 474$ GeV and $\tilde{m}_h = 691$ GeV. After the D-term corrections the scalar masses are : $\tilde{m}_q = \tilde{m}_{u^c} = \tilde{m}_{e^c} = 496$ GeV, $\tilde{m}_l = \tilde{m}_{d^c} = 404$ GeV, $\tilde{m}_{\nu^c} = 572$ GeV (for the third family) and $m_2 = 660$ GeV, $m_1 = 720$ GeV.

In the last part of this section we present a series of figures that show in detail how an acceptable top mass prediction can be achieved and how it is correlated with the sparticle spectrum. For the sake of illustration we take, as in the previous sections $\alpha_s = 0.120$, $M_b = 4.8$ GeV and the following input at the Planck scale :

$$\begin{aligned} M_{1/2} &= 300 \text{ GeV} \qquad & D &= 200 \text{ GeV} \\ \tilde{m}_h &= 700 - 1100 \text{ GeV} \qquad & \tilde{m}_F &= \tilde{m}_{F^c} = 500, 550, .., 900 \text{ GeV} \end{aligned} \tag{34}$$

These values correspond to a scan of the $\tilde{m}_h$–$\tilde{m}_{F,F^c}$ parameter space that is indicated in Fig. 22 with a box.

In Fig. 23 we plot the pole top mass prediction M_t against $\tilde{m}_h$ for several choices of the sfermion masses $\tilde{m}_{F,F^c} = 500, 550, .., 900$ GeV. We observe that M_t increases with increasing $\tilde{m}_h$ and decreasing $\tilde{m}_{F,F^c}$. The reason for such dependence is directly related with the value of the Higgs mixing parameter μ.

In Fig. 24 we show how the top mass prediction M_t correlates with μ. In this plot each line corresponds to a fixed $\tilde{m}_{F,F^c}$ mass (labeled by the number beside it) and along it $\tilde{m}_h$ is varying in the range indicated by Eq. (34). We see that decreasing $\tilde{m}_{F,F^c}$ shifts the lines to the right of the graph thus making μ less negative. Furthermore, as $\tilde{m}_h$ increases, from the bottom to the top of the graph, $|\mu|$ decreases. These dependencies lead to a small value for μ (at the top-right corner of this graph) which in turn lead to small SUSY bottom corrections that raise the top mass prediction to an acceptable value.

In Fig. 25 we show the correlation between the top mass M_t and the gluino mass $m_{\tilde{g}}$ predictions. We see that, for the choice of $M_{1/2} = 300$ GeV in Eq. (34), if the top mass is in the 170–180 GeV range then the gluino mass is in the 605–620 GeV range. It is worth stressing that the 422 model with D-terms offers the possibility of predicting light gluinos. This is exciting from the experimental point of view and theoretically desirable since it reduces the fine-tuning in the Higgs potential parameters.

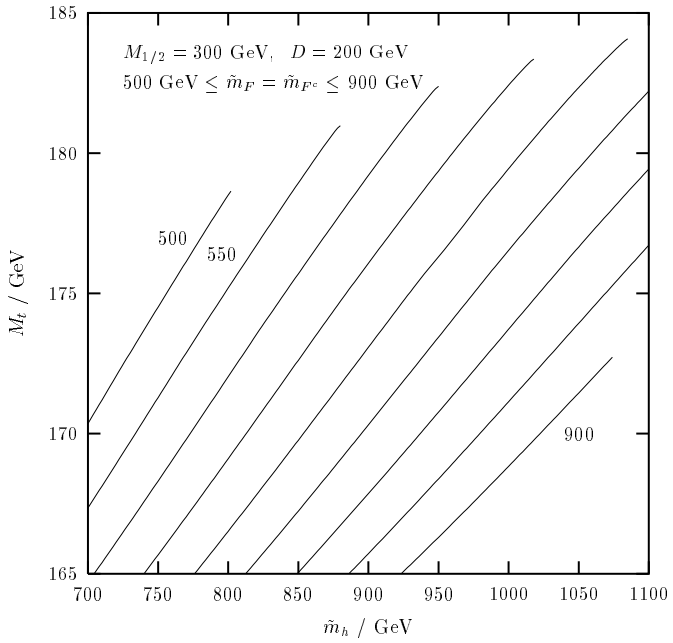

FIG. 23 Prediction for the top mass M_t against the soft mass for the unified Higgs bosons $\tilde{m}_h$ in Eq. (16). The numerical labels, for each line, indicate the value for the soft masses of the scalar fields $\tilde{m}_F = \tilde{m}_{F^c}$ used to generate the corresponding line ($\alpha_s = 0.120$.)

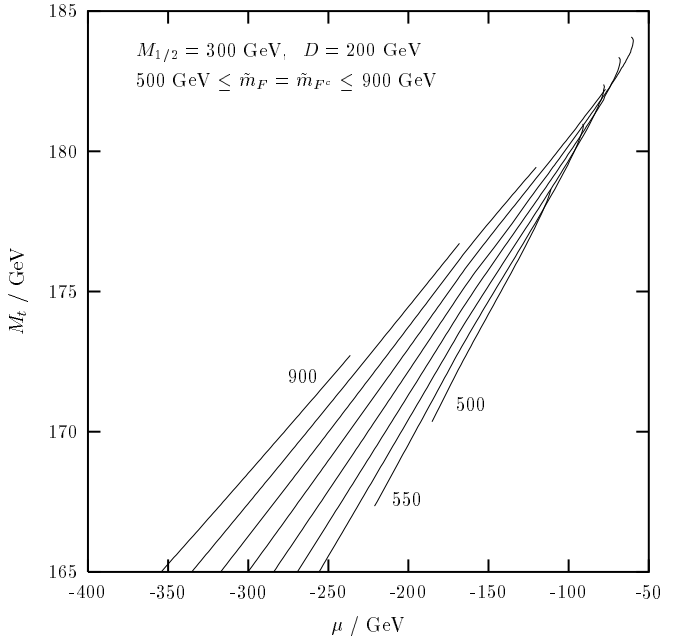

FIG. 24 Prediction for the top mass M_t against the Higgs mixing parameter μ. Each line corresponds to a fixed choice for the soft mass of the scalar fields $\tilde{m}_F = \tilde{m}_{F^c}$ and along it the soft mass for the unified Higgs bosons $\tilde{m}_h$ is varying (increasing from the bottom to the top of the plot.) We observe that M_t increases with decreasing $|\mu|$ ($\alpha_s = 0.120$.)

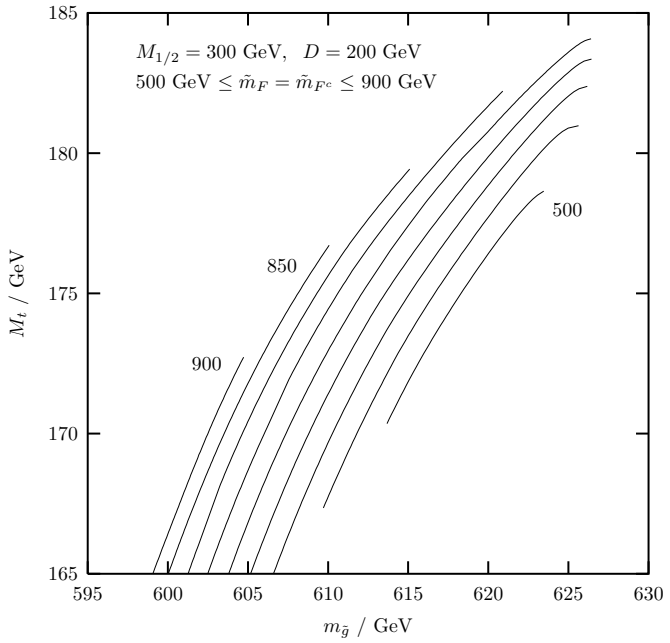

FIG. 25 Correlation between the top mass prediction M_t and the gluino mass prediction $m_{\tilde{g}}$. Each line corresponds to a fixed choice for the soft mass of the scalar fields $\tilde{m}_F = \tilde{m}_{F^c}$ (labeled with a number) and along it the soft mass for the unified Higgs bosons $\tilde{m}_h$ is varying (increasing from the bottom to the top of the plot.)

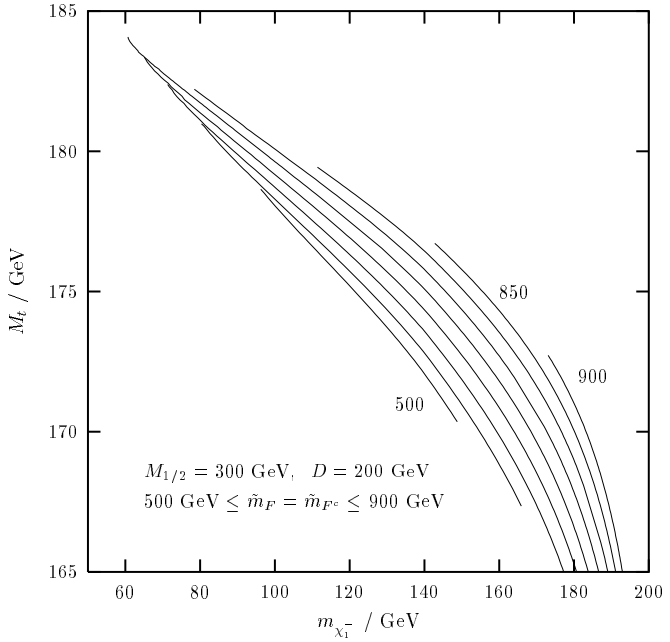

FIG. 26 Correlation between the top mass prediction M_t and the lightest chargino mass prediction $m_{\chi_1^-}$. Each line corresponds to a fixed choice for the soft mass of the scalar fields $\tilde{m}_F = \tilde{m}_{F^c}$ (labeled with a number) and along it the soft mass for the unified Higgs bosons $\tilde{m}_h$ is varying (increasing from the bottom to the top of the plot.)

In Fig. 26 we plot the top mass M_t against the lightest chargino mass $m_{\chi_1^-}$ prediction. In this model χ_1^- is roughly the charged higgsino which is lighter than the charged wino because $\mu < m_{\tilde{W}}$ at low energy. From this graph we read that 80 GeV $< m_{\chi_1^-} <$ 180 GeV which should be compared with experimental bound from LEP2 : $m_{\chi_1^-}^{exp} > 89$ GeV [32].

In Fig. 27 we show the correlation between the top mass M_t and the lightest neutralino mass $m_{\chi_1^0}$ predictions. We note that since μ can be comparable with of the bino mass, χ_1^0 can have a substantial higgsino component. From this plot we read that 60 GeV $< m_{\chi_1^0} <$ 105 GeV which should be compared with the experimental bound : $m_{\chi_1^0}^{exp} > 40$ GeV [32].

In Fig. 28 we plot M_t against the lightest charged slepton mass $m_{\tilde{\tau}_1}$ prediction. It is interesting to observe that the D-term correction to the left-handed charged sleptons in Eq. (29) is negative while for the right-handed charged sleptons in Eq. (30) it is positive. Thus the lightest stau is not right-handed ($\tilde{\tau}_2$) but left-handed ($\tilde{\tau}_1$). From this graph we see that the prediction for $m_{\tilde{\tau}_1}$ can vary significantly, roughly we find that only an upper bound can be imposed $m_{\tilde{\tau}_1} < 600$ GeV (the experimental lower bound is $m_{\tilde{\tau}_1}^{exp} > 81$ GeV. [32])

In Fig. 29 the prediction for the top mass M_t is plotted against the lightest sneutrino mass $m_{\tilde{\nu}_\tau}$. We note that for the choices of $\tilde{m}_{F,F^c} = 500, 550, 600, 650, 700$ GeV the $\tilde{\nu}_\tau$ mass is driven to zero as $\tilde{m}_h$ increases from the bottom to the top of the graph (thus, it is possible that $\tilde{\nu}_\tau$ could be the lightest SUSY particle (LSP).) Comparing this figure with Fig. 28 we see that the prediction for the $\tilde{\tau}_1$ and $\tilde{\nu}_\tau$ masses are similar. We find that the predicted upper bound for $m_{\tilde{\nu}_\tau} < 650$ GeV is compatible with the experimental lower bound $m_{\tilde{\nu}_\tau}^{exp} > 43$ GeV [32].

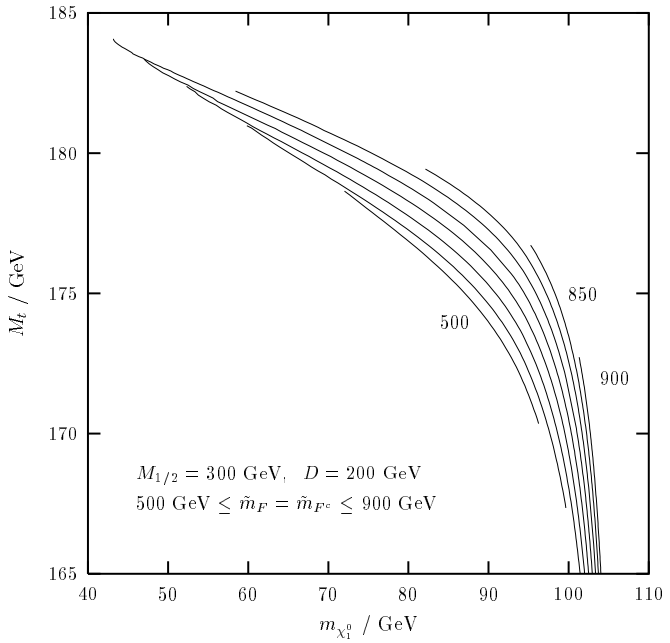

FIG. 27 Correlation between the top mass prediction M_t and the lightest neutralino mass prediction $m_{\chi_1^0}$. Each line corresponds to a fixed choice for the soft mass of the scalar fields $\tilde{m}_F = \tilde{m}_{F^c}$ (labeled with a number) and along it the soft mass for the unified Higgs bosons $\tilde{m}_h$ is varying (increasing from the bottom to the top of the plot.)

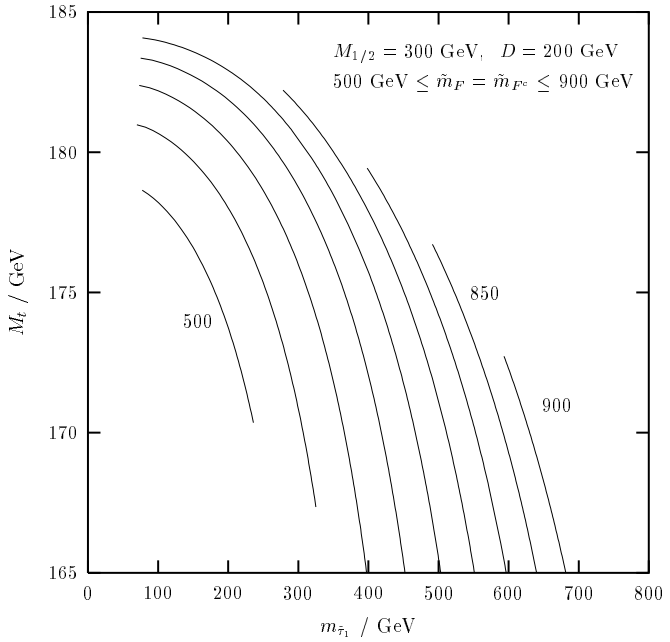

FIG. 28 Correlation between the top mass prediction M_t and the lightest charged slepton mass prediction $m_{\tilde{\tau}_1}$. Each line corresponds to a fixed choice for the soft mass of the scalar fields $\tilde{m}_F = \tilde{m}_{F^c}$ (labeled with a number) and along it the soft mass for the unified Higgs bosons $\tilde{m}_h$ is varying (increasing from the bottom to the top of the plot.)

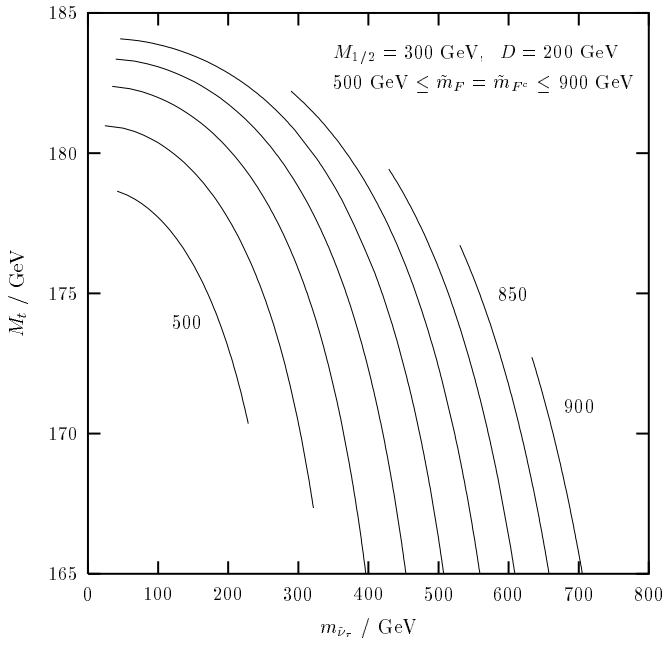

FIG. 29 Correlation between the top mass prediction M_t and the lightest sneutrino mass prediction m_{ν_3}. Each line corresponds to a fixed choice for the soft mass of the scalar fields $\tilde{m}_F = \tilde{m}_{F^c}$ (labeled with a number) and along it the soft mass for the unified Higgs bosons $\tilde{m}_h$ is varying (increasing from the bottom to the top of the plot.)

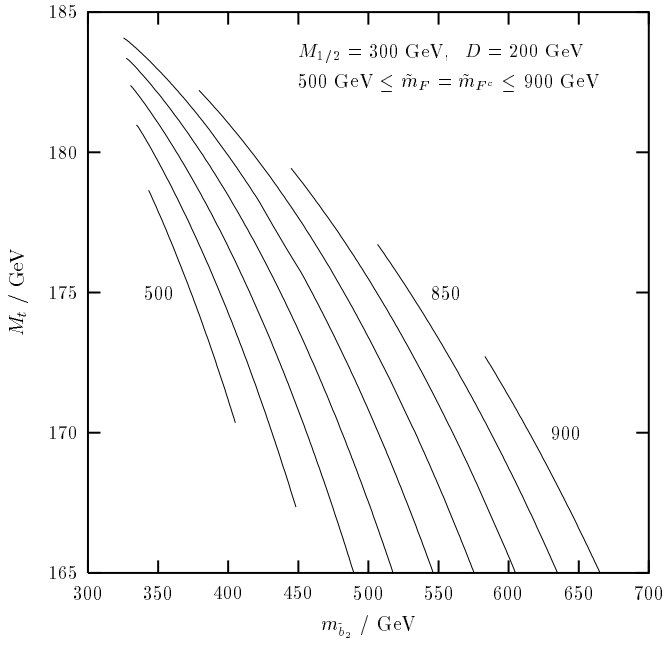

FIG. 30 Correlation between the top mass prediction M_t and the lightest sbottom mass prediction $m_{\tilde{b}_1}$. Each line corresponds to a fixed choice for the soft mass of the scalar fields $\tilde{m}_F = \tilde{m}_{F^c}$ (labeled with a number) and along it the soft mass for the unified Higgs bosons $\tilde{m}_h$ is varying (increasing from the bottom to the top of the plot.)

In Fig. 30 the top mass prediction M_t is plotted against the lightest squark mass, that is, the right-handed sbottom $\tilde{b}_2$. The reason why the right-handed down-type squarks are lighter than the other squarks is because of the negative D-term correction in Eq. (28). The prediction for $m_{\tilde{b}_2}$ is well above the experimental lower bound $m_{\tilde{b}_2}^{exp} > 75$ GeV [32].

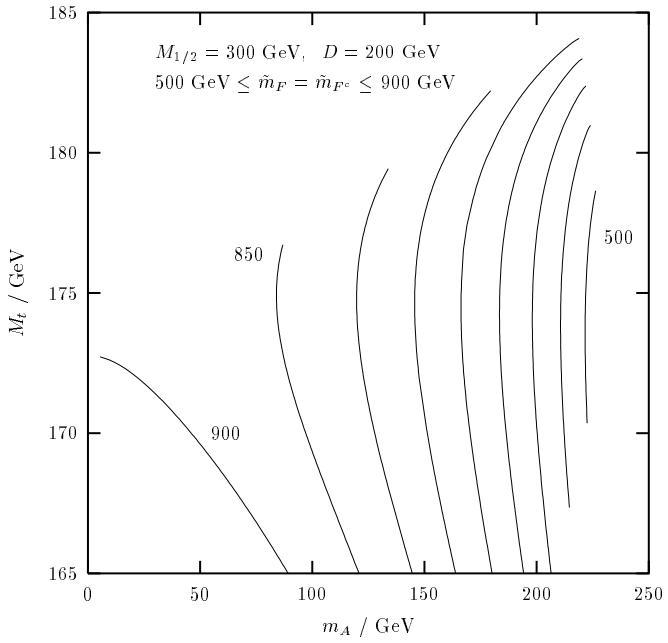

FIG. 31 Correlation between the top mass prediction M_t and the CP-odd Higgs boson mass prediction m_A. Each line corresponds to a fixed choice for the soft mass of the scalar fields $\tilde{m}_F = \tilde{m}_{F^c}$ (labeled with a number) and along it the soft mass for the unified Higgs bosons $\tilde{m}_h$ is varying (increasing from the bottom to the top of the plot.)

Finally in Fig. 31 we present the correlation between the predictions for the top mass M_t and the mass of the CP-odd Higgs boson m_A. We observe that m_A decreases for increasing $\tilde{m}_{F,F^c}$ masses. In fact, for $\tilde{m}_{F,F^c} = 900$ GeV we find that m_A is driven to zero. This graph shows that only an upper bound for the Higgs boson mass can be estimated : $m_A < 220$ GeV (the experimental lower bound is $m_A^{exp} > 84$ GeV [32].)

We would like to end this section by remarking that, as far as the top mass prediction is concerned, the results in this section are similar to the $SO(10)$ model [21, 23, 55, 57, 60, 61], since we have taken the case of universal gaugino and scalar

mass parameters, with the D-term corrections reducing to those in $SO(10)$. However we have included the neutrino Yukawa coupling in our analysis, and also the theory is different from $SO(10)$ above the GUT scale. The reason we worked in this limit was to make contact with the recent work on $SO(10)$, and to distinguish clearly the effects of D-terms from the effect of explicit non-universality. However we would like to emphasise that the results in Figs. 23-31 are not only valuable by themselves, but they also serve as a reference to which the results in section VI.C should be compared with. Generally, the non-universal 422 model with D-term corrections will lead to a set of predictions that is a combination of the results presented in sections VI.C and VI.D.

E. $b \to s\gamma$ and $\tau \to \mu\gamma$ with non-universal A-terms

It is well known that the decay $b \to s\gamma$ is a sensitive probe of new physics. In the standard model the loop diagram involving the W boson and top quark give a theoretical prediction for $\mathrm{BR}(b \to s\gamma) = (3.28 \pm 0.33) \times 10^{-4}$ [62] [21] at the next-to-leading order in QCD. This result turns out to be slightly larger than the official CLEO measurement (see first Ref. in [63]). [22] However the recent ALEPH results indicate a larger branching ratio [64]. We quote :

$$\begin{aligned} \mathrm{BR}(b \to s\gamma) &= (2.32 \pm 0.57 \pm 0.35) \times 10^{-4} \quad \text{CLEO} \\ \mathrm{BR}(b \to s\gamma) &= (3.11 \pm 0.88 \pm 0.72) \times 10^{-4} \quad \text{ALEPH} \end{aligned} \tag{35}$$

where the first error is statistical and the second is systematic. In view of the above large uncertainties we will take the conservative range :

$$1.0 \times 10^{-4} < \mathrm{BR}(b \to s\gamma) < 5.0 \times 10^{-4}. \tag{36}$$

[21] This is the value of K. Chetyrkin *et al.* in Ref. [62].

[22] Note that an updated preliminary value by CLEO has been reported : $\mathrm{BR}(b \to s\gamma) = (3.15 \pm 0.35 \pm 0.32) \times 10^{-4}$ (see second Ref. in [63].)

In supersymmetric extensions of the SM the inclusion of additional SUSY particles can spoil the above "agreement" [25]. The reason is because, generally, there is no guarantee that the sparticle contributions are small or that they conspire to cancel between themselves. Indeed, it is known that in two Higgs extensions of the SM the contribution from the charged Higgs–top quark loop $H^- t$ always interferes constructively with the SM one. Thus, the resulting branch ratio prediction is bigger and dependent on the unknown charged Higgs mass m_{H^-}. If m_{H^-} is light then the prediction for the BR($b \to s\gamma$) is larger than the experimental upper bound. On the other hand, for a heavy Higgs mass $m_{H^-} \sim 1$ TeV, agreement with Eq. (35) is still be possible.

The above situation can change drastically in SUSY models with third family Yukawa unification. The reason is because the new contributions arising from gluino-sbottom ($\tilde{g}\tilde{b}$), neutralino-sbottom ($\chi^0\tilde{b}$) and particularly from chargino-stop ($\chi^-\tilde{t}$) loops are enhanced by large large $\tan\beta \sim 40 - 50$ factors. In contrast to the charged Higgs contribution, the SUSY amplitudes can either add constructively or destructively with the $H^- t$ contribution or between themselves. In order to recover the original agreement with experiment a large part of the work in the literature [25] explores the idea of suppressing the $b \to s\gamma$ decay by canceling the $\chi^-\tilde{t}$ against the $H^- t$ amplitude (typically the gluino and neutralino amplitudes are small.) Many of these results are obtained in the context of SUGRA/GUT models with universal soft masses and trilinear terms at the Planck or GUT scale with large gaugino masses $M_{1/2} \sim 1$ TeV. Cancellation between $\chi^-\tilde{t}$ and $H^- t$ loops is possible because of two reasons, firstly the large gaugino mass leads to large stop masses thus suppressing the $\chi^-\tilde{t}$ amplitude making it comparable in magnitude to the $H^- t$ term. Secondly, the sign of μ is chosen to be positive. This means that the $\chi^-\tilde{t}$ contribution has the opposite sign of the $H^- t$ contribution thus allowing the cancellation to occur.

Clearly the above strategy is very attractive because it is based on universal soft

parameters which render it model independent. However, it fails to address two issues. Firstly a large $M_{1/2}$ leads to fine-tuning of the Z boson mass and secondly, a positive μ is in conflict with the successful prediction for the top mass in the context of GUT models with unified third family Yukawa couplings which, as we have seen, require negative μ.

In this section we explore a different solution to the enhanced $b \to s\gamma$ decay in SUSY models with $t - b - \tau$ Yukawa unification. The idea is to choose μ to be negative, for the reasons stated earlier, and to suppress $b \to s\gamma$ by allowing the trilinear soft A-terms to have a non-universal family dependent structure. We will avoid unnatural tuning of electroweak symmetry breaking by taking a low value for the gaugino masses, for example $M_{1/2} \sim 300\,(250)$ GeV at the Planck (GUT) scale. In this scheme we find that $b \to s\gamma$ is dominated by the chargino-stop loop.

The purpose of this section is to investigate the possibility of suppressing $b \to s\gamma$ by tuning the initial non-universal A-terms at the Planck scale such that, at low energy, they are cancelled by the flavour violating signals that naturally develop when the parameters of our model evolve from high to low energy by the use of RGEs. We will conclude by checking that the introduction of non-universal A-terms is also compatible with the present upper bound on $\mathrm{BR}(\tau \to \mu\gamma)$.

$b \to s\gamma$

The standard model, charged Higgs, chargino and gluino diagrams contributing to this decay are illustrated in Fig. 32.

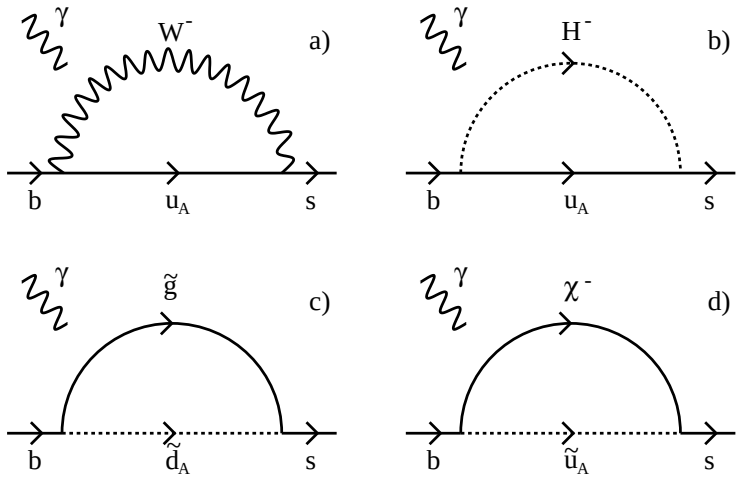

FIG. 32. Diagrams responsible for the $b \to s\gamma$ decay considered in this article (note that we did not compute the neutralino/sbottom loop which is typically found to be small.) The W boson loop a) illustrates the standard model contribution. The charged Higgs loop b) is present in two doublet Higgs extensions of the SM. The gluino contribution c) was found to be small. On the other hand, the chargino loop d) dominated the $b \to s\gamma$ decay.

In models with large $\tan\beta$ the corresponding dominant amplitudes are given by [65] :

$$A_{SM} = \frac{\alpha_w\sqrt{\alpha_e}}{4\sqrt{\pi}}\frac{1}{M_W^2}V_{ts}V_{tb}\,3x_{tw}\,F_{12}(x_{tw}) \quad (37)$$

$$A_{H^-} = \frac{\alpha_w\sqrt{\alpha_e}}{4\sqrt{\pi}}\frac{1}{M_W^2}V_{ts}V_{tb}\,x_{th}\,F_{34}(x_{th}) \quad (38)$$

$$A_{\chi^-} = \frac{\alpha_w\sqrt{\alpha_e}}{2\sqrt{\pi}}\sum_{j=1}^{2}\sum_{\alpha=1}^{6}\frac{1}{m^2_{\tilde{U}_\alpha}}H_{UL}^{j\alpha b}\left(G_{UL}^{j\alpha s}-H_{UR}^{j\alpha s}\right)\frac{m_{\chi_j^-}}{m_b}F_{43}(x_{\chi_j^-\tilde{U}_\alpha}) \quad (39)$$

$$A_{\tilde{g}} = \frac{\alpha_s\sqrt{\alpha_e}}{\sqrt{\pi}}C(R)e_D\sum_{\alpha=1}^{6}\frac{1}{m^2_{\tilde{D}_\alpha}}(V_R^{\tilde{d}d\dagger})_{b\alpha}(V_L^{\tilde{d}d})_{\alpha s}\frac{m_{\tilde{g}}}{m_b}F_4(x_{\tilde{g}\tilde{D}_\alpha}) \quad (40)$$

where $\alpha_w = g^2/(4\pi)$, $\alpha_e = e^2/(4\pi)$, M_W is the W boson mass, $m_{\tilde{U}_\alpha}$ and $m_{\tilde{D}_\alpha}$ the sup/sdown type squark mass eigenstates, V the CKM matrix, $x_{tw} = m_t^2/M_W^2$, $x_{th} = m_t^2/m_{H^-}^2$, $x_{\chi_j^-\tilde{U}_\alpha} = m^2_{\chi_j^-}/m^2_{\tilde{U}_\alpha}$, $x_{\tilde{g}\tilde{D}_\alpha} = m^2_{\tilde{g}}/m^2_{\tilde{D}_\alpha}$, $C(R) = 4/3$ and $e_D = -1/3$. The flavour matrices $V_{L,R}^{\tilde{d}d}$ describe the mismatch between the transformations that

diagonalize the down-type squark and quark mass matrices (See appendix A for details.) The functions F are defined by $F_{mn}(x) = \frac{2}{3}F_m(x) + F_n(x)$ with $F_{m,n}(x)$ as in Ref. [65]. The gaugino and higgsino vertex factors G and H are given by :

$$G_{UL}^{j\alpha A} = T_{j1}^{c}(V_L^{\tilde{u}d})_{\alpha A} \tag{41}$$

$$H_{UR}^{j\alpha A} = T_{j2}^{c}\sum_{B=1}^{3}(V_R^{\tilde{u}u})_{\alpha B}(Y_u)_{BB}V_{BA} \tag{42}$$

$$H_{UL}^{j\alpha A} = S_{2j}^{c\dagger}(Y_d)_{AA}(V_L^{\tilde{u}d\dagger})_{A\alpha} \tag{43}$$

where,

$$Y_u = \mathrm{diag}(m_u, m_c, m_t)/(\sqrt{2}M_W \sin\beta) = \lambda'_u/g \tag{44}$$

$$Y_d = \mathrm{diag}(m_d, m_s, m_b)/(\sqrt{2}M_W \cos\beta) = \lambda'_d/g. \tag{45}$$

and S^c, T^c diagonalize the chargino mass matrix. Finally the precise definition of the $V_L^{\tilde{u}d}$, $V_R^{\tilde{u}u}$ matrices that describe the mismatch between the transformations required to diagonalize the up-type squarks and quarks mass matrices can be found in appendix A.

The branch ratio $\mathrm{BR}(b \to s\gamma)$ can be computed from [65] :

$$\mathrm{BR}(b \to s\gamma) = \frac{\Gamma(b \to s\gamma)}{\Gamma(b \to ce\bar{\nu})}\mathrm{BR}(b \to ce\bar{\nu}) \tag{46}$$

where the decay rate for $b \to s\gamma$ is given by :

$$\Gamma(b \to s\gamma) = \frac{m_b^5}{16\pi}|A^\gamma(m_b)|^2. \tag{47}$$

The full expressions for $\Gamma(b \to ce\bar{\nu})$ and $A^\gamma(m_b)$ (the QCD corrected amplitude at the scale of the process ($\sim m_b$) – obtained from the total sum of amplitudes $A^\gamma(M_W) = A_{SM} + A_{H^-} + A_{\chi^-} + A_{\tilde{g}}$) can be found in Ref. [65].

It is interesting to note that the chargino amplitude has two distinct contributions. They are illustrated in Fig. 33. In Fig. 33 a) the helicity flip required in the decay is achieved at the higgsino vertex. Thus, along the internal squark line $\tilde{t}_L$–$\tilde{c}_L$, flavour

violation develops through a $(\Delta^u_{23})_{LL}$ mass insertion. [23] On the other hand, in Fig. 33 b) the two higgsino vertices require that the helicity flip must be accomplished through the $\tilde{t}_L$–$\tilde{c}_R$ line via a $(\Delta^u_{23})_{LR}$ mass insertion.

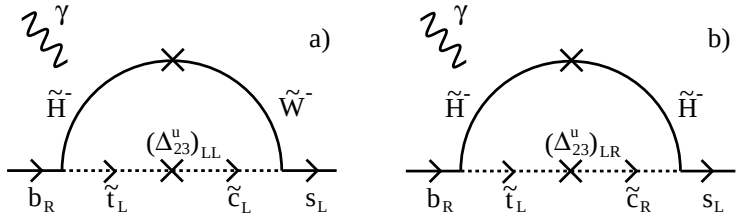

FIG. 33 Diagrams corresponding to the two contributions associated with the chargino amplitude of Eq. (39). In fig. a) flavour violation is introduced through a $(\Delta^u_{23})_{LL}$ mass insertion along the $\tilde{t}_L$–$\tilde{c}_L$ squark line. In fig. b) a $(\Delta^u_{23})_{LR}$ mass insertion is introduced along the $\tilde{t}_L$–$\tilde{c}_R$ chirality flipping squark line.

Remembering that we aim at reducing A_{χ^-} by introducing tree-level explicit sources of flavour violation through non-universal soft SUSY terms, the relevant question to address is whether it is more appropriate to relax universality of the soft mass terms for the fields in the F, F^c multiplets, thereby changing $(\Delta^u_{23})_{LL}$, or to modify the trilinear A-terms, thereby changing $(\Delta^u_{23})_{LR}$. For reasons that will became clear latter, when we study the $\tau \to \mu\gamma$ decay, we will take the latter approach.

Traditionally the SUSY trilinear terms are defined, at high energy, to be proportional to their associated Yukawa matrix, *i.e.* $(\tilde{A}_u)_{AB} = A_0(\lambda_u)_{AB}$ *etc.*. Although this assumption leads to obvious simplifications, models inspired by string theory have been proposed [67] in which the A-terms are not universal. Motivated by these results we parametrise the $\tilde{A}$'s by :

$$\begin{aligned} (\tilde{A}_u)_{AB} &= A_0 x_{AB}(\lambda_u)_{AB} \quad (\tilde{A}_d)_{AB} = A_0 x_{AB}(\lambda_d)_{AB} \\ (\tilde{A}_e)_{AB} &= A_0 x_{AB}(\lambda_e)_{AB} \quad (\tilde{A}_\nu)_{AB} = A_0 x_{AB}(\lambda_\nu)_{AB} \end{aligned} \tag{48}$$

where x_{AB} is a dimensionless matrix of order one that we conveniently choose to have

[23] The $(\Delta^u_{23})_{LL}$ parameter is the off-diagonal 23 entry of the left-handed up-type squark mass matrix in a basis where the up-type quark mass matrix is diagonal (see Ref. [66].)

the following structure :

$$x_{AB} = \begin{pmatrix} 1 & 1 & 1 \\ 1 & 1 & x \\ 1 & x & \frac{1}{10} \end{pmatrix} \tag{49}$$

We now turn to study the phenomenological implications of Eq. (49) to the BR($b \to s\gamma$). For illustrative purposes, and keeping in mind the successful prediction for the top mass in the 422 model with D-terms, we use, as in the previous section, the same $\alpha_s = 0.120$, $M_b = 4.8$ GeV and the same input at the Planck scale : $M_{1/2} = 300$ GeV, $\tilde{m}_F = \tilde{m}_{\bar{F}} = 500$ GeV, $\tilde{m}_h = 750$ GeV and $D = 200$ GeV. Moreover we fixed $A_0 = 2000$ GeV [24] and a negative sign for μ. At the GUT scale the Yukawa matrices were set as follows. The eigenvalues of λ_u, λ_d, λ_e were fixed by the requirement that the fermion masses at low energy were reproduced. The CKM mixing angles were assumed to be given by $\theta_i = \theta_i^u + \theta_i^d$ with $\theta_i^u = \theta_i^d$ (the $\theta_i^{u,d}$ are the angles that parameterise the rotation matrices that transform the left-handed up/down quarks into their physical mass basis.) The angles associated with the rotation required to transform the left handed charged leptons into their physical mass basis were given by $\theta_i^e = \theta_i^d$. Finally λ_ν was set equal to λ_u. For completeness we list in Table V the values of the Yukawa matrices at the SUSY scale $Q = M_S = 430$ GeV.

[24] $A_0(M_X) = 570$ GeV

TABLE V.

$$\lambda_u = \begin{pmatrix} 1.003 \times 10^{-5} & 1.118 \times 10^{-6} & 1.768 \times 10^{-8} \\ -3.608 \times 10^{-4} & 3.236 \times 10^{-3} & 7.012 \times 10^{-5} \\ 5.882 \times 10^{-4} & -1.973 \times 10^{-2} & 0.914 \end{pmatrix}$$

$$\lambda_d = \begin{pmatrix} 1.075 \times 10^{-3} & 1.213 \times 10^{-4} & 3.251 \times 10^{-6} \\ 2.384 \times 10^{-3} & 2.111 \times 10^{-2} & -4.461 \times 10^{-4} \\ -5.686 \times 10^{-4} & 1.910 \times 10^{-2} & 0.872 \end{pmatrix}$$

$$\lambda_e = \begin{pmatrix} 1.464 \times 10^{-4} & -1.637 \times 10^{-5} & 7.297 \times 10^{-7} \\ 3.436 \times 10^{-3} & 3.084 \times 10^{-2} & -6.077 \times 10^{-4} \\ 7.465 \times 10^{-4} & 9.409 \times 10^{-3} & 0.532 \end{pmatrix}$$

$$\lambda_\nu = \begin{pmatrix} 4.406 \times 10^{-6} & 4.908 \times 10^{-7} & 8.300 \times 10^{-9} \\ -1.585 \times 10^{-4} & 1.421 \times 10^{-3} & 3.539 \times 10^{-5} \\ 2.519 \times 10^{-4} & -1.141 \times 10^{-2} & 0.575 \end{pmatrix}$$

TABLE V. Values of the Yukawa matrices at the effective SUSY scale $Q = M_S = 430$ GeV. The correct quark and charged lepton masses as well as the CKM matrix are obtained after "running-down" these matrices firstly, from $Q = M_S$ to $Q = M_Z$, using the SM RGEs, and secondly from $Q = M_Z$ to $Q = 1$ GeV, using $SU(3)_c \times U(1)_{em}$ RGEs. (See section II.B for more details.)

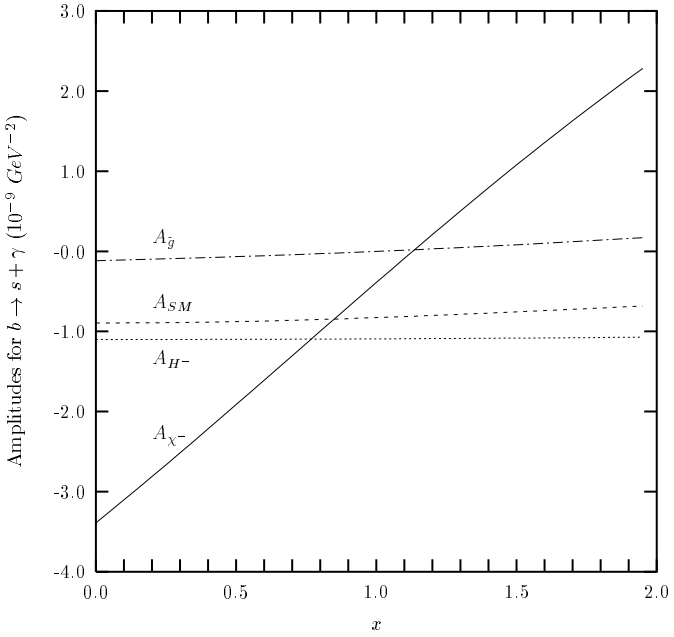

FIG. 34 Individual values for the amplitudes contributing to the $b \to s\gamma$ decay against the trilinear parameter x of Eq. (49). One observes that the chargino amplitude A_{χ^-} is sensitive to x and bigger than A_{SM}, A_{H^-} and $A_{\tilde{g}}$ for almost all the x values. Furthermore, the sign of A_{χ^-} changes as x increases from 0.0 to 2.0.

In Fig. 34 we plot the SM, charged Higgs, chargino and gluino amplitudes in Eqs. (37)–(40) against x. For $x \sim 0$ we approximately recover the usual universal A-term model. This is because the first and second family of the trilinear terms are small (due to small Yukawa entries) and the third family A-terms at low energy are not too sensitive to their initial value at high energy. We see that because μ is negative, the chargino amplitude is negative and interferes constructively with the other amplitudes. However, as x increases, the chargino amplitude becomes less negative and the magnitude of $|A_{\chi^-}|$ steadily decreases. At some point, around $x \sim 1.1$ the chargino amplitude vanishes. Beyond $x \sim 1.1$, A_{χ^-} is positive, thus it interferes destructively with the SM and Higgs amplitudes. Clearly, we see that by tuning x it is easy to find a region where $b \to s\gamma$ is suppressed.

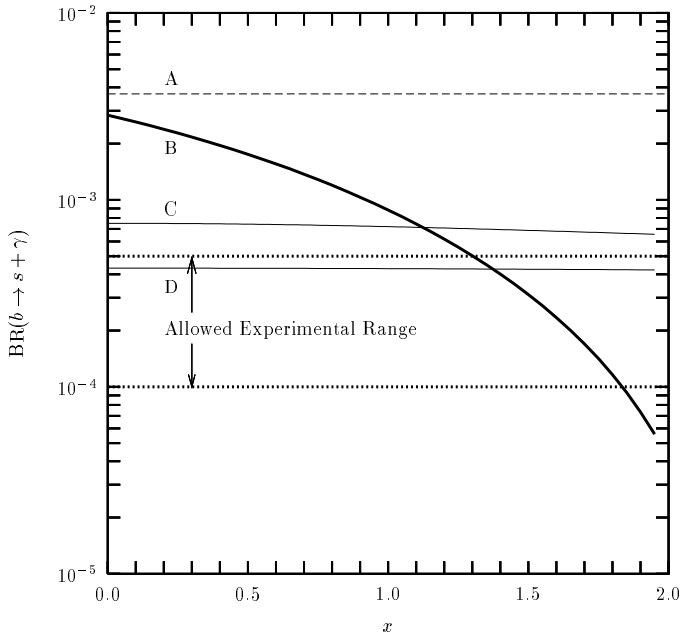

FIG. 35 Branch ratio for the $b \to s\gamma$ decay against the trilinear parameter x in Eq. (49). The dashed line A corresponds to the result one obtains when $A_0 = 0$. The solid line B was computed using the SM, charged Higgs, gluino and higgsino contributions. For the line C we used the SM and Higgs contributions only. The line D was obtained using the SM amplitude alone. The allowed experimental range is indicated by the area between the two dotted lines. We observe that for the line B an acceptable prediction is obtained for $x \sim 1.60$.

In Fig. 35 we show the BR($b \to s\gamma$) against x. The area between the dashed lines indicates the experimental allowed range in Eq. (36). The dashed line A corresponds to the result one obtains when $A_0 = 0$. The solid lines D and C are plotted for illustrative purposes; they correspond to the BR($b \to s\gamma$) that is obtained when only the SM amplitude, and the SM plus the charged Higgs amplitudes are considered respectively. The solid line B indicates the BR($b \to s\gamma$) prediction when all the amplitudes in Eqs. (37)-(40) are considered. We observe that, due to a light charged Higgs mass $m_H^- \sim 130$ GeV, the value of the BR($b \to s\gamma$) when only the SM+H^-t loops are considered lies above the experimental range. On the other hand, the BR($b \to s\gamma$) when the chargino contribution is included (line B) starts at $x \sim 0$ very large but is driven into compatibility with experiment at around $x \sim 1.60 \pm 0.15$.

$$\tau \to \mu\gamma$$

In the previous section we showed that the parameterization of the trilinear terms by Eq. (49) lead to a suppressed BR($b \to s\gamma$) compatible with the experimental data. However, one should be careful about other possible implications derived from this new source of flavour violation. Clearly Eq. (49) also introduces lepton flavour violating signals through the $\tilde{A}_{e,\nu}$ matrices in Eq. (48). The purpose of this section is to check that the decay $\tau \to \mu\gamma$ (for the successful value of x fixed by $b \to s\gamma$) is not in conflict with the experimental upper bound on BR($\tau \to \mu\gamma$) $< 3.0 \times 10^{-6}$ [68].

The effective lagrangian for the $\tau \to \mu\gamma$ decay is :

$$\mathcal{L}_{\tau\to\mu\gamma} = \tfrac{1}{2}\bar{\psi}_\mu(p-q)\left(A^R P_R + A^L P_L\right)\sigma^{\alpha\beta}\psi_\tau(p)F_{\alpha\beta} \tag{50}$$

where $P_{R,L}$ are projection operators and $F_{\alpha\beta}$ the electromagnetic field tensor. The branch ratio can be computed using :

$$\mathrm{BR}(\tau \to \mu\gamma) = \frac{12\pi^2}{G_F^2}\left(|A^R|^2 + |A^L|^2\right) \tag{51}$$

where $A^R = A^R_{\chi^-} + A^R_{\chi^0}$ and $A^L = A^L_{\chi^0}$. Numerically we found that the decay is dominated by the chargino-sneutrino loop diagram illustrated in Fig. 36.

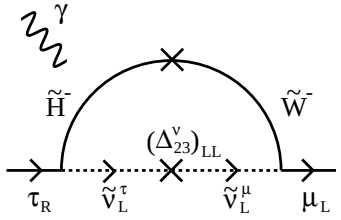

FIG. 36 Chargino diagram involved in the $\tau \to \mu\gamma$ decay (the neutralino diagram was found to be subdominant.) In this process lepton flavour violation develops through the $(\Delta^\nu_{23})_{LL}$ mass insertion along the $\tilde{\nu}^\tau_L$–$\tilde{\nu}^\mu_L$ sneutrino line.

The corresponding amplitude is given by :

$$A^R_{\chi^-} = \frac{\alpha_w\sqrt{\alpha_e}}{2\sqrt{\pi}}\sum_{j=1}^{2}\sum_{\alpha=1}^{3}\frac{1}{m^2_{\tilde{\nu}_\alpha}}H^{j\alpha\tau}_{\nu L}G^{j\alpha\mu}_{\nu L}\frac{m_{\chi^-_j}}{m_\tau}J(x_{\chi^-_j\tilde{\nu}_\alpha}) \tag{52}$$

where $m_{\tilde{\nu}_\alpha}$ is the physical mass of the sneutrinos, $x_{\chi_j^- \tilde{\nu}_\alpha} = m^2_{\chi_j^-}/m^2_{\tilde{\nu}_\alpha}$ and J a dimensionless function. [25] The gaugino and higgsino vertex factors are given by :

$$\begin{aligned} G_{\nu L}^{j\alpha A} &= T^c_{j1}(V_{LL}^{\tilde{\nu}e})_{\alpha A} \\ H_{\nu L}^{j\alpha A} &= S^{c\dagger}_{2j}(Y_e)_{AA}(V_{LL}^{\tilde{\nu}e\dagger})_{A\alpha} \end{aligned} \tag{53}$$

where $Y_e = \mathrm{diag}(m_e, m_\mu, m_\tau)/(\sqrt{2}M_W \cos\beta) = \lambda'_e/g$. Finally the sneutrino/charged lepton flavour matrix is defined by $V_L^{\tilde{\nu}e} = S_{LL}^{\tilde{\nu}} T^{e\dagger}$ where $S_{LL}^{\tilde{\nu}}$ diagonalizes the sneutrino mass matrix and T^e is the matrix that rotates the left-handed charged leptons into their physical mass eigenstates (see appendix A for details.)

We see from Fig. 36 that the τ decay develops through the sneutrino $\tilde{\nu}_L^\tau$–$\tilde{\nu}_L^\mu$ scalar line via the $(\Delta^\nu_{23})_{LL}$ mass insertion. Comparing the bottom with the tau decay, we note that while in the former decay the presence of right-handed up-type squarks allows the diagram in Fig. 33 b) to exist, in the latter decay, the corresponding lepton analogue of such diagram does not exist since the effective low energy theory does not include right-handed sneutrinos ($\tilde{\nu}_R$).

We can now justify why we preferred to consider non-universal A-terms rather than non-universal soft SUSY masses. If we had chosen to introduce non-universal soft squark masses then unification of quarks and leptons in the F and F^c multiplets would demand similar non-universal slepton masses. In this scenario it would be difficult to simultaneously suppress $b \to s + \gamma$ and keep $\mathrm{BR}(\tau \to \mu\gamma)$ below the experimental bound. The reason is because both decays can proceed via a $(\Delta_{23})_{LL}$ mass insertion. In contrast, when non-universal A-terms are introduced, we can control $b \to s\gamma$ via the $(\Delta^u_{23})_{LR}$ insertion, while leaving the prediction for $\mathrm{BR}(\tau \to \mu\gamma)$ approximately unchanged because the leptonic decay proceeds via the $(\Delta^\nu_{23})_{LL}$ insertion.

[25] Explicitly, $J(x) = [x^2 - 4x + 3 + 2\ln(x)]/[2(x-1)^3]$.

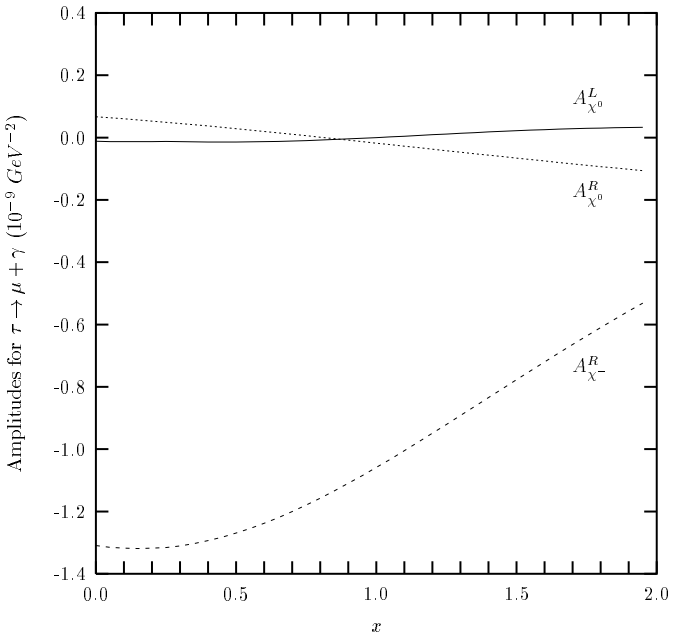

FIG. 37 Values for the chargino A^R_χ and neutralino amplitudes $A^{L,R}_{\chi^0}$ contributing to the $\tau \to \mu\gamma$ decay against the trilinear parameter x in Eq. (49). We observe that $A^{L,R}_{\chi^0}$ are small compared with A^R_χ. Moreover, the magnitude of A^R_χ slowly decreases as x increases.

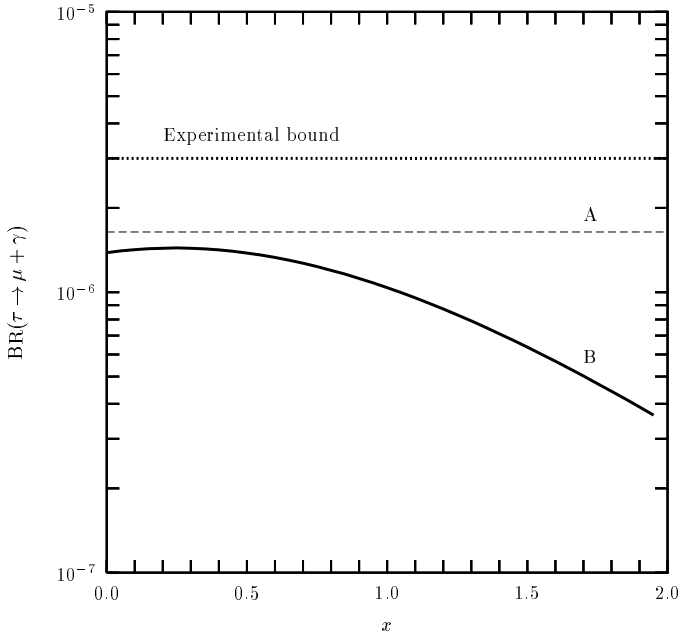

FIG. 38 Branch ratio for the $\tau \to \mu\gamma$ decay against the trilinear parameter x in Eq. (49). The dashed line A corresponds to the result when $A_0 = 0$. We observe that the solid line B is driven to smaller values as x increases. In fact, for large $x \sim 2.0$, the predicted branch ratio is roughly one order of magnitude smaller than the present experimental bound (here indicated by the dotted line.)

In Fig. 37 and Fig. 38 we show how the amplitudes and the branch ratio of the $\tau \to \mu\gamma$ decay depend on the trilinear parameter x in Eq. (49). We see that, for $x \sim 0$, the prediction for the tau decay is close to the experimental limit $\mathrm{BR}(\tau \to \mu\gamma) < 3.0 \times 10^{-6}$. However as x increases the magnitude of the chargino amplitude $|A_{\chi^-}|$ slowly decreases thus driving the prediction for $\mathrm{BR}(\tau \to \mu\gamma)$ to smaller values. For $x \sim 1.60$ the predicted $\mathrm{BR}(\tau \to \mu\gamma)$ is about one order of magnitude below the experimental upper bound.

In summary, we have verified that by introducing non-universal A-terms one can simultaneously satisfy the present experimental constraints on $b \to s\gamma$ and $\tau \to \mu\gamma$ even when μ is negative.

Finally we point that the success in suppressing the $b \to s\gamma$ decay is not without some tuning. Indeed we found that the suppression works well only for a restricted range of $x \sim 1.60 \pm 0.15$. Thus taking as a measure of tuning x the ratio $\delta = \delta x/x$ we find $\delta \sim 19$ %. Nevertheless, it is unclear if it is more natural to expect $b \to s\gamma$ to be suppressed by flavour physics, implying tuning in the flavour parameters, or by suppressing the charged Higgs and chargino amplitudes by demanding large m_{H^-} and stop masses, implying tuning in setting M_Z.

VII. CONCLUSION

We have studied Yukawa unification, including the effects of a physical neutrino mass consistent with the Superkamiokande observations. We began our study by reviewing the usual mSUGRA scenario with universal soft mass parameters, but including the effect of the neutrino Yukawa coupling. Assuming hierarchical neutrino masses, and mixing angles arising mainly from the neutrino sector (so that the charged lepton Yukawa matrix has no large off-diagonal entries) we saw that the usual predictions are not much affected. [26] For example the usual result that positive μ is not allowed, and negative μ leads to top quark masses which are too small is still valid.

We then analysed a string/D-brane inspired $SU(4)\otimes SU(2)_L\otimes SU(2)_R$ model since this allows the most general non-universal scalar and gaugino masses, and is therefore the perfect laboratory for studying the effects of non-universality. We explored the sensitivity of the predictions to variations in all these non-universal soft masses, and showed that the usual results can change considerably as a function of the degree of non-universality of the soft parameters. We then switched on the usual D-term contributions which arise in $SO(10)$, and which by themselves are enough to allow successful electroweak symmetry breaking, and permit small corrections to the b-quark mass which implies an acceptable large top quark mass. We studied the effect of the D-terms in the $SU(4)\otimes SU(2)_L\otimes SU(2)_R$ model, for the sake of clarity working in the (approximate) $SO(10)$ limit of the model, in order to distinguish clearly the effect of the D-terms from that of explicit non-universality. Including D-terms as the only source of non-universality, we studied the sparticle spectrum in some detail, although these results should be considered in conjunction with the effect of the explicit non-universal scalar masses and non-universal gaugino masses considered previously, since in a realistic $SU(4)\otimes SU(2)_L\otimes SU(2)_R$ model both effects will simulaneously be

[26] Large off-diagonal entries in the neutrino Yukawa matrix will not affect our results very much since the right-handed neutrinos decouple from the right-hand sides of the RGEs at high energy.

present.

We then turned to rare decays such as $b \to s\gamma$ and $\tau \to \mu\gamma$ which severely constrain Yukawa unification. Assuming that the only source of non-universality is due to D-terms, we showed how non-universal trilinear parameters can lead to cancellations of the important effects and so provide information about the family-dependent supersymmetry breaking soft Lagrangian. Again, the effect of more general non-universal scalar masses and non-universal gaugino masses associated with the $SU(4)\otimes SU(2)_L\otimes SU(2)_R$ model will modify the results, but the main message remains clear: family-dependent non-universality will play an important role in $b \to s\gamma$, and such effects should be considered in conjunction with the effects of family-independent non-universality. We have shown that successful Yukawa unification can be achieved if both types of non-universality are simultaneously present.

In summary Yukawa unification is well motivated from both a theoretical point of view, and from the point of view of predicting large $\tan\beta$ which helps to raise the Higgs mass. We have found that Yukawa unification is perfectly viable providing the soft masses are non-universal in both family-independent and family-dependent ways, and we have explored the specific correlations between the soft parameters required in order to satisfy all the constraints simultaneously. In our view the sensitivity of Yukawa unification to soft SUSY breaking parameters is to be welcomed, since it provides a window into the soft supersymmetry breaking Lagrangian.

ACKNOWLEDGMENTS

The work of M.O. was supported by JNICT under contract grant : PRAXIS XXI/BD/5536/95.

APPENDIX A
Notation and Conventions

In this appendix we briefly summarize our conventions and explain in detail the notation concerning the diagonalization of the mass matrices. The superpotential of the MSSM+ν^c model is given by :

$$\begin{aligned}\mathcal{W} = \epsilon_{\alpha\beta}(\quad & u^c_A(\lambda_u)_{AB} q^\alpha_B h^\beta_u - d^c_A(\lambda_d)_{AB} q^\alpha_B h^\beta_d \\ & + \nu^c_A(\lambda_\nu)_{AB} l^\alpha_B h^\beta_u - e^c_A(\lambda_e)_{AB} l^\alpha_B h^\beta_d + \mu h^\alpha_u h^\beta_d) + \tfrac{1}{2}(M_\nu)_{AB}\nu^c_A\nu^c_B \end{aligned} \tag{54}$$

where $\epsilon_{12} = -\epsilon_{21} = 1$, $A, B = 1, .., 3$ are flavour indices and $\alpha, \beta = 1, 2$ are $SU(2)_L$ indices. The Yukawa matrices are diagonalized by the following transformations :

$$S^u \lambda_u T^{u\dagger} = \lambda'_u \quad S^d \lambda_d T^{d\dagger} = \lambda'_d \quad S^e \lambda_e T^{e\dagger} = \lambda'_e \quad S^\nu \lambda_\nu T^{\nu\dagger} = \lambda'_\nu \tag{55}$$

where the primed λ's are diagonal. In this notation the CKM matrix is given by $V = T^u T^{d\dagger}$. The full lagrangian of the model also includes trilinear, soft scalar masses and gaugino masses given by :

$$\begin{aligned}\mathcal{V} = \epsilon_{\alpha\beta}(\quad & \tilde{u}^c_A(\tilde{A}_u)_{AB}\tilde{q}^\alpha_B h^\beta_u - \tilde{d}^c_A(\tilde{A}_d)_{AB}\tilde{q}^\alpha_B h^\beta_d \\ & + \tilde{\nu}^c_A(\tilde{A}_\nu)_{AB}\tilde{l}^\alpha_B h^\beta_u - \tilde{e}^c_A(\tilde{A}_e)_{AB}\tilde{l}^\alpha_B h^\beta_d + m_3 h^\alpha_u h^\beta_d) + \text{h.c.} \end{aligned} \tag{56}$$

$$\begin{aligned}\mathcal{L} = & \tfrac{1}{2}(m_2^2|h_u|^2 + m_1^2|h_d|^2 + \tilde{q}^*_A(\tilde{m}^2_q)_{AB}\tilde{q}_B + \tilde{l}^*_A(\tilde{m}^2_l)_{AB}\tilde{l}_B + \\ & \tilde{u}^c_A(\tilde{m}^2_{u^c})_{AB}\tilde{u}^{c*}_B + \tilde{d}^c_A(\tilde{m}^2_{d^c})_{AB}\tilde{d}^{c*}_B + \tilde{e}^c_A(\tilde{m}^2_{e^c})_{AB}\tilde{e}^{c*}_B + \tilde{\nu}^c_A(\tilde{m}^2_{\nu^c})_{AB}\tilde{\nu}^{c*}_B) + \text{h.c.} \end{aligned} \tag{57}$$

$$\mathcal{L} = \tfrac{1}{2}M_1\lambda_1\lambda_1 + \tfrac{1}{2}M_2\lambda^a_2\lambda^a_2 + \tfrac{1}{2}M_3\lambda^m_3\lambda^m_3 + \text{h.c.} \tag{58}$$

The chargino and neutralino mass matrices can be conveniently written in the basis of the following 4-component gaugino and higgsino fields : [27]

$$\tilde{W}^- = \begin{pmatrix} -i\lambda^- \\ i\bar{\lambda}^+ \end{pmatrix} \quad \tilde{H}^- = \begin{pmatrix} \tilde{H}^2_d \\ i\bar{\tilde{H}}^1_u \end{pmatrix} \tag{59}$$

[27] $\lambda^\pm = (\lambda^1_2 \mp i\lambda^2_2)/\sqrt{2}$

$$\tilde{B} = \begin{pmatrix} -i\lambda_1 \\ i\bar{\lambda}_1 \end{pmatrix} \quad \tilde{W}^0 = \begin{pmatrix} -i\lambda_2^3 \\ i\bar{\lambda}_2^3 \end{pmatrix} \quad \tilde{H}_d^0 = \begin{pmatrix} \tilde{H}_d^1 \\ \bar{\tilde{H}}_d^1 \end{pmatrix} \quad \tilde{H}_u^0 = \begin{pmatrix} \tilde{H}_u^2 \\ \bar{\tilde{H}}_u^2 \end{pmatrix}. \tag{60}$$

Thus,

$$\mathcal{L} = -\left(\bar{\tilde{W}}_L^- \; \bar{\tilde{H}}_L^-\right) \begin{pmatrix} M_2 & \sqrt{2}M_W s_\beta \\ \sqrt{2}M_W c_\beta & \mu \end{pmatrix} \begin{pmatrix} \tilde{W}_R^- \\ \tilde{H}_R^- \end{pmatrix} + \text{h.c.} \tag{61}$$

and,

$$\mathcal{L} = -\frac{1}{2}\left(\bar{\tilde{B}}\, \bar{\tilde{W}}^0 \; \bar{\tilde{H}}_d^1 \, \bar{\tilde{H}}_u^2\right) \begin{pmatrix} M_1 & 0 & -M_Z c_\beta s_\theta & M_Z s_\beta s_\theta \\ 0 & M_2 & M_Z c_\beta c_\theta & -M_Z s_\beta c_\theta \\ -M_Z c_\beta s_\theta & M_Z c_\beta c_\theta & 0 & -\mu \\ M_Z s_\beta s_\theta & -M_Z s_\beta c_\theta & -\mu & 0 \end{pmatrix} \begin{pmatrix} \tilde{B} \\ \tilde{W}^0 \\ \tilde{H}_d^1 \\ \tilde{H}_u^2 \end{pmatrix} \tag{62}$$

where $s_\beta = \sin\beta$, $c_\beta = \cos\beta$ ($\tan\beta = v_2/v_1 =$ the ratio of the up/down Higgs VEVs) and θ the weak mixing angle. The chargino mass matrix M^C in Eq. (61) and the neutralino matrix M^N in Eq. (62) are diagonalized by :

$$S^C M^C T^{C\dagger} = \text{Diag}(m_{\chi_1^-}, m_{\chi_2^-}) \tag{63}$$

$$S^N M^N S^{N\dagger} = \text{Diag}(m_{\chi_1^0}, m_{\chi_2^0}, m_{\chi_3^0}, m_{\chi_4^0}) \tag{64}$$

The mass matrices for the charged scalar sparticles are written in the following basis :

$$\begin{pmatrix} \tilde{u}_L \\ \tilde{u}_R \end{pmatrix} = \begin{pmatrix} \tilde{u} \\ \tilde{u}^{c*} \end{pmatrix} \qquad \begin{pmatrix} \tilde{d}_L \\ \tilde{d}_R \end{pmatrix} = \begin{pmatrix} \tilde{d} \\ \tilde{d}^{c*} \end{pmatrix} \qquad \begin{pmatrix} \tilde{e}_L \\ \tilde{e}_R \end{pmatrix} = \begin{pmatrix} \tilde{e} \\ \tilde{e}^{c*} \end{pmatrix} \tag{65}$$

Explicitly we find :

$$\left(\tilde{u}_L^\dagger \; \tilde{u}_R^\dagger\right) \begin{pmatrix} \tilde{m}_q^2 + m_u^\dagger m_u + M_Z^2 Z_u c_{2\beta} & -\mu\lambda_u^\dagger v_1 + \tilde{A}_u^\dagger v_2 \\ -\mu\lambda_u v_1 + \tilde{A}_u v_2 & \tilde{m}_{u^c}^2 + m_u m_u^\dagger + M_Z^2 Z_{u^c} c_{2\beta} \end{pmatrix} \begin{pmatrix} \tilde{u}_L \\ \tilde{u}_R \end{pmatrix} \tag{66}$$

$$\left(\tilde{d}_L^\dagger \; \tilde{d}_R^\dagger\right) \begin{pmatrix} \tilde{m}_q^2 + m_d^\dagger m_d + M_Z^2 Z_d c_{2\beta} & -\mu\lambda_d^\dagger v_2 + \tilde{A}_d^\dagger v_1 \\ -\mu\lambda_d v_2 + \tilde{A}_d v_1 & \tilde{m}_{d^c}^2 + m_d m_d^\dagger + M_Z^2 Z_{d^c} c_{2\beta} \end{pmatrix} \begin{pmatrix} \tilde{d}_L \\ \tilde{d}_R \end{pmatrix} \tag{67}$$

$$\left(\tilde{e}_L^\dagger \; \tilde{e}_R^\dagger\right) \begin{pmatrix} \tilde{m}_l^2 + m_e^\dagger m_e + M_Z^2 Z_e c_{2\beta} & -\mu\lambda_e^\dagger v_2 + \tilde{A}_e^\dagger v_1 \\ -\mu\lambda_e v_2 + \tilde{A}_e v_1 & \tilde{m}_{e^c}^2 + m_e m_e^\dagger + M_Z^2 Z_{e^c} c_{2\beta} \end{pmatrix} \begin{pmatrix} \tilde{e}_L \\ \tilde{e}_R \end{pmatrix} \tag{68}$$

The light sneutrino mass matrix in the $\tilde{\nu}_L = \tilde{\nu}$ basis, after the heavy right-handed sneutrinos are integrated out, is given by :

$$\tilde{\nu}_L^\dagger \left(\tilde{m}_l^2 + M_Z^2 Z_{\nu_L} c_{2\beta}\right) \tilde{\nu}_L \tag{69}$$

The Z factors in Eqs.(66)-(69) are defined by $Z_f = I_f - Q_f s_\theta^2$ where I_f is the isospin and Q_f the electric charge of the f field :

$$\begin{aligned} Z_u &= (+\tfrac{1}{2}) - (+\tfrac{2}{3})s_\theta^2 \quad Z_{u^c} = (0) - (-\tfrac{2}{3})s_\theta^2 \\ Z_d &= (-\tfrac{1}{2}) - (-\tfrac{1}{3})s_\theta^2 \quad Z_{d^c} = (0) - (+\tfrac{1}{3})s_\theta^2 \\ Z_e &= (-\tfrac{1}{2}) - (-1)s_\theta^2 \quad Z_{e^c} = (0) - (+1)s_\theta^2 \\ Z_\nu &= (+\tfrac{1}{2}) - (\ \ 0)s_\theta^2 \end{aligned} \tag{70}$$

The diagonalization of the up-type squark squared mass matrix $M^{\tilde{u}2}$ of Eq. (66), down-type squark matrix $M^{\tilde{d}2}$ of Eq. (67), charged slepton matrix $M^{\tilde{e}2}$ of Eq. (68) and sneutrino matrix of Eq. (69) is achieved in the following way :

$$S^{\tilde{u}} M^{\tilde{u}2} S^{\tilde{u}\dagger} = \mathrm{Diag}(m_{\tilde{U}_1}, .., m_{\tilde{U}_6}) \tag{71}$$

$$= \mathrm{Diag}(m_{\tilde{u}_1}, m_{\tilde{c}_1}, m_{\tilde{t}_1}, m_{\tilde{u}_2}, m_{\tilde{c}_2}, m_{\tilde{t}_2}) \tag{72}$$

$$S^{\tilde{d}} M^{\tilde{d}2} S^{\tilde{d}\dagger} = \mathrm{Diag}(m_{\tilde{D}_1}, .., m_{\tilde{D}_6}) \tag{73}$$

$$= \mathrm{Diag}(m_{\tilde{d}_1}, m_{\tilde{s}_1}, m_{\tilde{b}_1}, m_{\tilde{d}_2}, m_{\tilde{s}_2}, m_{\tilde{b}_2}) \tag{74}$$

$$S^{\tilde{e}} M^{\tilde{e}2} S^{\tilde{e}\dagger} = \mathrm{Diag}(m_{\tilde{E}_1}, .., m_{\tilde{E}_6}) \tag{75}$$

$$= \mathrm{Diag}(m_{\tilde{e}_1}, m_{\tilde{\mu}_1}, m_{\tilde{\tau}_1}, m_{\tilde{e}_2}, m_{\tilde{\mu}_2}, m_{\tilde{\tau}_2}) \tag{76}$$

$$S^{\tilde{\nu}}_{LL} M^{\tilde{\nu}2}_{LL} S^{\tilde{\nu}\dagger}_{LL} = \mathrm{Diag}(m_{\tilde{\nu}_1}, m_{\tilde{\nu}_2}, m_{\tilde{\nu}_3}) \tag{77}$$

.

Finally it is convenient to define the following matrices that are, in a way, supersymmetric generalizations of the CKM matrix, *i.e.* they describe the flavour properties of vertices that involve the interaction between a SUSY scalar particle and a standard

model fermion :

$$
\begin{aligned}
(V_R^{\tilde{u}u})_{\alpha A} &= \textstyle\sum_{B=1}^{3} S^{\tilde{u}}_{\alpha B+3} S^{u\dagger}_{BA} & (V_R^{\tilde{u}u\dagger})_{A\alpha} &= \textstyle\sum_{B=1}^{3} S^{u}_{AB} S^{\tilde{u}\dagger}_{B+3\alpha} \\
(V_L^{\tilde{d}d})_{\alpha A} &= \textstyle\sum_{B=1}^{3} S^{\tilde{d}}_{\alpha B} T^{d\dagger}_{BA} & (V_L^{\tilde{d}d\dagger})_{A\alpha} &= \textstyle\sum_{B=1}^{3} T^{d}_{AB} S^{\tilde{d}\dagger}_{B\alpha} \\
(V_R^{\tilde{d}d})_{\alpha A} &= \textstyle\sum_{B=1}^{3} S^{\tilde{d}}_{\alpha B+3} S^{d\dagger}_{BA} & (V_R^{\tilde{d}d\dagger})_{A\alpha} &= \textstyle\sum_{B=1}^{3} S^{d}_{AB} S^{\tilde{d}\dagger}_{B+3\alpha} \\
(V_L^{\tilde{u}d})_{\alpha A} &= \textstyle\sum_{B=1}^{3} S^{\tilde{u}}_{\alpha B} T^{d\dagger}_{BA} & (V_L^{\tilde{u}d\dagger})_{A\alpha} &= \textstyle\sum_{B=1}^{3} T^{d}_{AB} S^{\tilde{u}\dagger}_{B\alpha} \\
(V_{LL}^{\tilde{\nu}e})_{\alpha A} &= \textstyle\sum_{B=1}^{3} (S^{\tilde{\nu}}_{LL})_{\alpha B} T^{e\dagger}_{BA} & (V_{LL}^{\tilde{\nu}e\dagger})_{A\alpha} &= \textstyle\sum_{B=1}^{3} T^{e}_{AB} (S^{\tilde{\nu}\dagger}_{LL})_{B\alpha}
\end{aligned}
\tag{78}
$$

APPENDIX B

The supersymmetry mass scale

In this section we will define the effective SUSY scale M_S which we used to represent the average sparticle masses. Above M_S the theory was described by the MSSM+ν^c and below it we had the Standard Model. Traditionally it is convenient to introduce three T_i scales that describe the effect of the decoupling of the SUSY particles on the gauge couplings [34] :

$$T_1 = m_{\tilde{q}}^{11/25} m_{\tilde{l}}^{9/25} m_{\tilde{H}}^{4/25} m_H^{1/25} \tag{79}$$

$$T_2 = m_{\tilde{q}}^{9/25} m_{\tilde{W}}^{8/25} m_{\tilde{H}}^{4/25} m_{\tilde{l}}^{3/25} m_H^{1/25} \tag{80}$$

$$T_3 = m_{\tilde{q}}^{1/2} m_{\tilde{g}}^{1/2} \tag{81}$$

where $m_{\tilde{q}}$, $m_{\tilde{l}}$, $m_{\tilde{H}}$, m_H, $m_{\tilde{W}}$ and $m_{\tilde{g}}$ are the squark, slepton, higgsino, heavy CP-even Higgs boson, wino and gluino masses respectively. In models with gauge unification at M_X the prediction for $\alpha_s(M_{\rm Z})$ depends on M_{SUSY} given by [5] :

$$M_{SUSY} = T_1^{-25/19}\, T_2^{100/19}\, T_3^{-56/19} \tag{82}$$

Combining the equations above we obtain [8] :

$$M_{SUSY} = m_{\tilde{H}} \left(\frac{m_{\tilde{W}}}{m_{\tilde{g}}}\right)^{28/19} \left[\left(\frac{m_{\tilde{l}}}{m_{\tilde{q}}}\right)^{3/19} \left(\frac{m_H}{m_{\tilde{H}}}\right)^{3/19} \left(\frac{m_{\tilde{W}}}{m_{\tilde{H}}}\right)^{4/19}\right] \tag{83}$$

In this article we did not use the above scale to describe the average sparticle masses since as was emphasized in Refs. [5, 8], M_{SUSY} is only related to the overall sparticle masses in the unlikely case of degenerate SUSY spectrum. Instead, we introduced a new scale M_S which was defined such that the sum of the squares of the threshold corrections induced by the decoupling of the SUSY spectrum on the gauge couplings is minimal :

$$\frac{\partial}{\partial M_S} \left\{\sum_{i=1}^{3} \frac{B_i}{2\pi} \ln\left(\frac{M_S}{T_i}\right)\right\}^2 = 0 \qquad \text{where} \qquad B_i = (\tfrac{5}{2}, \tfrac{25}{6}, 4) \tag{84}$$

Explicitly we find that M_S is given by :

$$M_{\rm S} = T_1^{225/1426}\, T_2^{625/1426}\, T_3^{576/1426} \quad (85)$$

$$= m_{\tilde{q}}^{612/1426}\, m_{\tilde{g}}^{228/1426}\, m_{\tilde{W}}^{200/1426}\, m_{\tilde{l}}^{156/1426}\, m_{\tilde{H}}^{136/1426}\, m_H^{34/1426} \quad (86)$$

where the exponent values of the $m_{\tilde{q}}$,..,m_H terms are : 0.43, 0.20, 0.14, 0.11, 0.10 and 0.02 respectively. It is interesting to note that the unphysical nature of M_{SUSY} can be immediately identified through the appearance of negative exponents (see Eq. (82)) whereas the T_i's in Eqs. (79)-(81) and M_S in Eq. (85) and Eq. (86) are weighed by positive numbers.

In Table VI we list the low energy values of the masses of the gauginos, the effective SUSY scales in Eqs. (79)-(81), and the value of the new supersymmetry scale M_S defined in Eq. (86) against the often used M_{SUSY} of Eq. (83). We observe that while M_S is a good average of the T_i's, M_{SUSY} fails to represent a meaningful effective SUSY mass.

TABLE VI.

Case	$m_{\tilde{B}}$	$m_{\tilde{W}}$	$m_{\tilde{g}}$	T_1	T_2	T_3	M_S	M_{SUSY}
A	173	334	942	440	454	874	588	68
B	356	674	1787	851	887	1650	1132	150
C	174	334	942	438	433	879	577	53
D	356	674	1789	818	820	1662	1091	103
E	173	334	976	449	474	903	610	76
F	355	673	1845	889	935	1700	1181	172
G	173	334	976	451	466	907	607	68
H	356	673	1845	876	911	1707	1166	150
I	264	503	1415	718	714	1319	915	116

TABLE VI. Predicted values for the bino ($m_{\tilde{B}}$), wino ($m_{\tilde{W}}$) and gluino ($m_{\tilde{g}}$) masses at low energies and for the three SUSY scales T_i and the effective M_S, M_{SUSY} scales defined in Eqs. (86),(83) (masses given in GeV units.). The first column indicates the input for each model as defined by list of values in Table I.

APPENDIX C
Tables for the SUSY corrections

In this appendix we present some examples which illustrate the magnitude of the SUSY corrections to the bottom and tau mass.

In Table VII we systematically list the values of all the parameters, evaluated at low energy, that are needed to compute the gluino correction. The columns refer to : the input taken according to Table I; the value of the strong gauge coupling; the ratio of the MSSM VEVs; the mass of the gluino; the value of the Higgs mixing parameter μ; the masses of the physical bottom squarks; the value of the dimensionless function $I_{\tilde{g}} = m_{\tilde{g}}\mu I(m^2_{\tilde{g}}, m^2_{\tilde{b}_1}, m^2_{\tilde{b}_2})$; [28] and finally, in the last column, the value of the gluino correction (in percentage %.) In Table VIII we list similar values appropriate for the evaluation of the higgsino correction. For example, $\alpha_t = \lambda_t^2/4\pi$, $m_{\tilde{t}_{1,2}}$ are stop masses and $I_{\tilde{H}} = A_t\mu I(\mu^2, m^2_{\tilde{t}_1}, m^2_{\tilde{t}_2})$. Comparing Table VII with Table VIII we read that $\Delta^{\tilde{g}} m_b \sim -20\%$ dominates over $\Delta^{\tilde{H}} m_b \sim 6$ %.

In Table IX we present, in the last column, the values for the bino corrections to the tau mass $\Delta^{\tilde{B}} m_\tau$. In this table we also give the values for $\alpha' = g'^2/4\pi$, for the bino mass $m_{\tilde{B}}$, for the stau masses and for $I_{\tilde{B}} = m_{\tilde{B}}\mu I(m^2_{\tilde{B}}, m^2_{\tilde{\tau}_1}, m^2_{\tilde{\tau}_2})$. We read that, on average, $\Delta^{\tilde{B}} m_\tau$ is -2.45 %.

Finally we computed Δm_d and Δm_s which we show in Table X. Two comments deserve attention. Firstly, $\Delta^{\tilde{H}} m_{d,s} \simeq 0$ due to small $\lambda_{d,s}$ Yukawa couplings. Secondly, we see that the gluino contribution is not universal, *i.e.* $\Delta^{\tilde{g}} m_d \simeq \Delta^{\tilde{g}} m_s \not\simeq \Delta^{\tilde{g}} m_b$ due to $m_{\tilde{d},\tilde{s}} \not\simeq m_{\tilde{b}}$. In conjunction, they lead to non-universal SUSY corrections $\Delta m_{d,s} \not\simeq \Delta m_b$, thus slightly affecting the ratio $\lambda_{d,s}(M_X)/\lambda_b(M_X)$ [69].

[28] $I(x,y,z) = -\frac{xy\ln(x/y)+yz\ln(y/z)+zx\ln(z/x)}{(x-y)(y-z)(z-x)}$

TABLE VII.

Case	α_3	$\tan\beta$	$m_{\tilde{g}}$	μ	$m_{\tilde{b}_1}$	$m_{\tilde{b}_2}$	$I_{\tilde{g}}$	$\Delta^{\tilde{g}} m_b$
A	0.0904	42.16	942	-417	775	691	-0.305	-24.65
B	0.0848	44.16	1787	-795	1431	1316	-0.311	-24.72
C	0.0906	35.94	942	-339	790	725	-0.238	-16.43
D	0.0850	37.51	1789	-636	1475	1373	-0.238	-16.11
E	0.0960	47.15	976	-494	794	692	-0.358	-34.36
F	0.0896	49.40	1845	-942	1452	1323	-0.367	-34.44
G	0.0960	41.99	976	-445	804	719	-0.313	-26.81
H	0.0897	44.06	1845	-847	1480	1364	-0.320	-26.82
I	0.0920	47.34	1415	-703	1144	1035	-0.347	-32.03

TABLE VII. Values of the parameters required to compute the gluino correction to the bottom quark mass $\Delta^{\tilde{g}} m_b \sim -20\%$ (all evaluated at low energy.) The gluino mass is given by $m_{\tilde{g}}$, the sbottom masses by $m_{\tilde{b}_{1,2}}$ and the dimensionless function $I_{\tilde{g}}$ is given by $I_{\tilde{g}} = m_{\tilde{g}} \mu I(m^2_{\tilde{g}}, m^2_{\tilde{b}_1}, m^2_{\tilde{b}_2})$.

TABLE VIII.

Case	α_t	$\tan\beta$	A_t	μ	$m_{\tilde{t}_1}$	$m_{\tilde{t}_2}$	$I_{\tilde{H}}$	$\Delta^{\tilde{H}} m_b$
A	0.0476	42.16	-780	-417	812	665	0.408	6.51
B	0.0482	44.16	-1410	-795	1457	1291	0.401	6.80
C	0.0363	35.94	-879	-339	831	690	0.385	4.00
D	0.0364	37.51	-1605	-636	1504	1345	0.376	4.09
E	0.0597	47.15	-728	-494	826	676	0.406	9.10
F	0.0602	49.40	-1302	-942	1472	1303	0.399	9.45
G	0.0499	41.99	-814	-445	842	692	0.416	6.94
H	0.0504	44.06	-1465	-847	1506	1338	0.409	7.23
I	0.0573	47.34	-1055	-703	1170	1013	0.400	8.64

TABLE VIII. Values of the parameters required to compute the higgsino correction to the bottom quark mass $\Delta^{\tilde{H}} m_b \sim 6$ % (all evaluated at low energy.) The higgsino mass is approximately given by $|\mu|$, the stop masses are given by $m_{\tilde{t}_{1,2}}$ and the dimensionless function $I_{\tilde{H}}$ is given by $I_{\tilde{H}} = A_t \mu I(\mu^2, m^2_{\tilde{t}_1}, m^2_{\tilde{t}_2})$.

TABLE IX.

Case	α'	$\tan\beta$	$m_{\tilde{B}}$	μ	$m_{\tilde{\tau}_1}$	$m_{\tilde{\tau}_2}$	$I_{\tilde{B}}$	$\Delta^{\tilde{B}} m_\tau$
A	0.0104	42.16	173	-417	348	178	-0.669	-2.33
B	0.0105	44.16	356	-795	653	387	-0.656	-2.42
C	0.0104	35.94	174	-339	343	207	-0.507	-1.51
D	0.0105	37.51	356	-636	657	424	-0.494	-1.55
E	0.0104	47.15	173	-494	355	143	-0.860	-3.36
F	0.0105	49.40	355	-942	652	352	-0.818	-3.37
G	0.0104	41.99	173	-445	350	175	-0.715	-2.49
H	0.0105	44.06	356	-847	655	387	-0.696	-2.56
I	0.0104	47.34	264	-703	549	329	-0.641	-2.52

TABLE IX. Values of the parameters required to compute the bino correction to the tau lepton mass $\Delta^{\tilde{B}} m_\tau \sim -2.45\%$. (all evaluated at low energy.) The bino mass is given by $m_{\tilde{B}}$, the stau masses by $m_{\tilde{\tau}_{1,2}}$ and the dimensionless function $I_{\tilde{B}}$ is given by $I_{\tilde{B}} = m_{\tilde{B}} \mu I(m^2_{\tilde{B}}, m^2_{\tilde{\tau}_1}, m^2_{\tilde{\tau}_2})$

TABLE X.

Case	$\Delta^{\tilde{g}} m_d$	$\Delta^{\tilde{H}} m_d$	$\Delta^{\tilde{g}} m_s$	$\Delta^{\tilde{H}} m_s$	Δm_d	Δm_s	Δm_b
A	-19.24	0.00	-19.25	0.01	-19.24	-19.23	-17.20
B	-19.28	0.00	-19.28	0.01	-19.28	-19.27	-17.04
C	-12.95	0.00	-12.95	0.01	-12.95	-12.94	-11.35
D	-12.72	0.00	-12.72	0.01	-12.72	-12.71	-11.16
E	-26.38	0.00	-26.39	0.02	-26.38	-26.37	-24.40
F	-26.38	0.00	-26.38	0.02	-26.38	-26.36	-24.19
G	-20.92	0.00	-20.92	0.01	-20.92	-20.91	-18.87
H	-20.91	0.00	-20.92	0.01	-20.91	-20.90	-18.67
I	-24.40	0.00	-24.40	0.02	-24.40	-24.38	-22.55

TABLE X. Gluino and higgsino SUSY corrections to the down and strange masses $\Delta^{\tilde{g},\tilde{H}} m_{d,s}$ and the total correction to the down, strange and bottom quark masses $\Delta m_{d,s,b}$ (in percentage values.)

APPENDIX D

Boundary conditions for the gauge and gaugino masses

In this appendix we review the origin of Eq. (20) that relates the gauge and the gaugino masses of the $SU(3)_c \otimes SU(2)_L \otimes U(1)_Y$ MSSM and of the $SU(4) \otimes SU(2)_L \otimes SU(2)_R$ Pati-Salam Model.

We start by considering the constraint on the $U(1)_Y$, $SU(2)_R$ and $SU(4)$ gauge couplings g', g_{2R} and g_4. The covariant derivative for the heavy Higgs boson H that breaks the GUT symmetry is :

$$D_\mu H = \partial_\mu H + i g_{2R} \tau_R^a W_{R\mu}^a H + i g_4 T^m G_\mu^m H \tag{87}$$

where $\tau_R^a = \frac{1}{2}\sigma^a$ and T^m are the $SU(2)_R$ and $SU(4)$ group generators with associated gauge bosons W_R^a and G^m ($a = 1, .., 3$ and $m = 1, .., 15$). When H develops a non-vanishing VEV $\langle H_\nu \rangle = \sqrt{2} V_\nu$ along the neutrino direction the quadratic interaction $|D_\mu H|^2$ generates the following mass terms :

$$2 g_{2R}^2 V_\nu^2 (\tau_R^a \tau_R^b)_{22} W_R^{a\mu} W_{R\mu}^b \tag{88}$$

$$4 g_{2R} g_4 V_\nu^2 (\tau_R^3)_{22} (T^{15})_{44} W_R^{3\mu} G_\mu^{15} \tag{89}$$

$$2 g_4^2 V_\nu^2 (T^m T^n)_{44} G^{m\mu} G_\mu^n. \tag{90}$$

where $\tau_R^3 = \mathrm{diag}(\frac{1}{2}, -\frac{1}{2})$ and $T^{15} = \sqrt{\frac{3}{2}}\,\mathrm{Diag}(\frac{1}{6}, \frac{1}{6}, \frac{1}{6}, -\frac{1}{2})$ are diagonal matrices. Upon explicit substitution of the group generators (and after adding to the above expressions similar terms associated with the $\bar{H}$ Higgs field, with a VEV $\langle \bar{H}_\nu \rangle = \sqrt{2}\bar{V}_\nu$) the mixing between the W_R^3, G^{15} gauge bosons can be written as :

$$\frac{1}{2} V^2 \begin{pmatrix} W_R^{3\mu} & G^{15\mu} \end{pmatrix} \begin{pmatrix} g_{2R}^2 & -\sqrt{\frac{3}{2}} g_4 g_{2R} \\ -\sqrt{\frac{3}{2}} g_4 g_{2R} & \frac{3}{2} g_4^2 \end{pmatrix} \begin{pmatrix} W_{\mu R}^3 \\ G_\mu^{15} \end{pmatrix} \tag{91}$$

where $V^2 = V_\nu^2 + \bar{V}_\nu^2$. The matrix above can be diagonalized by a unitary matrix parameterised by the rotation angle α given by :

$$\sin\alpha = \frac{g_{2R}}{\sqrt{g_{2R}^2 + \frac{3}{2} g_4^2}} \qquad \cos\alpha = \frac{\sqrt{\frac{3}{2}} g_4}{\sqrt{g_{2R}^2 + \frac{3}{2} g_4^2}} \tag{92}$$

to yield a massless B state (the MSSM bino) and a heavy gauge boson X with a mass $m_X^2 = V^2(g_{2R}^2 + \frac{3}{2}g_4^2)$. These are related to the W_R^3, G^{15} bosons through :

$$\begin{pmatrix} B \\ X \end{pmatrix} = \begin{pmatrix} \cos\alpha & \sin\alpha \\ -\sin\alpha & \cos\alpha \end{pmatrix} \begin{pmatrix} W_R^3 \\ G^{15} \end{pmatrix} \quad , \quad \begin{pmatrix} W_R^3 \\ G^{15} \end{pmatrix} = \begin{pmatrix} \cos\alpha & -\sin\alpha \\ \sin\alpha & \cos\alpha \end{pmatrix} \begin{pmatrix} B \\ X \end{pmatrix} \tag{93}$$

Finally, in order to obtain the first equation in Eq. (20) we need to relate g' to g_{2R} and g_4. This can be achieved by examining, for example, the kinetic term for the fermions in the F representation :

$$\mathcal{L} = i\bar{F}\gamma^\mu D_\mu F \sim -\bar{F}\gamma^\mu \left[g_4 T^{15} G_\mu^{15}\right] F \sim -\bar{u}\gamma^\mu \left[\sqrt{\tfrac{3}{2}} g_4 \left(\tfrac{1}{6}\right) (\sin\alpha B_\mu)\right] u \tag{94}$$

and comparing it to the $U(1)_Y$ neutral current Lagrangian :

$$\mathcal{L} = -\bar{u}\gamma^\mu \left[g' \left(\tfrac{1}{6}\right) B_\mu\right] u \tag{95}$$

We get :

$$g' = \sqrt{\tfrac{3}{2}} g_4 \sin\alpha \tag{96}$$

Thus combining Eq. (92) and (96) we find :

$$\frac{1}{g'^2} = \frac{1}{g_{2R}^2} + \frac{1}{\frac{3}{2}g_4^2} \tag{97}$$

which agrees with Eq. (20) after replacing $g'^2 = \frac{3}{5}g_1^2$.

In the second part of this appendix we will justify the second equation in Eq. (20). We start by considering the following Higgs-gaugino-higgsino interaction :

$$\mathcal{L} = i\sqrt{2} H^\dagger \left(g_{2R}\tau_R^a \lambda_R^a + g_4 T^m \lambda_4^m\right) \tilde{H} + \text{h.c.} \tag{98}$$

where H is the heavy Higgs boson, $\tilde{H}$ the heavy higgsino field, and λ_R^a, λ_4^m the $SU(2)_R$, $SU(4)$ gauginos (a similar expression applies to $\bar{H}$). When the Higgs bosons H, $\bar{H}$ develop their VEVs, we obtain (after appropriately substituting the generator matrices τ_R^3, T^{15}) :

$$\mathcal{L} = -g_{2R}(-i\lambda_R^3)\left[V_\nu \tilde{H}_\nu + \bar{V}_\nu \tilde{\bar{H}}_\nu\right] + \sqrt{\tfrac{3}{2}} g_4 (-i\lambda_4^{15})\left[V_\nu \tilde{H}_\nu + \bar{V}_\nu \tilde{\bar{H}}_\nu\right] + \text{h.c.} \tag{99}$$

From Eq. (99) it is clear that the gauginos only couple to the $V_\nu\tilde{H}_\nu+\bar{V}_\nu\tilde{\bar{H}}_\nu$ combination of higgsinos. Thus, it is convenient to define new fields $\tilde{N}_1$ and $\tilde{N}_2$ through :

$$\begin{pmatrix}\tilde{N}_1\\ \tilde{N}_2\end{pmatrix} = \begin{pmatrix}\cos\theta_N & \sin\theta_N\\ -\sin\theta_N & \cos\theta_N\end{pmatrix}\begin{pmatrix}\tilde{H}_\nu\\ \tilde{\bar{H}}_\nu\end{pmatrix} \tag{100}$$

where $\tan\theta_N = \bar{V}_\nu/V_\nu$. The bosonic partners of $\tilde{N}_1$, $\tilde{N}_2$ have VEVs given by $\langle N_1\rangle = \sqrt{2}V_1 = \sqrt{2}V_\nu\cos\theta_N + \sqrt{2}\bar{V}_\nu\sin\theta_N = \sqrt{2}(V_\nu^2+\bar{V}_\nu^2)^{1/2}$ and $\langle N_2\rangle = 0$. The gaugino mass matrix in the $(-i\lambda_R^3, -i\lambda_4^{15}, \tilde{N}_1)$ basis can be written as :

$$M_\lambda = \begin{pmatrix} M_{2R} & 0 & g_{2R}V_1\\ 0 & M_4 & -\sqrt{\frac{3}{2}}g_4V_1\\ g_{2R}V_1 & -\sqrt{\frac{3}{2}}g_4V_1 & 0\end{pmatrix} \tag{101}$$

where the 13, 23 entries derive from Eq. (99) and M_{2R}, M_4 are explicit light soft masses for the $SU(2)_{2R}$, $SU(4)$ gauginos. The two heavy eigenvalues of the above matrix are approximately given by $M_{\lambda_{2,3}} \sim \pm(g_{2R}^2+\frac{3}{2}g_4^2)^{1/2}V_1$. The lightest eigenvalue (the bino mass) can easily be computed from $M_1 = \mathrm{Det}M_\lambda/(M_{\lambda_1}M_{\lambda_2})$. We find :

$$M_1 = \frac{\frac{3}{2}g_4^2}{g_{2R}^2+\frac{3}{2}g_4^2}M_{2R} + \frac{g_{2R}^2}{g_{2R}^2+\frac{3}{2}g_4^2}M_4 \tag{102}$$

Finally, replacing the result of Eq. (97) into Eq. (102) gives us the expression we wanted to prove :

$$\frac{M_1}{g'^2} = \frac{M_{2R}}{g_{2R}^2} + \frac{M_4}{\frac{3}{2}g_4^2} \tag{103}$$

We would like to conclude this appendix with the following observation. The rotation that diagonalizes the W_R^3–G^{15} gauge bosons mass matrix (see Eq. (91)) also simultaneously block diagonalizes the gaugino mass matrix in Eq. (101). Indeed we note that :

$$\begin{pmatrix} c_\alpha & s_\alpha & 0\\ -s_\alpha & c_\alpha & 0\\ 0 & 0 & 1\end{pmatrix} M_\lambda \begin{pmatrix} c_\alpha & -s_\alpha & 0\\ s_\alpha & c_\alpha & 0\\ 0 & 0 & 1\end{pmatrix} \sim \begin{pmatrix} M_{\lambda_1} & \mathcal{O}(M) & 0\\ \mathcal{O}(M) & \mathcal{O}(M) & \mathcal{O}(V_1)\\ 0 & \mathcal{O}(V_1) & 1\end{pmatrix} \tag{104}$$

where $s_\alpha = \sin\alpha$, $c_\alpha = \cos\alpha$ and $\mathcal{O}(M)$ is a number of order M_{2R} and/or M_4. Thus we find from Eq. (104) that $M_{\lambda_1} = c_\alpha^2 M_{2R} + s_\alpha^2 M_4$ which is nothing less than the bino mass of Eq. (102) re-written in terms of the gauge mixing angle α defined in Eq. (92).

APPENDIX E
Expressions for the D-terms

The D-term corrections to the soft masses in Eqs. (26)-(33) arise when the rank of the Pati-Salam group is reduced from five to four due to gauge symmetry breaking. In this appendix we show that the coefficients of the corrections are related to the charge carried by the fields under the $U(1)$ broken generator and that their magnitude depends on the difference between the soft masses of the heavy Higgs that break the GUT symmetry.

We start by carefully reporting our index conventions. The matrix elements of the fields of the $SU(4) \otimes SU(2)_L \otimes SU(2)_R$ model in Eqs. (15)-(17) are indicated by :

$$\begin{array}{ll} F^c_{\dot{\alpha} i} : (\bar{4}, 1, \bar{2}) & \bar{H}_{\dot{\theta} p} : (\bar{4}, 1, \bar{2}) \\ & \qquad\qquad h_\rho{}^{\dot{\sigma}} : (1, \bar{2}, 2) \\ F^{\gamma k} : (4, 2, 1) & H^{\dot{\eta} r} : (4, 1, 2) \end{array} \tag{105}$$

where $i, k, p, r = 1, .., 4$ are $SU(4)$ indices, $\dot{\alpha}, \dot{\theta}, \dot{\eta}, \dot{\sigma} = 1, 2$ are $SU(2)_R$ indices and $\gamma, \rho = 1, 2$ are $SU(2)_L$ indices. The position of the indices is the following, the first/second index refers to the line/column of the matrices in Eqs. (15)-(17). Moreover up/down indices are related to the representation of the multiplet. For example, the lower ρ index of h indicates that h transforms in the $\bar{2}$ (anti-matter) representation of $SU(2)$ under the $SU(2)_L$ symmetry, whereas the upper $\dot{\sigma}$ index indicates that h transforms in the fundamental representation of $SU(2)$ under the $SU(2)_R$ symmetry.

The D-term contributions from the $SU(2)_{2R}$ and $SU(4)$ groups are given by :

$$\mathcal{V} = \tfrac{1}{2} g^2_{2R} \sum_{a=1}^{3} D^a_{2R} D^a_{2R} + \tfrac{1}{2} g^2_4 \sum_{m=1}^{15} D^m_4 D^m_4. \tag{106}$$

We focus on the $a = 3$ and $m = 15$ contributions of Eq. (106) which involve the

$$\tau^3_R = \mathrm{diag}(\tfrac{1}{2}, -\tfrac{1}{2}) \qquad\qquad T^{15} = \sqrt{\tfrac{3}{2}}\, \mathrm{diag}(\tfrac{1}{6}, \tfrac{1}{6}, \tfrac{1}{6}, -\tfrac{1}{2}) \tag{107}$$

diagonal generators of the $SU(2)_{2R}$ and $SU(4)$ groups. Using the notation of Eq. (105) we find that D^3_{2R}, D^{15}_4 are given by :

$$D^2_{2R} = \bar{H}^\dagger_{\dot\theta p}(-\tau^{3*}_R)_{\dot\theta\dot\omega}\bar{H}_{\dot\omega p} + H^{\dagger\dot\eta r}(\tau^3_R)_{\dot\eta\dot\xi}H^{\dot\xi r} + \tilde{F}^{c\dagger}_{\dot\alpha i}(-\tau^{3*}_R)_{\dot\alpha\dot\beta}\tilde{F}^c_{\dot\beta i} + h^\dagger_\rho{}^{\dot\sigma}(\tau^3_R)_{\dot\sigma\dot\pi}h_\rho{}^{\dot\pi} \quad (108)$$

$$D^{15}_4 = \bar{H}^\dagger_{\dot\theta p}(-T^{15*})_{pq}\bar{H}_{\dot\theta q} + H^{\dagger\dot\eta r}(T^{15})_{rs}H^{\dot\eta s} + \tilde{F}^{c\dagger}_{\dot\alpha i}(-T^{15*})_{ij}\tilde{F}^c_{\dot\alpha j} + \tilde{F}^{\dagger\gamma k}(T^{15})_{kl}\tilde{F}^{\gamma l} \quad (109)$$

Assuming that the heavy Higgs develop VEVs along the neutrino directions :

$$\langle\bar{H}\rangle = \bar{H}_{\dot24} = \bar{H}_\nu \qquad \langle H\rangle = H^{\dot24} = H_\nu \quad (110)$$

we can expand D^3_{2R}, D^{15}_4 :

$$\begin{aligned} D^3_{2R} &= \bar{H}^\dagger_\nu(-\tau^{3*}_R)_{\dot2\dot2}\bar{H}_\nu + H^\dagger_\nu(\tau^3_R)_{\dot2\dot2}H_\nu + \\ &\quad \tilde{d}^{c\dagger}(-\tau^{3*}_R)_{\dot1\dot1}\tilde{d}^c + \tilde{e}^{c\dagger}(-\tau^{3*}_R)_{\dot1\dot1}\tilde{e}^c + \tilde{u}^{c\dagger}(-\tau^{3*}_R)_{\dot2\dot2}\tilde{u}^c + \tilde{\nu}^{c\dagger}(-\tau^{3*}_R)_{\dot2\dot2}\tilde{\nu}^c + \\ &\quad h^\dagger_d(\tau^3_R)_{\dot1\dot1}h_d + h^\dagger_u(\tau^3_R)_{\dot2\dot2}h_u \\ &= +\tfrac{1}{2}|\bar{H}_\nu|^2 - \tfrac{1}{2}|H_\nu|^2 - \tfrac{1}{2}|\tilde{d}^c|^2 - \tfrac{1}{2}|\tilde{e}^c|^2 + \tfrac{1}{2}|\tilde{u}^c|^2 + \tfrac{1}{2}|\tilde{\nu}^c|^2 + \tfrac{1}{2}|h_d|^2 - \tfrac{1}{2}|h_u|^2 \end{aligned} \quad (111)$$

$$\begin{aligned} D^{15}_4 &= \bar{H}^\dagger_\nu(-T^{15*})_{44}\bar{H}_\nu + H^\dagger_\nu(T^{15})_{44}H_\nu + \\ &\quad \tilde{d}^{c\dagger}(-T^{15*})_{11}\tilde{d}^c + \tilde{e}^{c\dagger}(-T^{15*})_{44}\tilde{e}^c + \tilde{u}^{c\dagger}(-T^{15*})_{11}\tilde{u}^c + \tilde{\nu}^{c\dagger}(-T^{15*})_{44}\tilde{\nu}^c + \\ &\quad \tilde{q}^\dagger(T^{15})_{11}\tilde{q} + \tilde{l}^\dagger(T^{15})_{44}\tilde{l} \\ &= \sqrt{\tfrac{3}{2}}\,[+\tfrac{1}{2}|\bar{H}_\nu|^2 - \tfrac{1}{2}|H_\nu|^2 - \tfrac{1}{6}|\tilde{d}^c|^2 + \tfrac{1}{2}|\tilde{e}^c|^2 - \tfrac{1}{6}|\tilde{u}^c|^2 + \tfrac{1}{2}|\tilde{\nu}^c|^2 + \tfrac{1}{6}|\tilde{q}|^2 - \tfrac{1}{2}|\tilde{l}|^2] \end{aligned} \quad (112)$$

One can summarize the results of Eqs. (111)-(112) by writing :

$$D^3_{2R} = D_H + \sum_\phi I_\phi|\phi|^2 \qquad D^{15}_4 = \sqrt{\tfrac{3}{2}}D_H + \sqrt{\tfrac{3}{2}}\sum_\phi\left(\tfrac{B-L}{2}\right)_\phi|\phi|^2 \quad (113)$$

where $D_H = \frac{1}{2}(|\bar{H}_\nu|^2 - |H_\nu|^2)$ and ϕ denotes any of the light fields $\tilde{u}^c$, $\tilde{d}^c$, $\tilde{e}^c$, $\tilde{\nu}^c$, $\tilde{q}$, $\tilde{l}$, h_u, h_d. The factor I_ϕ refers to the charge carried by ϕ with respect to the $SU(2)_R$ group and $(B-L)/2$ to the semi-difference between the baryon and lepton numbers of ϕ. These are can be read from the coefficients of the terms in Eqs. (111)-(112) and are collected in Table XI.

TABLE XI.

	$\tilde{u}^c$	$\tilde{d}^c$	$\tilde{e}^c$	$\tilde{\nu}^c$	$\tilde{q}$	$\tilde{l}$	h_u	h_d
I_ϕ	$+\frac{1}{2}$	$-\frac{1}{2}$	$-\frac{1}{2}$	$+\frac{1}{2}$	0	0	$-\frac{1}{2}$	$+\frac{1}{2}$
$\left(\frac{B-L}{2}\right)_\phi$	$-\frac{1}{6}$	$-\frac{1}{6}$	$+\frac{1}{2}$	$+\frac{1}{2}$	$+\frac{1}{6}$	$-\frac{1}{2}$	0	0

TABLE XI. Charges carried by the light scalar fields under the $SU(2)_{2R}$ and (Baryon-Lepton)/2 symmetries.

Finally, using Eq. (113) into Eq. (106) gives :

$$\mathcal{V} = \tfrac{1}{2}g_{2R}^2 D_{2R}^3 D_{2R}^2 + \tfrac{1}{2}g_4^2 D_4^{15} D_4^{15} \tag{114}$$

$$= \tfrac{1}{2}g_{2R}^2 [\, 2D_H \sum_\phi I_\phi |\phi|^2] + \tfrac{1}{2}g_4^2 [\, 2\,\tfrac{3}{2} D_H \sum_\phi \left(\tfrac{B-L}{2}\right)_\phi |\phi|^2] \tag{115}$$

$$= \tfrac{1}{2}(|\bar{H}_\nu|^2 - |H_\nu|^2) \sum_\phi \Big\{ g_{2R}^2 I_\phi + \tfrac{3}{2} g_4^2 \Big(\tfrac{B-L}{2}\Big)_\phi \Big\} |\phi|^2 \tag{116}$$

The equation above deserves two comments. Firstly, we see that the broken $U(1)$ generator X resulting from the GUT symmetry breaking :

$$SU(4) \otimes SU(2)_{2R} \to SU(3)_c \otimes U(1)_Y \otimes U(1)_X \tag{117}$$

is given by $X = I + (B-L)/2$ whereas the unbroken hypercharge is $Y = -I + (B-L)/2$. Secondly, comparing Eq. (116) with Eqs. (26)-(33) we find :

$$D^2 = \tfrac{1}{8}(|\bar{H}_\nu|^2 - |H_\nu|^2) \tag{118}$$

From Eq. (118) alone, one might be tempted to conclude that the natural scale for the D-term is of the order of the mass of the heavy Higgs. However this is not true.

The scale of the D-term in Eq. (118) can be estimated upon the minimization of the heavy Higgs potential given by :

$$\mathcal{V} = \tfrac{1}{8}(g_{2R}^2 + \tfrac{3}{2}g_4^2)(\bar{H}_\nu^2 - H_\nu^2)^2 + \lambda_S^2(\bar{H}_\nu H_\nu - M_H^2)^2 + m_{\bar{H}}^2 \bar{H}_\nu^2 + m_H^2 H_\nu^2 \tag{119}$$

where the first term is a D-term, the second an F_S-term where S is the gauge singlet of Eq. (18) and $M_H \sim 10^{16}$ GeV, and $m_{\bar{H}}$, m_H soft scalar masses.

The minimization conditions for $\mathcal{V}$, re-written as combinations of $\partial\mathcal{V}/\partial\bar{H}_\nu \pm \partial\mathcal{V}/\partial H_\nu = 0$, are given by :

$$[\, g_H^2(\bar{H}_\nu^2 - H_\nu^2)^2 + \lambda_S^2(\bar{H}_\nu H_\nu - M_H^2)\,](\bar{H}_\nu + H_\nu) = -m_{\bar{H}}^2\bar{H}_\nu - m_H^2 H_\nu \tag{120}$$

$$[\, g_H^2(\bar{H}_\nu^2 + H_\nu^2)^2 - \lambda_S^2(\bar{H}_\nu H_\nu - M_H^2)\,](\bar{H}_\nu - H_\nu) = -m_{\bar{H}}^2\bar{H}_\nu \ + m_H^2 H_\nu \tag{121}$$

where $g_H^2 = \frac{1}{4}(g_{2R}^2 + \frac{3}{2}g_4^2)$. In the limit of negligible soft masses the right-hand side of Eqs. (120)-(121) vanishes. Thus, we find that $\bar{H}_\nu = H_\nu = M_H$, implying that $D = 0$. This result could had been anticipated since, if $m_{\bar{H}} = m_H$ then the Higgs potential is invariant under the exchange of the $\bar{H}_\nu \leftrightarrow H_\nu$ fields. When the soft masses are not zero, but still much smaller than M_H a perturbative solution to Eqs. (120)-(121) is appropriate. In terms of the new parameters m, $\bar{m}$ defined by :

$$\bar{H}_\nu = M_H - \bar{m} \qquad H_\nu = M_H - m \tag{122}$$

the minimization conditions are :

$$2\lambda_S^2(\bar{m} + m)M = m_{\bar{H}}^2 + m_H^2 \qquad 4g_H^2(\bar{m} - m)M = m_{\bar{H}}^2 - m_H^2 \tag{123}$$

Thus we find :

$$\bar{m} = \frac{1}{\lambda^2 + 2g_H^2}\left(\frac{m_{\bar{H}}^2}{M}\right) \qquad m = \frac{1}{\lambda^2 + 2g_H^2}\left(\frac{m_H^2}{M}\right) \tag{124}$$

and finally :

$$D^2 = \frac{m_H^2 - m_{\bar{H}}^2}{4\lambda_S^2 + 2g_{2R}^2 + 3g_4^2} \tag{125}$$

We see that, in spite of D being the difference of two GUT scale masses, it actually scales with the difference between the heavy soft Higgs masses. The reason is because $D^2 \sim \epsilon M_H^2$ where $\epsilon = (m_H^2 - m_{\bar{H}}^2)/M_H^2$ is a very small parameter which measures the amount of the $\bar{H}_\nu \leftrightarrow H_\nu$ symmetry breaking of the potential $\mathcal{V}$ in Eq. (119).

References

[1] H. P. Nilles, Phys. Rep. **110**, 1 (1984) ; H. E. Haber and G. L. Kane, Phys. Rep. **117**, 75 (1985) ; A. B. Lahanas and D. V. Nanopoulos, Phys. Rep **145**, 1 (1987); H. E. Haber, Presented at Theoretical Advanced Study Institute (TASI 92): From Black Holes and Strings to Particles, Boulder, CO, 3-28 Jun 1992. Published in Boulder TASI 92:0589-688, `hep-ph/9305248`.

[2] M. B. Einhorn and D. R. T. Jones, Nucl. Phys. **B196**, 475 (1982); J. Ellis, S. Kelley and D. V. Nanopoulos, Phys. Lett. **B249**, 441 (1990); *ibid.*, Phys. Lett. **B260**, 131 (1991); U. Amaldi, W. de Boer and H. Fürstenau, Phys. Lett. **B260**, 447 (1991); P. Langacker and M. Luo, Phys. Rev. **D44**, 817 (1991); R. Barbieri and L. J. Hall, Phys. Rev. Lett. **68**, 752 (1992); M. Carena, Talk given at International Europhysics Conference on High-energy Physics (HEP 95), Brussels, Belgium, 27 Jul - 2 Aug 1995, `hep-ph/9603370`.

[3] J. Ellis, S. Kelley and D. V. Nanopoulos, Nucl. Phys. **B373**, 55 (1992).

[4] G. G. Ross and R. G. Roberts, Nucl. Phys. **B377**, 571 (1992).

[5] P. Langacker and N. Polonsky, Phys. Rev. **D47**, 4028 (1993).

[6] P. Langacker and N. Polonsky, Phys. Rev. **D49**, 1454 (1994).

[7] S. Kelley, J. L. Lopez and D. V. Nanopoulos, Phys. Lett. **B274**, 387 (1992).

[8] M. Carena, S. Pokorski and C. E. M. Wagner, Nucl. Phys. **B406**, 59 (1993).

[9] H. Arason, D. J. Castaño, E. J. Piard and P. Ramond, Phys. Rev. **D47**, 232 (1993).

[10] B. C. Allanach, S. F. King, Phys. Lett. **B353**, 477 (1995).

[11] H. Georgi and S. Glashow, Phys. Rev. Lett. **32**, 438 (1974).

[12] J. C. Pati, A. Salam, Phys. Rev. **D10**, 275 (1974).

[13] Y. Fukuda *et al.*, Super-Kamiokande Collaboration, Phys. Lett. **B433**, 9 (1998); *ibid.* Phys. Lett. **B436**, 33 (1998); *ibid.* Phys. Rev. Lett. **81**, 1562 (1998).

[14] B. Ananthanarayan, G. Lazarides and Q. Shafi, Phys. Rev. **D44**, 1613 (1991).

[15] V. Barger, M. S. Berger, P. Ohmann, Phys. Rev. **D47**, 1093 (1993).

[16] D. J. Castaño, E. J. Piard and P. Ramond, Phys. Rev. **D49** 4882 (1994).

[17] G. Kane, C. Kolda, L. Roszkowski, J. Wells, Phys. Rev. **D49**, 6173 (1994).

[18] M. Carena, M. Olechowski, S. Pokorski and C. E. M. Wagner, Nucl. Phys. **B419**, 213 (1994); *ibid.* Nucl. Phys. **B426**, 269 (1994).

[19] L. J. Hall, R. Rattazzi and U. Sarid, Phys. Rev. **D50**, 7048 (1994).

[20] M. Olechowski and S. Pokorski, Phys. Lett. **B344**, 201 (1995).

[21] H. Baer, M. A. Díaz, J. Ferrandis and X. Tata, Phys. Rev. **D61**, 111701 (2000).

[22] M. Carena and C. E. M. Wagner, Talk given at 2nd IFT Workshop on Yukawa Couplings and the Origins of Mass, Gainesville, FL, 11-13 Feb 1994, `hep-ph/9407209`.

[23] R. Rattazzi and U. Sarid, Phys. Rev. **D53**, 1553 (1996).

[24] M. Drees, Phys. Lett. **B181**, 279 (1986); J. S. Hagelin and S. Kelley, Nucl. Phys. **B342**, 95 (1990); Y. Kawamura and M. Tanaka, Prog. Theor. Phys. **91**, 949 (1994); H.-C. Cheng and L. J. Hall, Phys. Rev. **D51**, 5289 (1995); C. Kolda and S. P. Martin, Phys. Rev. **D53**, 3871 (1996).

[25] R. Barbieri, G. F. Giudice, Phys. Lett. **B309**, 86 (1993); N. Oshimo, Nucl. Phys. **B404**, 20 (1993); Y. Okada, Phys. Lett. **B315**, 119 (1993); V. Barger,

M. S. Berger, P. Ohmann, R. J. N. Phillips, Phys. Rev. **D51**, 2438 (1995); R. Garisto, J. Ng, Phys. Lett. **B315**, 372 (1993); J. L. Lopez, D. V. Nanopoulos, G. T. Park, Phys. Rev. **D48**, 974 (1993) M. A. Díaz, Phys. Lett. **B322**, 207 (1994); F. M. Borzumati, M. Olechowski, S. Pokorski, Phys. Lett. **B349**, 311 (1995); J. Wu, R. Arnowitt, P. Nath, Phys. Rev. **D51**,1371 (1995); B. de Carlos, J. A. Casas, Phys. Lett. **B349**, 300 (1995); S. Bertolini, F. Vissani, Z. Phys. **C67**, 513 (1997); T. Blazěk, S. Raby, Phys. Rev. **D59**, 095002 (1999); H. Baer, M. Brhlik, M. A. Díaz, J. Ferrandis, P. Mercadante, P. Quintana, X. Tata `hep-ph/0005027`; G. Barenboim, K. Huitu and M. Raidal, hep-ph/0005159; E. Ma and M. Raidal, hep-ph/0006253; (and references therein.)

[26] I. Antoniadis and G. K. Leontaris, Phys. Lett. **B216**, 333 (1989).

[27] Gary Shiu, S.H.Henry Tye, Phys. Rev. **D58** (1998) 106007, hep-th/9805157.

[28] O. V. Tarasov, A. A. Vladimirov, A. Y. Zharkov, Phys. Lett. **B93**, 429 (1980); S. G. Gorshny, A. L. Kataev, S. A. Larin, Phys. Lett. **B135**, 457 (1984).

[29] H. Arason, D. J. Castaño, B. Kesthelyi, S. Mikaelian, E. J. Piard, P. Ramond and B. D. Wright, Phys. Rev. **D46**, 3945 (1992).

[30] M. E. Machacek and M. T. Vaughn, Nucl. Phys. **B222**, 83 (1983); *ibid.*, Nucl. Phys. **B236**, 221 (1984); *ibid.*, Nucl. Phys. **B249**, 70 (1985).

[31] N. K. Falck, Z. Phys **C30**, 247 (1986); S. P. Martin and M. T. Vaughn, Phys. Rev. **D50**, 2282 (1994).

[32] D. E. Groom *et al.* (Particle Data Group), Eur. Phys. Jour. **C15**, 1 (2000) (URL:http://pdg.lbl.gov)

[33] L. Hall, Nucl. Phys. **B178**, 75 (1981).

[34] B. D. Wright, Submitted to Phys. Rev. **D**, `hep-ph/9404217`.

[35] G. Gamberini, G. Ridolfi and F. Zwirner, Nucl. Phys. **B331**, 331 (1990).

[36] P. H. Chankowski, Phys. Rev. **D41**, 2877 (1990).

[37] A. Dedes, A. B. Lahanas and K. Tamvakis, Phys. Rev. **D53**, 3793 (1996).

[38] V. Barger, M. S. Berger, P. Ohmann, Phys. Rev. **D49**, 4908 (1994).

[39] R. Arnowitt and P. Nath, Phys. Rev. **D46**, 3981 (1992); *ibid.*, Invited talk at 8th Les Rencontres de Physique de la Vallee d'Aoste: Results and Perspectives in Particle Physics, La Thuile, Italy, 6-12 Mar 1994, `hep-ph/9406403`.

[40] R. Hempfling and B. A. Kniehl, Phys. Rev. **D51**, 1386 (1995).

[41] D. M. Pierce, J. A. Bagger, K. T. Matchev and R. Zhang, Nucl. Phys. **B491**, 3 (1997).

[42] M. Gell-Mann, P. Ramond, R. Slansky, in Sanibel Talk, CALT-68-709, Feb. 1979 and in *Supergravity* (North Holland, Amsterdam 1979); T. Yanagida in *Proc. of the Workshop on Unified Theory and Baryon Number of the Universe*, KEK, Japan (1979); R. N. Mohapatra, G. Senjanovic, Phys. Rev. Lett. **44**, 912 (1980).

[43] The Top Averaging Group and CDF and D0 Collaborations (Luc Demortier *et al.*). FERMILAB-TM-2084, Sep. 1999.

[44] V. Barger, M. S. Berger, P. Ohmann, R. J. N. Phillips, Phys. Lett. **B314**, 351 (1993).

[45] B. Pendleton, G. G. Ross, Phys. Lett. **B98**, 291 (1981); C. T. Hill, Phys. Rev. **D24**, 691 (1981).

[46] S. F. King, Phys. Lett. **B325**, 129 (1994); B. C. Allanach, S. F. King, Nucl. Phys. **B456**, 57 (1995).

[47] S. F. King and Q. Shafi, Phys. Lett. **B422**, 135 (1998).

[48] Y. Kawamura, H. Murayama and M. Yamaguchi, Phys. Lett. **B324**, 52 (1994); *ibid.*, Phys. Rev. **D51**, 1337 (1995).

[49] R. Hempfling, Phys. Rev. **D52**, 4106 (1995).

[50] M. Olechowski and S. Pokorski, Nucl. Phys. **B404**, 590 (1993).

[51] M. Drees and M. M. Nojiri, Nucl. Phys. **B369**, 54 (1992).

[52] W. Majerotto and B. Mösslacher, Z. Phys. **C48**, 273 (1990).

[53] V. Barger, M. S. Berger and P. Ohmann, Phys. Rev. **D51**, 2438 (1995).

[54] R. Rattazzi, U. Sarid and L. J. Hall, Presented at the second IFT Workshop on Yukawa Couplings and the Origins of Mass, 11-13 February 1994, Gainesville, Florida, `hep-ph/9405313`.

[55] N. Polonsky and A. Pomarol, Phys. Rev. **D51**, 6532 (1995).

[56] N. Polonsky and A. Pomarol, Phys. Rev. Lett. **73**, 2292 (1994).

[57] A. Lleyda and C. Muñoz, Phys. Lett. **B317**, 82 (1993).

[58] A. E. Faraggi, J. Hagelin, S. Kelley, and D. V. Nanopoulos, Phys. Rev. **D45**, 3272 (1992);

[59] J. Ellis, G. Ridolfi, F. Zwirner, Phys. Lett. **B262**, 477 (1991).

[60] H. Murayama, M. Olechowski and S. Pokorski, Phys. Lett. **B371**, 57 (1996)

[61] D. Matalliotakis and H. P. Nilles, Nucl. Phys. **B435**, 115 (1995).

[62] A. J. Buras, M. Misiak, M. Münz, S. Pokorski, Nucl. Phys. **B424**, 374 (1994); K. Adel, Y. Yao, Phys. Rev. **D49**, 4945 (1994); A. Ali, C. Greub, Phys. Lett. **B361**, 146 (1995); C. Greub, T. Hurth, Talk presented at the Second International Conference on B Physics and CP Violation, Honolulu, Hawaii, March 1997,

hep-ph/9708214; A. J. Buras, A. Kwiatkowski, N. Pott, Phys. Lett. **B414**, 157 (1997); K. Chetyrkin, M. Misiak, M. Münz, Phys. Lett. **B400**, 206 (1997); M. Ciuchini, G. Degrassi, P. Gambino, G. F. Giudice, Nucl. Phys. **B527**, 21 (1998).

[63] CLEO collaboration (M. S. Alam *et al.*), Phys. Rev. Lett. **74**, 2885 (1995); CLEO collaboration (S. Ahmed), hep-ex/9908022.

[64] ALEPH collaboration (R. Barate *et al.*), Phys. Lett. **B429**, 169 (1998).

[65] S. Bertolini, F. Borzumati, A. Masiero, G. Ridolfi, Nucl. Phys. **B353**, 591 (1991).

[66] F. Gabbiani, A. Masiero, Nucl. Phys. **B322**, 235 (1989).

[67] E. Gabrielli, S. Khalil, E. Torrente-Lujan, hep-ph/0005303.

[68] CLEO Collaboration (K. E. Edwards *et al.*), Phys. Rev. **D55**, 3919 (1997).

[69] T. Blažek, S. Raby and S. Pokorski, Phys. Rev. **D52**, 4151 (1995).

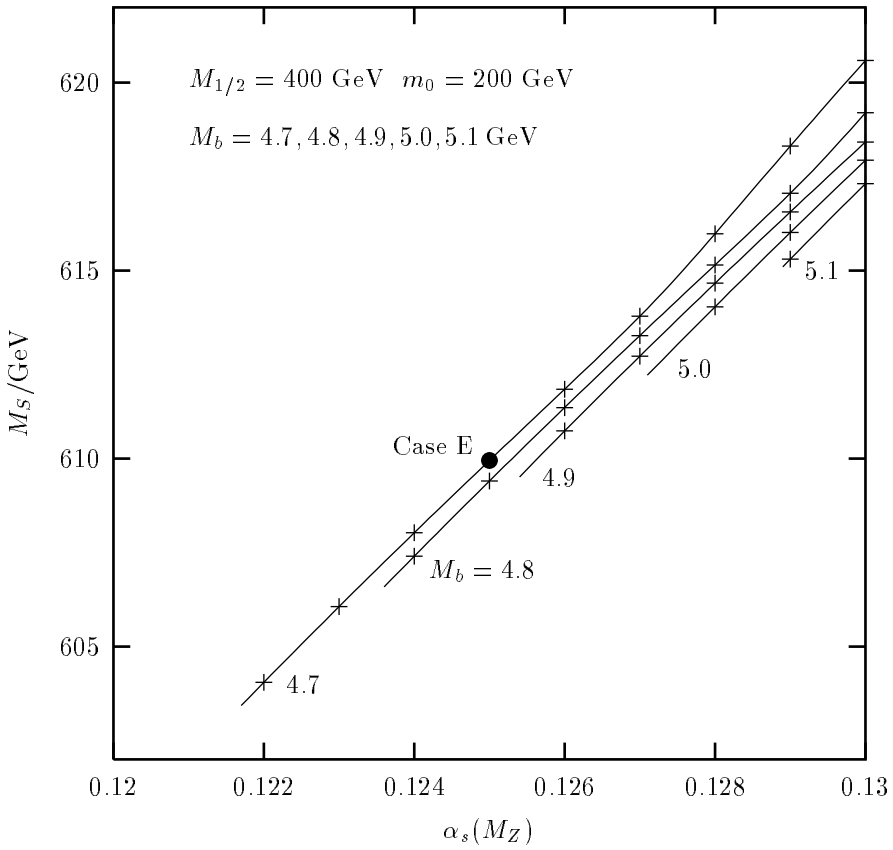
$M_{1/2} = 400$ GeV $m_0 = 200$ GeV
$M_b = 4.7, 4.8, 4.9, 5.0, 5.1$ GeV
620
615
610
605
M_S/GeV
0.12
0.122
0.124
0.126
0.128
0.13
$\alpha_s(M_Z)$
Case E
4.7
$M_b = 4.8$
4.9
5.0
5.1

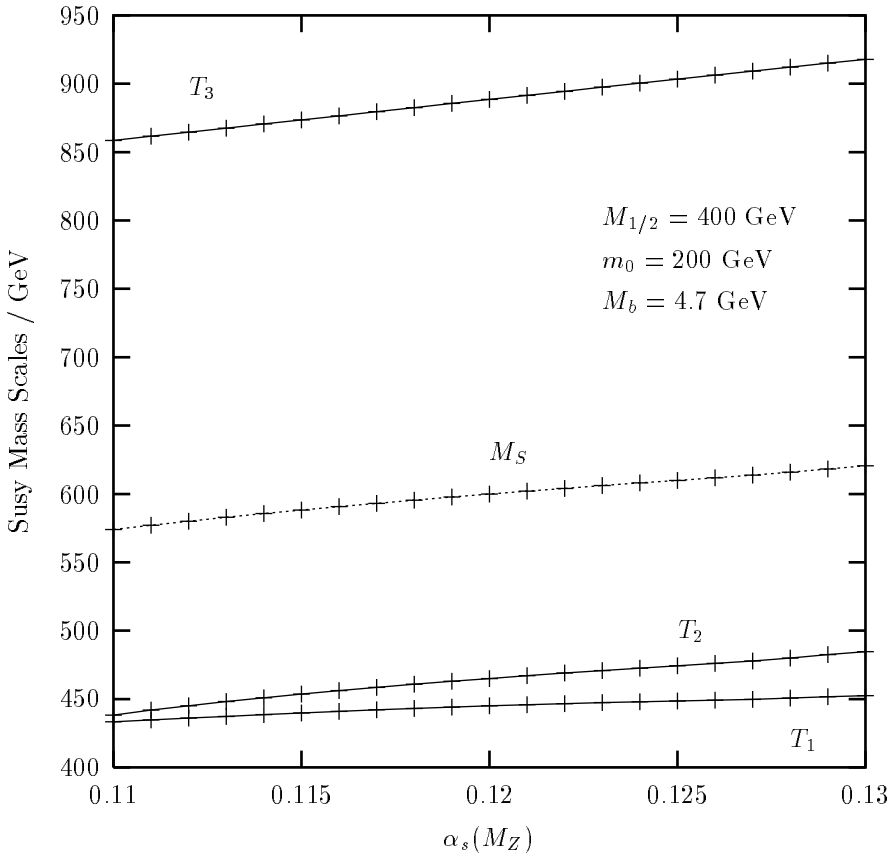
950
900
850
800
750
700
650
600
550
500
450
400
0.11
0.115
0.12
0.125
0.13
Susy Mass Scales / GeV
$\alpha_s(M_Z)$
T_3
M_S
T_2
T_1
$M_{1/2} = 400$ GeV
$m_0 = 200$ GeV
$M_b = 4.7$ GeV

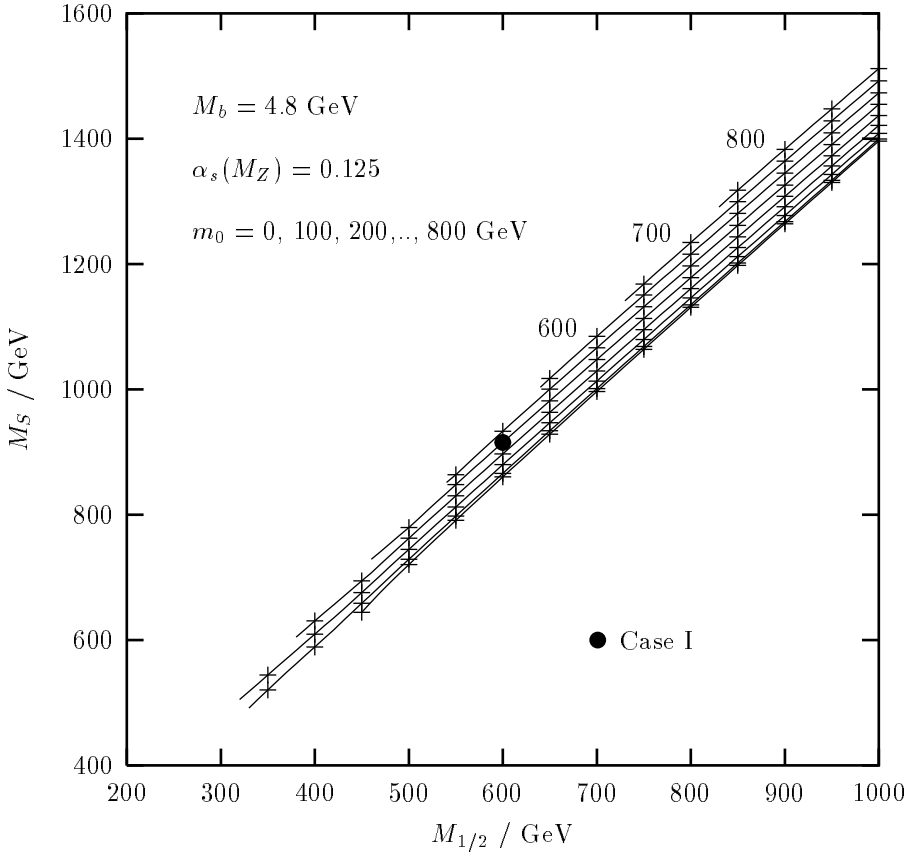
$M_b = 4.8$ GeV
$\alpha_s(M_Z) = 0.125$
$m_0 = 0,\ 100,\ 200,..,\ 800$ GeV
800
700
600
Case I
M_S / GeV
$M_{1/2}$ / GeV
1600
1400
1200
1000
800
600
400
200
300
400
500
600
700
800
900
1000

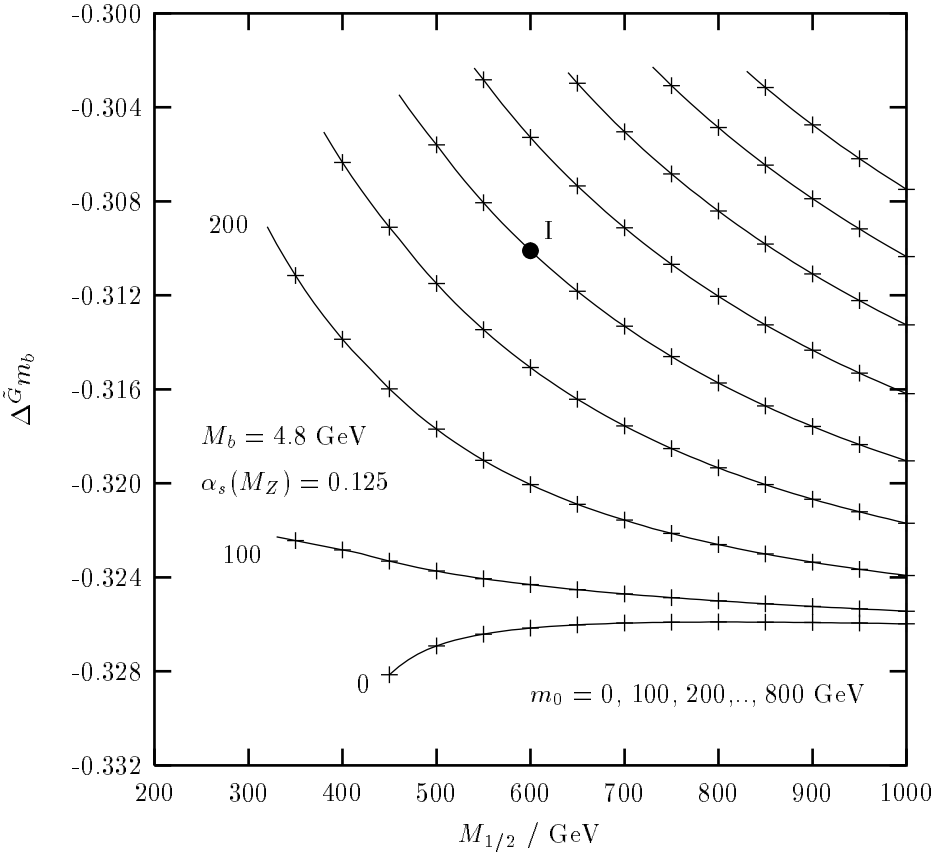
-0.300
-0.304
-0.308
-0.312
-0.316
-0.320
-0.324
-0.328
-0.332
200
300
400
500
600
700
800
900
1000
$\Delta^{\tilde{G}} m_b$
$M_{1/2}$ / GeV
200
I
100
0
$M_b = 4.8$ GeV
$\alpha_s(M_Z) = 0.125$
$m_0 = 0, 100, 200, .., 800$ GeV

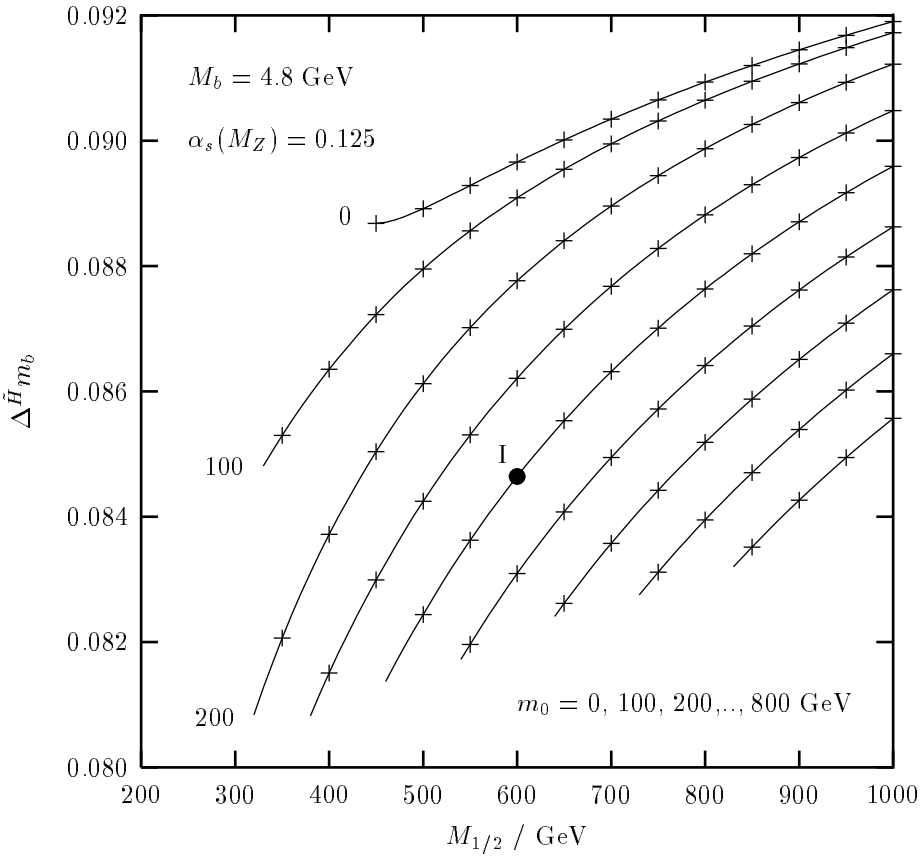
0.092
0.090
0.088
0.086
0.084
0.082
0.080
$\Delta^{\tilde{H}} m_b$
$M_b = 4.8$ GeV
$\alpha_s(M_Z) = 0.125$
0
100
200
I
$m_0 = 0,\ 100,\ 200,..,\ 800$ GeV
200
300
400
500
600
700
800
900
1000
$M_{1/2}$ / GeV

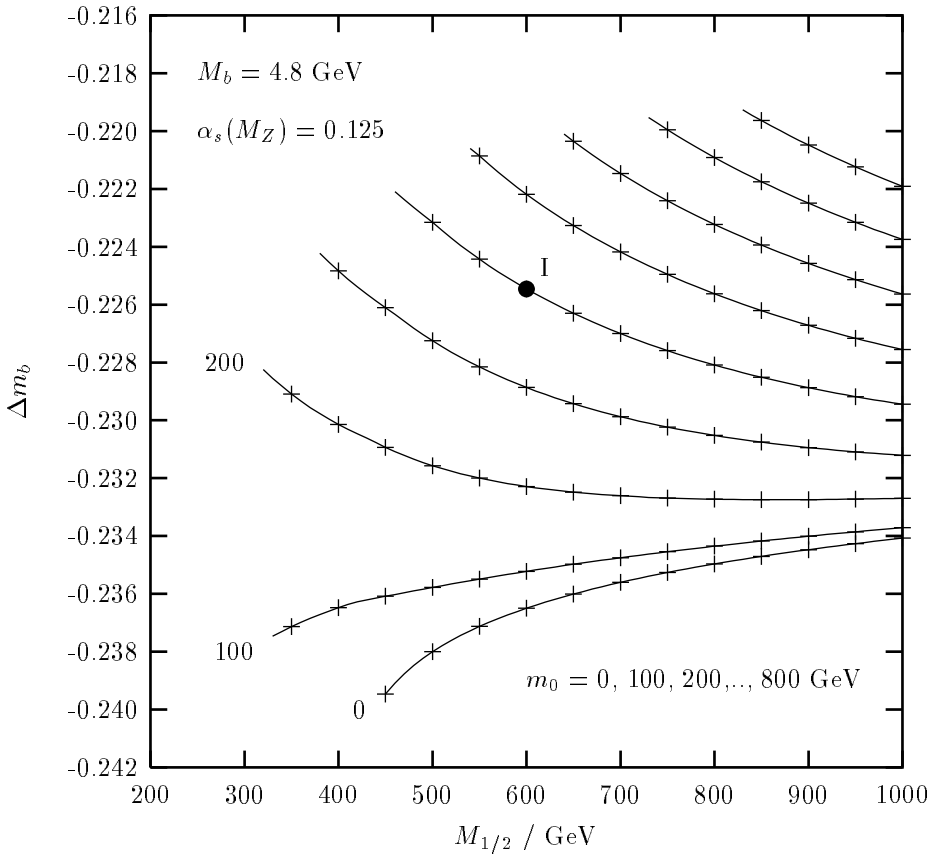
-0.216
-0.218
-0.220
-0.222
-0.224
-0.226
-0.228
-0.230
-0.232
-0.234
-0.236
-0.238
-0.240
-0.242
Δm_b
$M_b = 4.8$ GeV
$\alpha_s(M_Z) = 0.125$
I
200
100
0
$m_0 = 0, 100, 200, .., 800$ GeV
200
300
400
500
600
700
800
900
1000
$M_{1/2}$ / GeV

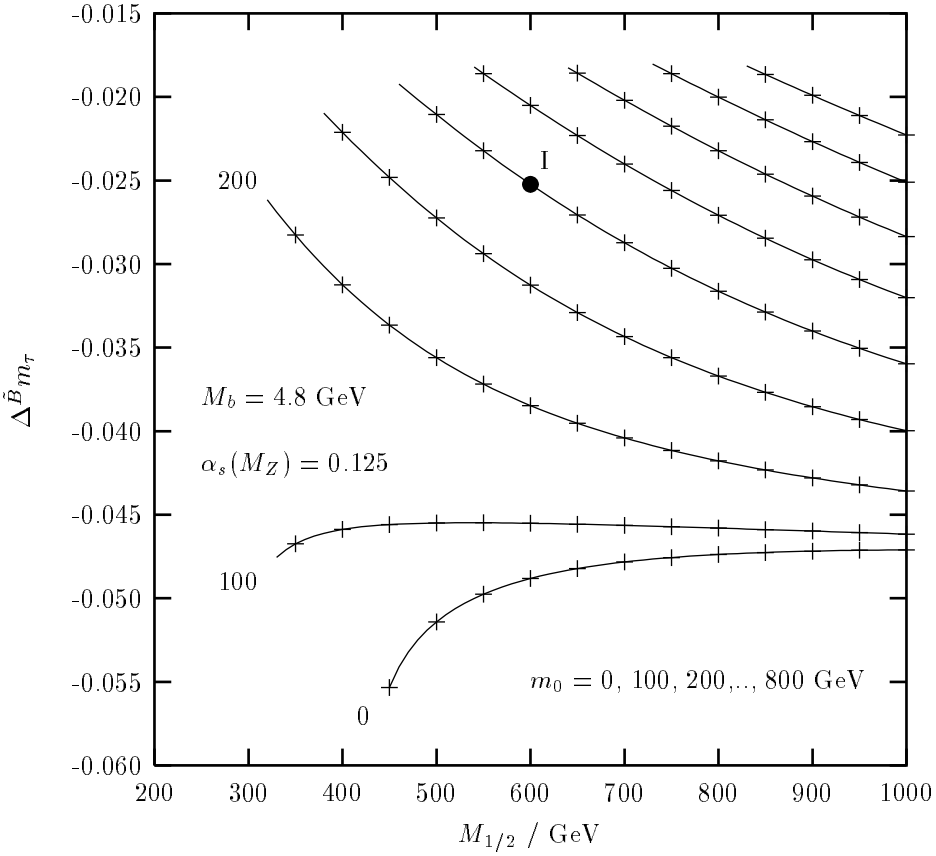
-0.015
-0.020
-0.025
-0.030
-0.035
-0.040
-0.045
-0.050
-0.055
-0.060
200
300
400
500
600
700
800
900
1000
$\Delta^{\tilde{B}} m_\tau$
$M_{1/2}$ / GeV
I
200
100
0
$M_b = 4.8$ GeV
$\alpha_s(M_Z) = 0.125$
$m_0 = 0, 100, 200, .., 800$ GeV

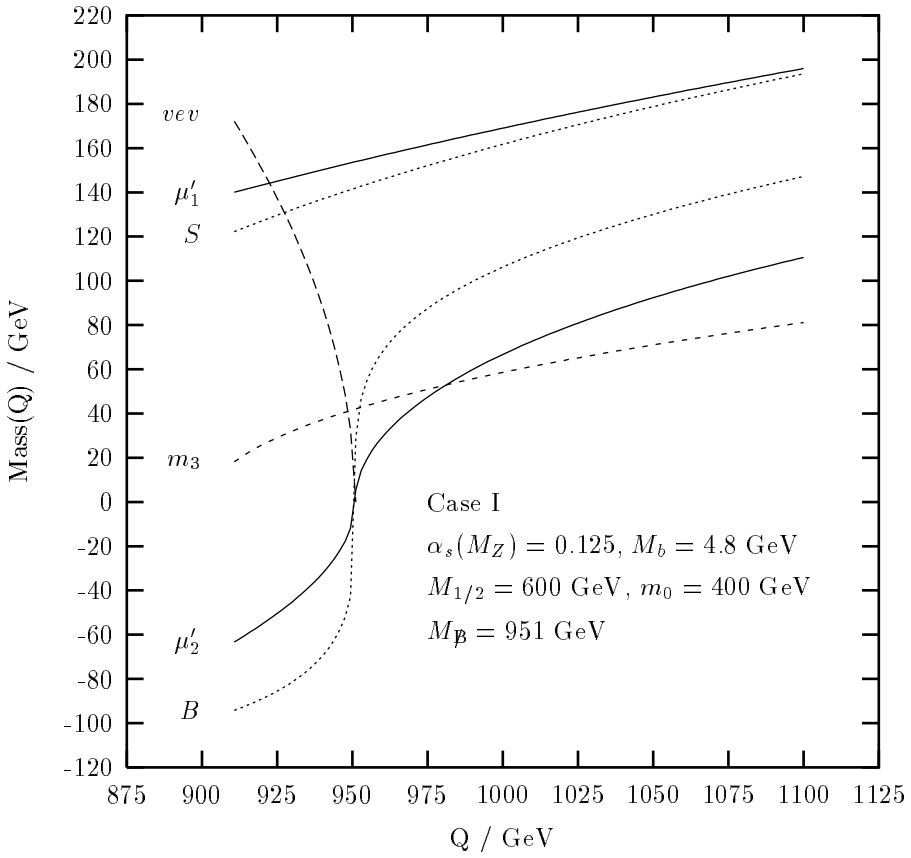
220
200
180
160
140
120
100
80
60
40
20
0
-20
-40
-60
-80
-100
-120
875
900
925
950
975
1000
1025
1050
1075
1100
1125
Mass(Q) / GeV
Q / GeV
vev
μ_1'
S
m_3
μ_2'
B
Case I
$\alpha_s(M_Z) = 0.125$, $M_b = 4.8$ GeV
$M_{1/2} = 600$ GeV, $m_0 = 400$ GeV
$M_{\not B} = 951$ GeV

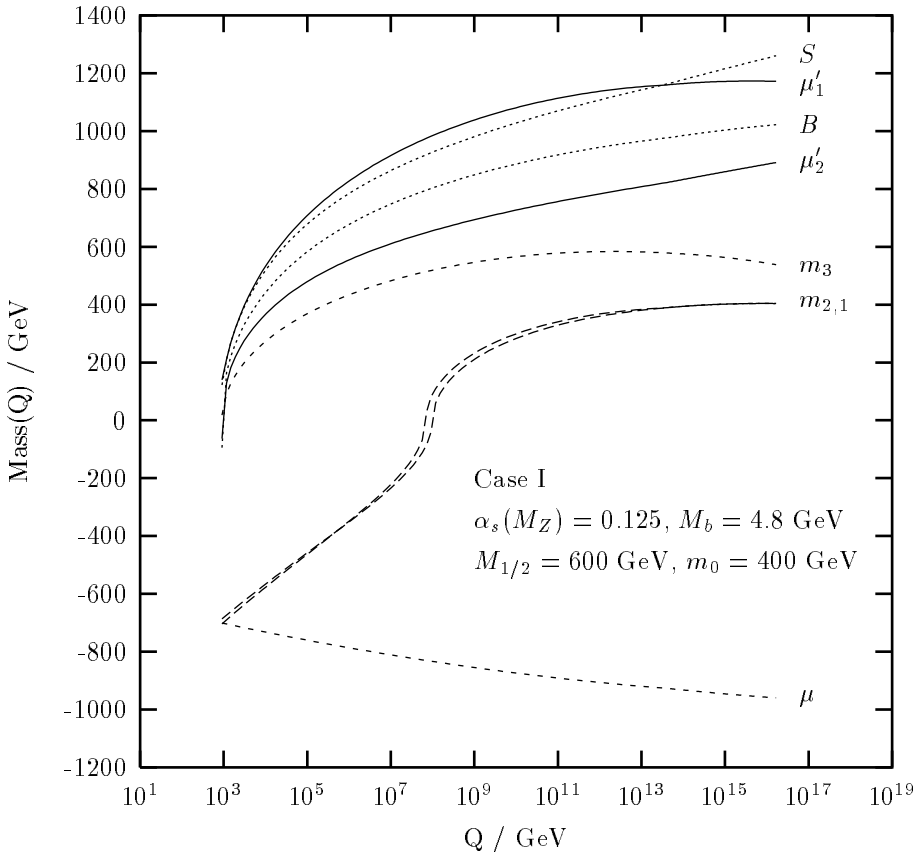
1400
1200
1000
800
600
400
200
0
-200
-400
-600
-800
-1000
-1200
10^1
10^3
10^5
10^7
10^9
10^{11}
10^{13}
10^{15}
10^{17}
10^{19}
Mass(Q) / GeV
Q / GeV
S
μ_1'
B
μ_2'
m_3
$m_{2,1}$
μ
Case I
$\alpha_s(M_Z) = 0.125$, $M_b = 4.8$ GeV
$M_{1/2} = 600$ GeV, $m_0 = 400$ GeV

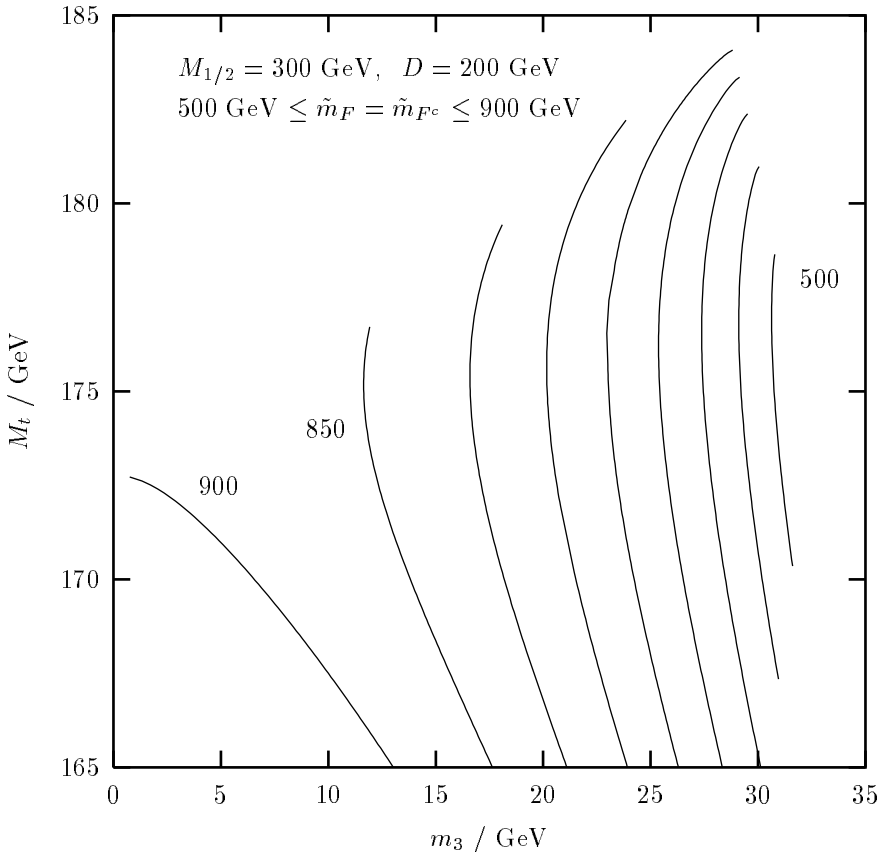
$M_{1/2} = 300$ GeV, $D = 200$ GeV
500 GeV $\leq \tilde{m}_F = \tilde{m}_{F^c} \leq$ 900 GeV
900
850
500
185
180
175
170
165
0
5
10
15
20
25
30
35
M_t / GeV
m_3 / GeV

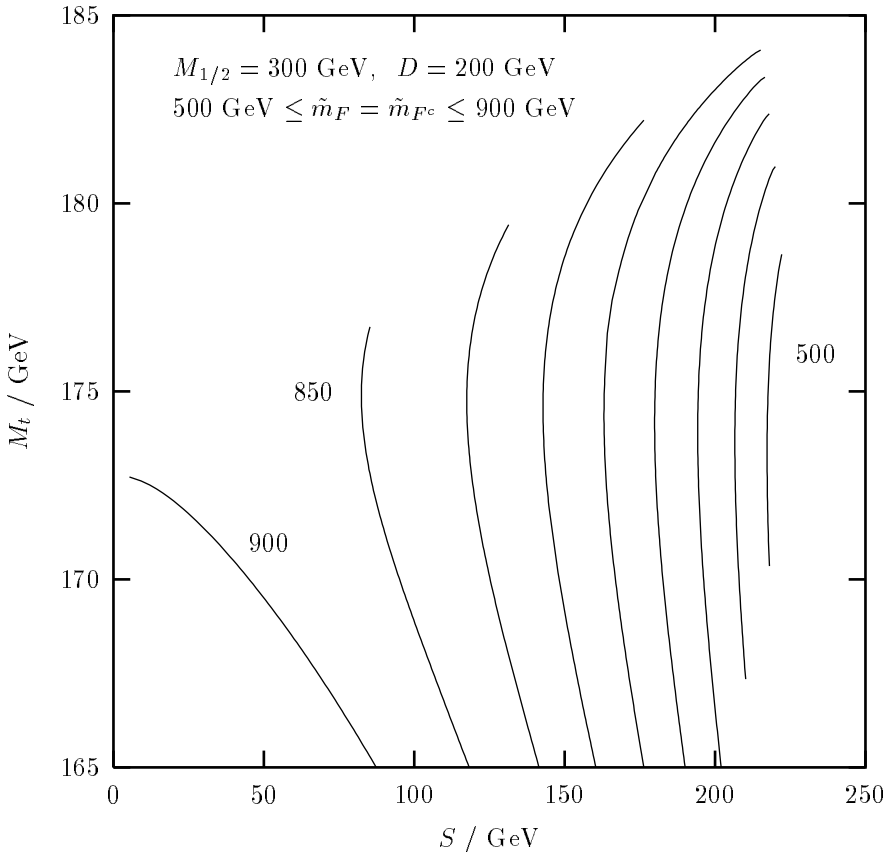
$M_{1/2} = 300$ GeV, $D = 200$ GeV
500 GeV $\leq \tilde{m}_F = \tilde{m}_{F^c} \leq$ 900 GeV
900
850
500
185
180
175
170
165
0
50
100
150
200
250
M_t / GeV
S / GeV

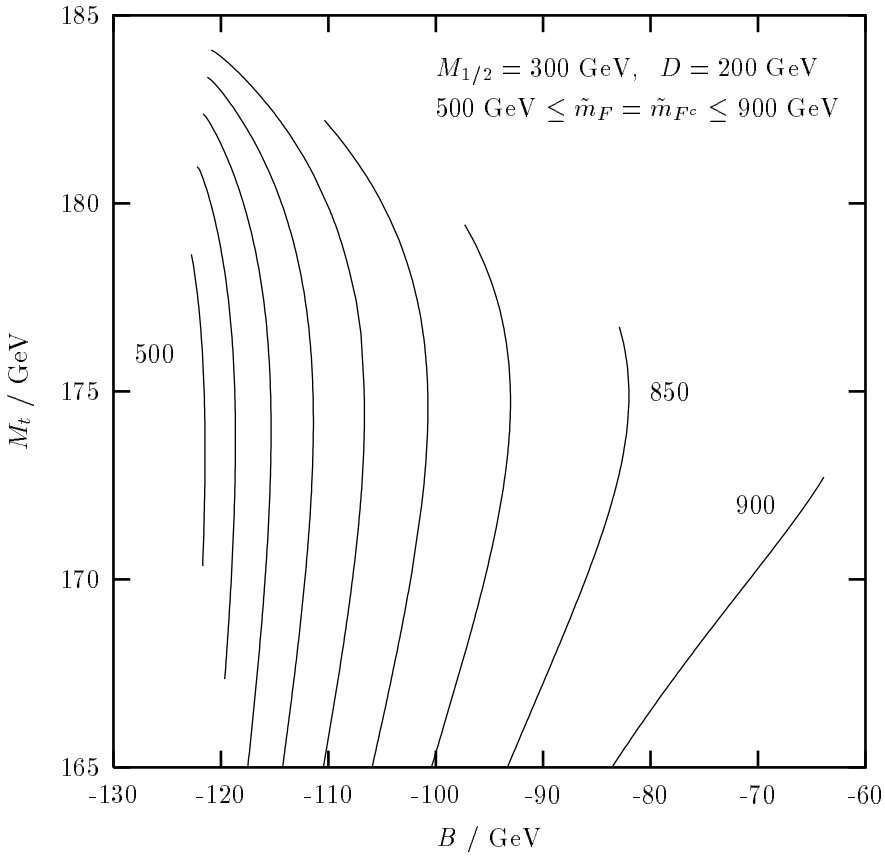
$M_{1/2} = 300$ GeV, $D = 200$ GeV
500 GeV $\leq \tilde{m}_F = \tilde{m}_{F^c} \leq$ 900 GeV
500
850
900
185
180
175
170
165
-130
-120
-110
-100
-90
-80
-70
-60
M_t / GeV
B / GeV

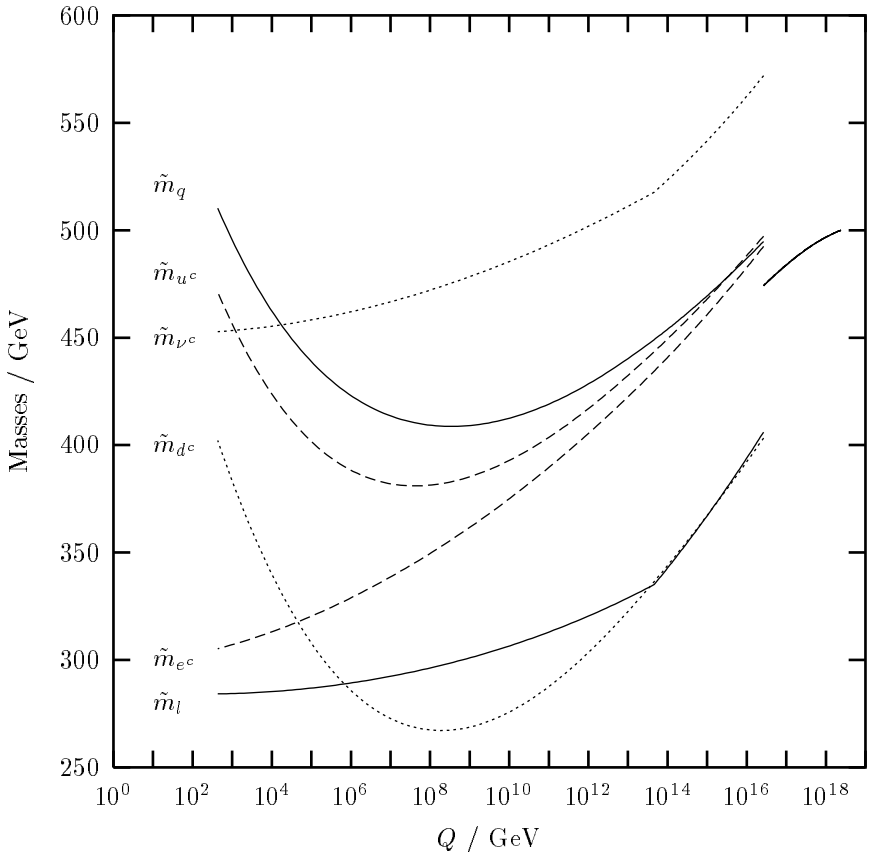
600
550
500
450
400
350
300
250
Masses / GeV
$\tilde{m}_q$
$\tilde{m}_{u^c}$
$\tilde{m}_{\nu^c}$
$\tilde{m}_{d^c}$
$\tilde{m}_{e^c}$
$\tilde{m}_l$
10^0
10^2
10^4
10^6
10^8
10^{10}
10^{12}
10^{14}
10^{16}
10^{18}
Q / GeV

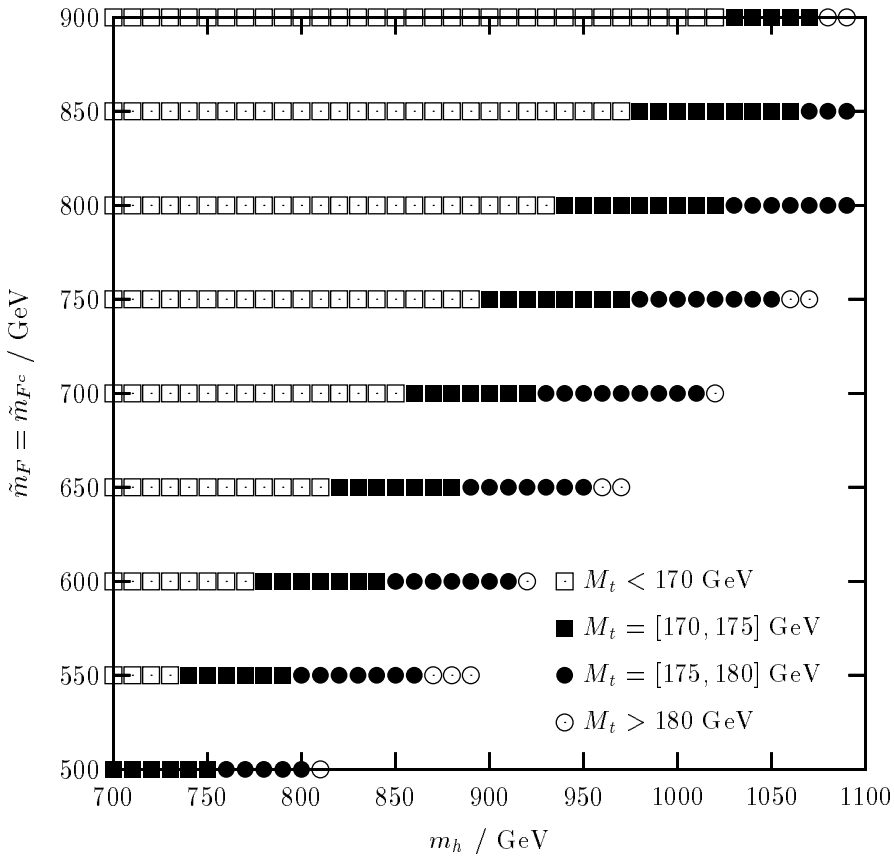
900
850
800
750
700
650
600
550
500
700
750
800
850
900
950
1000
1050
1100
$\tilde{m}_F = \tilde{m}_{F^c}$ / GeV
m_h / GeV
$M_t < 170$ GeV
$M_t = [170, 175]$ GeV
$M_t = [175, 180]$ GeV
$M_t > 180$ GeV